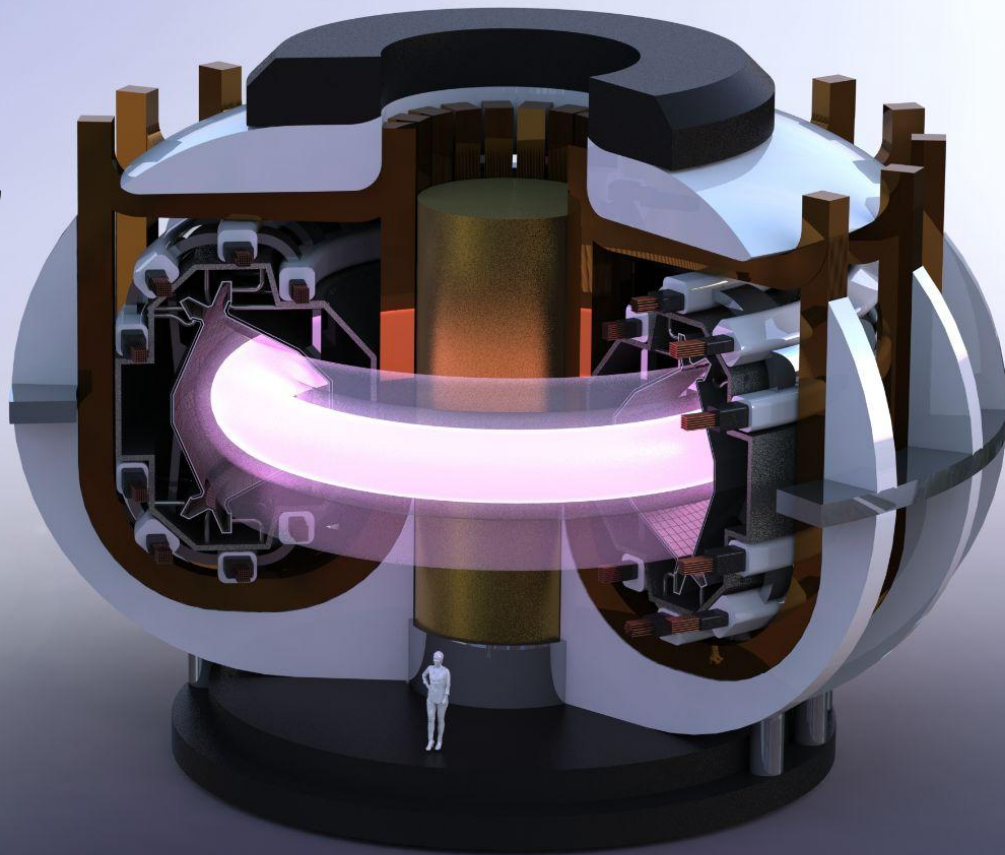




**Modular
Adjustable
Negative-Triangularity
ARC**

A Fusion Pilot Plant



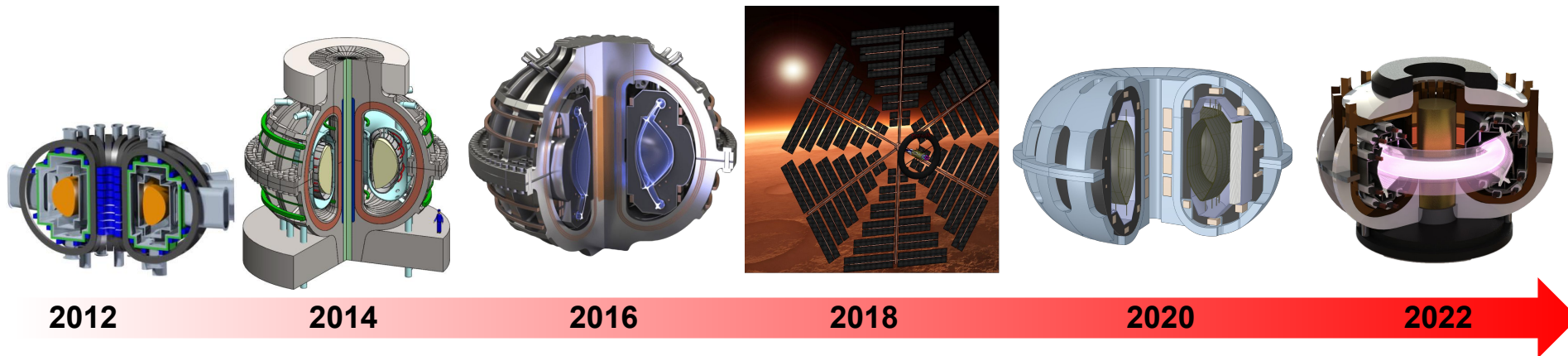
22.63 Fusion Engineering

APPH 9143



COLUMBIA ENGINEERING
The Fu Foundation School of Engineering and Applied Science

MIT fusion design class (22.63): **the last 10 years**



VULCAN

- PMI science facility
- D-D fuel
- Demountable HTS joints
- HFS current drive

G. Olynyk et al., *Fusion Eng. and Design*, 87(3), 2012.

Y. Podpaly et al., *Fusion Eng. and Design*, 87(3), 2012.

D. G. Whyte et al., *Fusion Eng. and Design*, 87(3), 2012.

H. Barnard et al., *Fusion Eng. and Design*, 87(3), 2012.

ARC

- D-T fusion pilot plant
- FLiBe liquid immersion blanket
- Demountable HTS joints
- Steady state AT operation

B. N. Sorbom et al., *Fusion Eng. and Design*, 100, 2015.

ARC+divertor

- Added advanced divertor solution to ARC design
- Studied ARC diagnostics

A. Q. Kuang et al., *Fusion Eng. and Design*, 137 (2018).

Fission-fusion interplanetary spacecraft

- D-T mirror-driven subcritical fission assembly

ARCH

- High-temperature ARC for hydrogen production
- Disruption-tolerant vacuum vessel (LSVV)
- High energy density L-mode operation with radiative heat exhaust
- Joint with Princeton

S. Frank et al., *Nuclear Fusion*, 62(12), 2022.

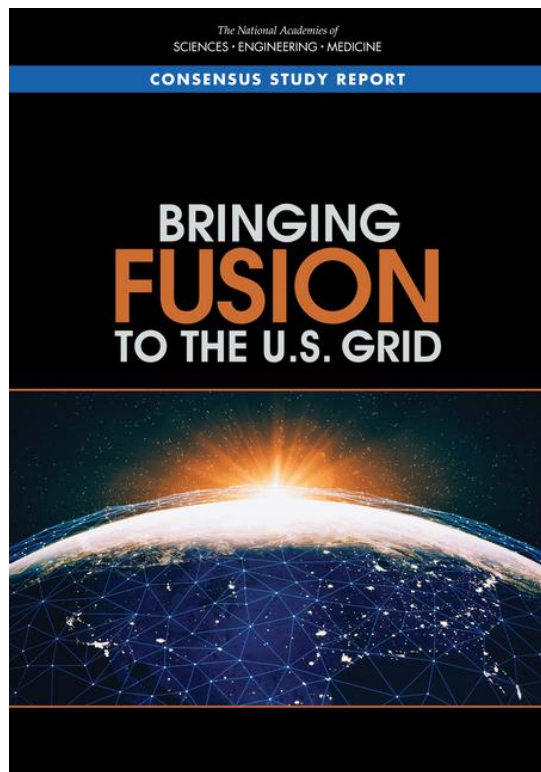
MANTA

- NASEM-compliant fusion pilot plant
- Negative triangularity
- FLiBe liquid immersion blanket
- Demountable HTS joints
- Joint with Columbia



images not to scale

NASEM 2021 report: fusion pilot plant recommendations



Key targets for a U.S. fusion pilot plant (FPP)

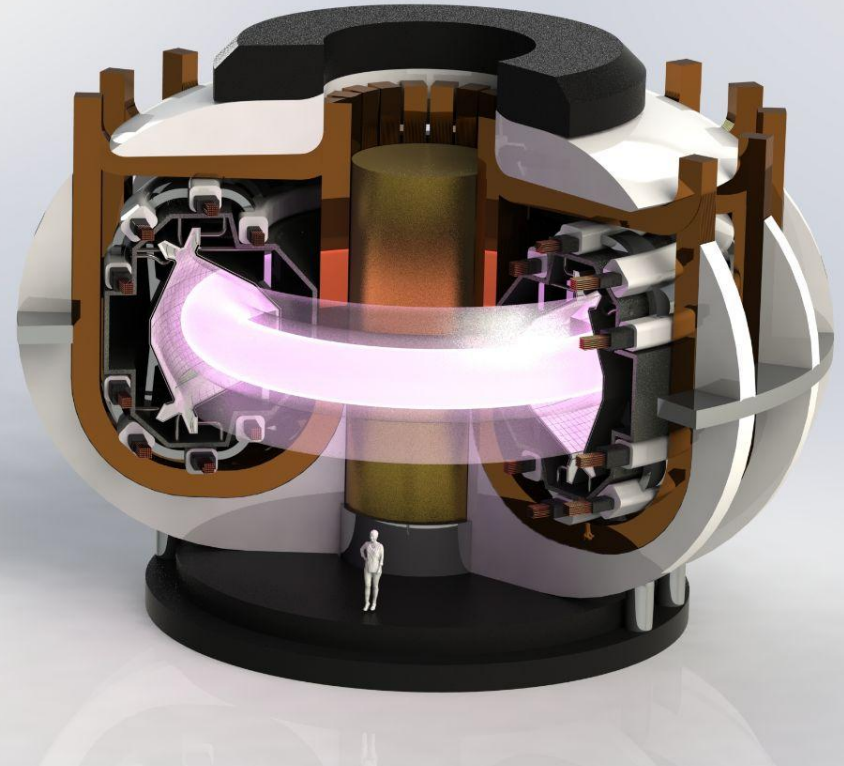
- $Q_{\text{electrical}} > 1$
- Net electricity ≥ 50 MWe (peak) for 3 hours
- TBR ~ 1 or higher for tritium self-sufficiency
- Overnight cost $< \$5\text{B}$
- Demonstrate successful operation through several environmental cycles

Education goals

- Learn/use modern computational design tools
- Work in groups but intertwine design features
- Big thanks to group leaders: E. Peterson, M. Wigram, S. Ferry, S. Frank, N. Mandell, O. Nelson, C. Hansen, R. Bielajew, T. Mouratidis

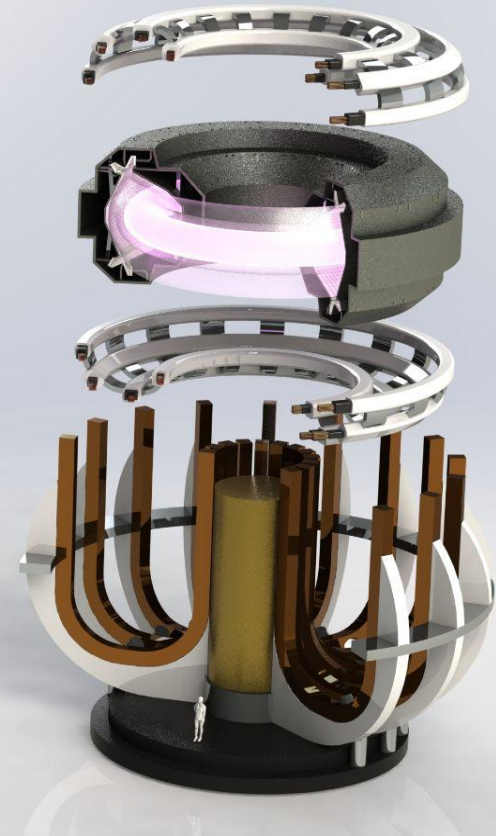
MANTA exceeds NASEM requirements through several key innovations

1. Large aspect ratio, low elongation, and negative triangularity **reduces physics and technology risks**
2. **Variable fusion power** at constant, manageable divertor power exhaust
3. **Pulsed plasma** but **constant electricity** production > 50 MWe
4. Flexible **replacement strategy** enables testing multiple designs through many environmental cycles
5. Tritium breeding **beyond sufficient for operation** and inventory



Presentation outline

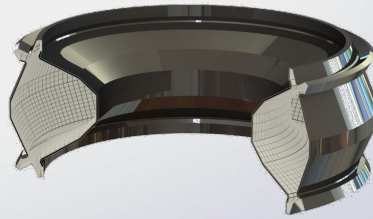
- **Core:** Self-consistent physics meets power goals
- **Magnets:** High fields with demountable joints
- **Power Handling:** Reactor will not melt
- **Neutronics:** Radiation load is tolerable
- **Fuel Cycle:** More tritium is bred than fused
- **Maintenance:** Rapid modular replacements
- **Integration:** All major systems are compatible
- **Economics:** MANTA is profitable and under budget



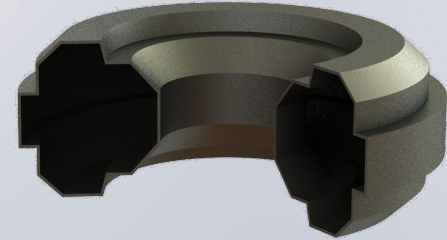
This project designed and integrated six unique modules



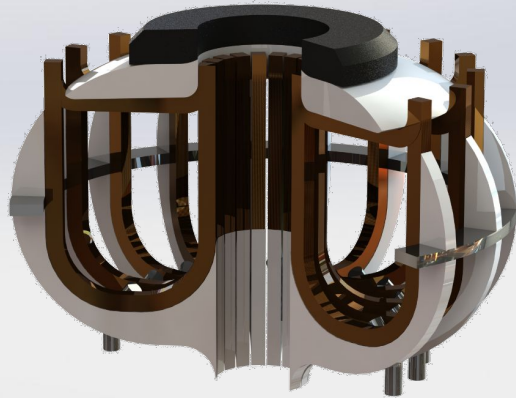
Core Plasma



Vacuum Vessel



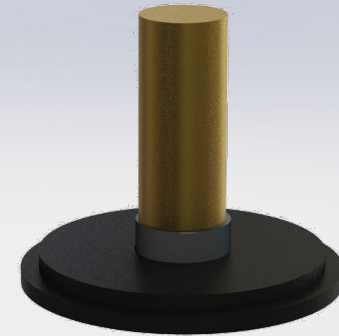
FLiBe Blanket



TF Magnets



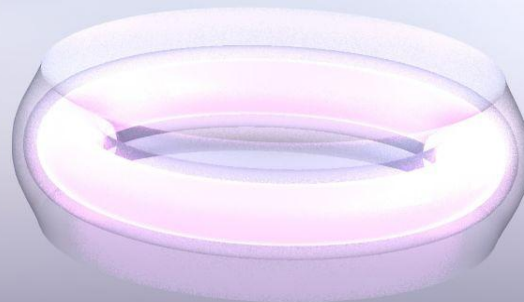
PF Magnets



Central Solenoid

Core Scenario and Edge Integration

Leonardo Corsaro
Raymond Diab
Stuart Benjamin
Jacob van de Lindt
Jamal Johnson
Matthew Pharr
Priyansh Lunia



Mentors: Carlos Paz-Soldan, Sam Frank, Noah Mandell, Chris Hansen



22.63 Fusion Engineering

APPH 9143



COLUMBIA | ENGINEERING
The Fu Foundation School of Engineering and Applied Science

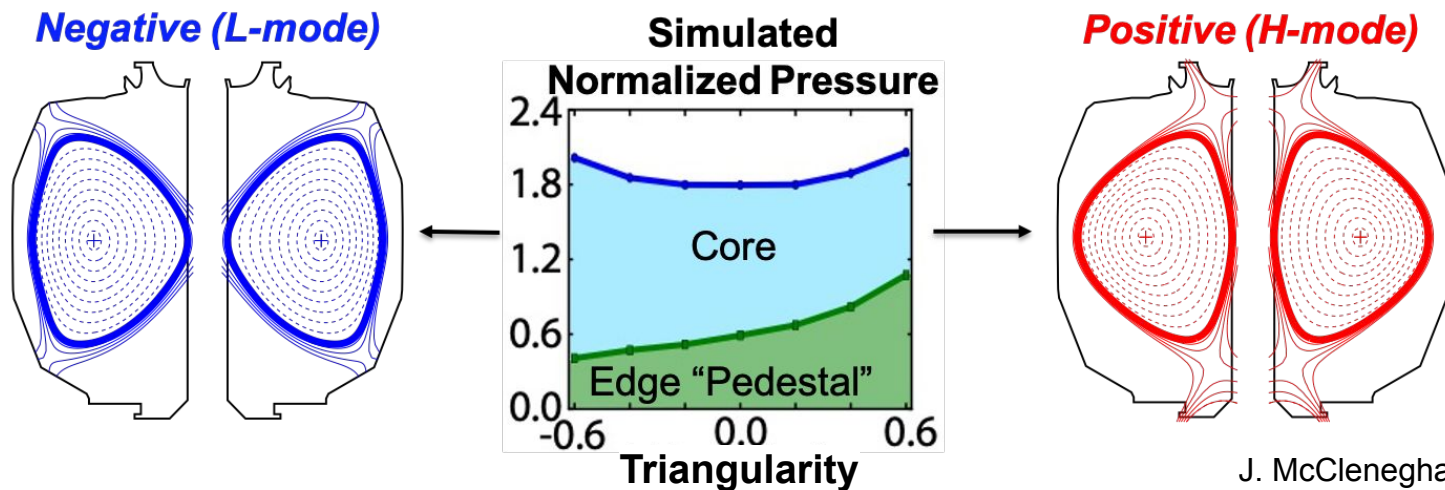
Negative triangularity (NT) enables reactor-relevant core performance

Hypothesis: Improved confinement L-mode provides edge integration solution

Edge localized modes → Removed by being in L-mode

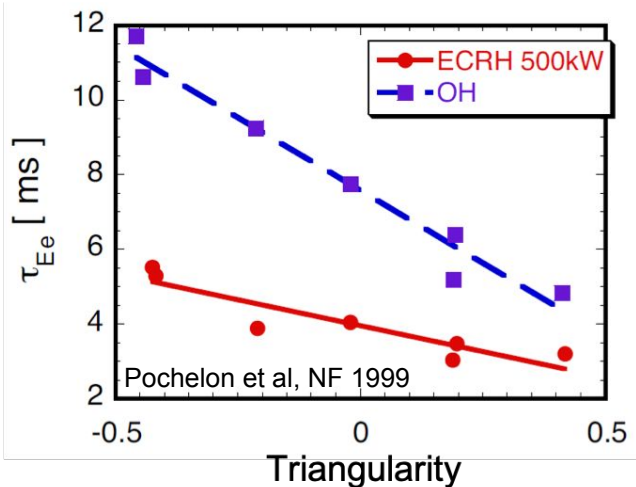
Divertor heat fluxes → Reduced via high radiation & large strike radius

Confinement → Better than usual L-mode due to plasma shape effects

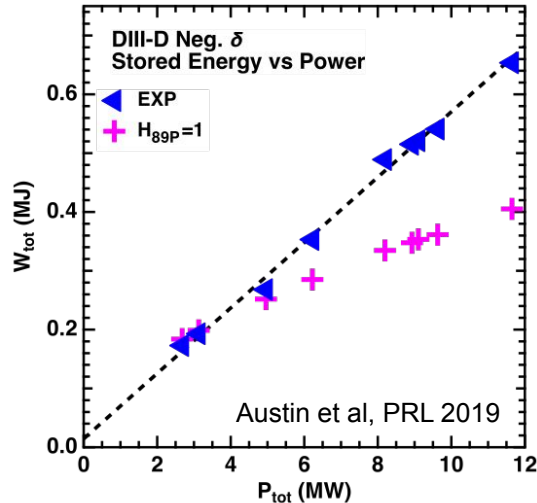


Existing tokamak data supports improved negative triangularity L-mode confinement

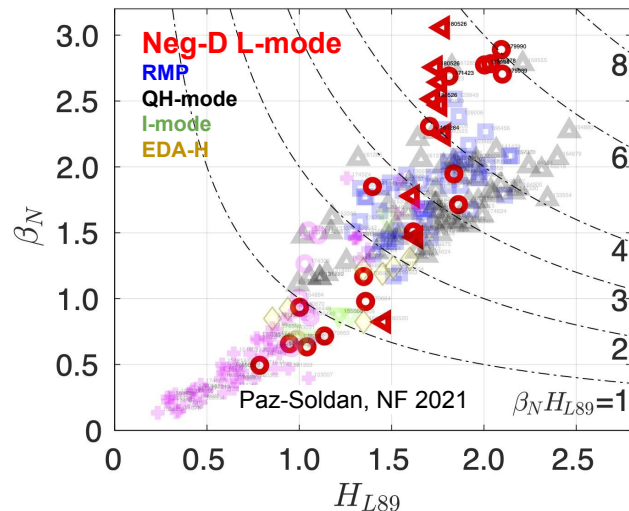
Improved energy confinement



Weaker power degradation



High normalized performance



**Existing TCV and DIII-D data is promising
→ more data from DIII-D campaign (Jan 2023)**

Radiative L-mode at negative triangularity allows adjustable fusion power with constant P_{SOL} to the divertor

Inductive pulsed L-mode:

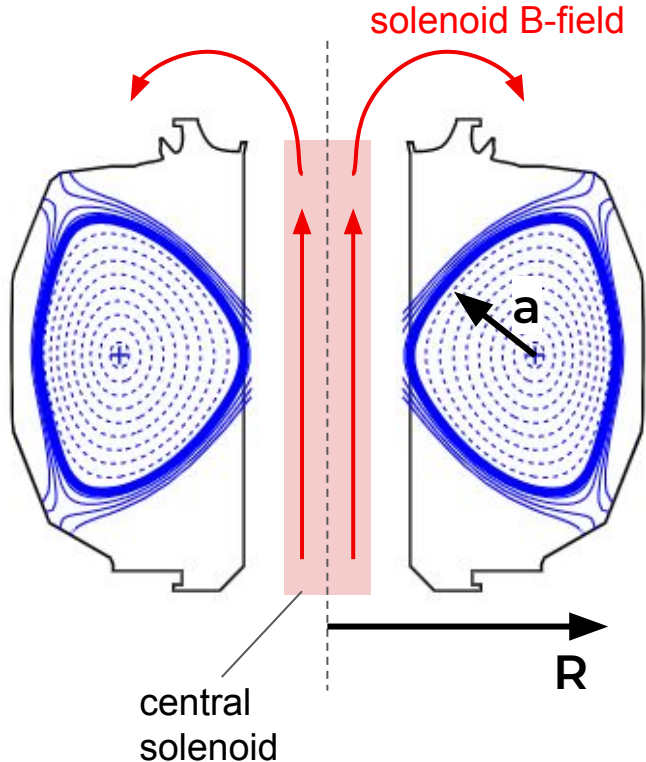
High B and high radiative fractions allows high gain outside of steady state

- No need for RF current drive + no H-mode pedestal allows **variable density**
- Variable density allows **variable fusion power output**
- Variable radiative fraction allows **constant P_{SOL}** as power is varied
- Low P_{SOL} consistent with no H-mode

Negative triangularity shaping:

- Ensures H-mode will not be accidentally accessed
- Improves L-mode confinement to lower current

Inductive design motivates large aspect ratio (R/a)



Inductive pulsed L-mode

Increasing major radius R :

- larger solenoid radius
- larger flux swing
- longer pulses

Keeping minor radius (a) small:

- plasma volume is the biggest cost scaling parameter

MANTA's core scenario differs from ARC due to flexible heat-exhaust solutions in negative triangularity radiative L-mode

| <u>Parameter</u> | <u>ARC</u> | <u>MANTA</u> |
|------------------|------------|--------------|
|------------------|------------|--------------|

| | | |
|-----------------------|-----|---------|
| P_{fus} [MW] | 525 | 250-500 |
|-----------------------|-----|---------|

| | | |
|-----------------------|------|----|
| P_{aux} [MW] | 38.6 | 10 |
|-----------------------|------|----|

| | | |
|-----------------------|----|----|
| P_{sol} [MW] | 93 | 25 |
|-----------------------|----|----|

| | | |
|---|------|---------|
| $f_{\text{rad}} = P_{\text{rad}}/P_{\text{heat}}$ | 0.35 | 0.6-0.8 |
|---|------|---------|

| | | |
|------------|-----|----|
| I_p [MA] | 7.8 | 10 |
|------------|-----|----|

| | | |
|--------------|-----|-------|
| B_{T0} [T] | 9.2 | 11.08 |
|--------------|-----|-------|

| | | |
|---------|-----|------|
| R [m] | 3.3 | 4.55 |
|---------|-----|------|

| | | |
|---------|------|-----|
| a [m] | 1.13 | 1.2 |
|---------|------|-----|

| | | |
|--------------|-----|-----|
| aspect ratio | 2.9 | 3.8 |
|--------------|-----|-----|

| | | |
|-----------------------|-----|-----|
| V [m ³] | 141 | 181 |
|-----------------------|-----|-----|

| | | |
|----------|------|-----|
| κ | 1.84 | 1.4 |
|----------|------|-----|

| | | |
|----------|-----|------|
| H_{89} | 2.8 | 1.75 |
|----------|-----|------|

| | | |
|-----------|------|------|
| β_N | 2.59 | 1.48 |
|-----------|------|------|

Variable power output is now possible

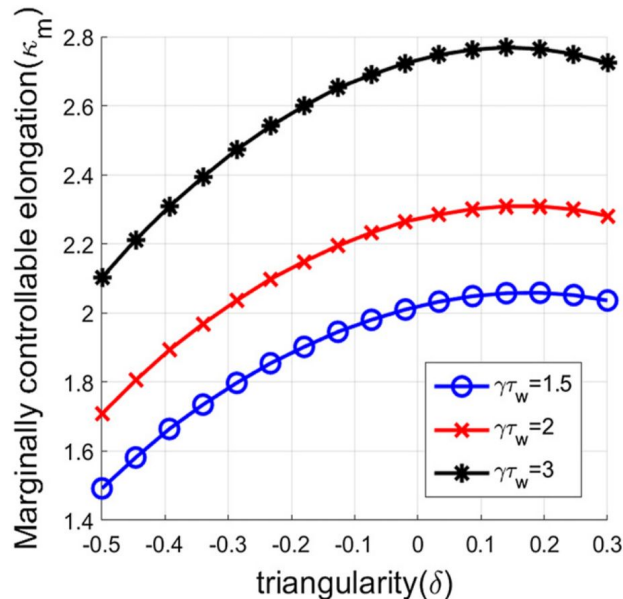
MANTA has a higher radiative fraction, lower P_{sol} relative to ARC

MANTA is optimised at a higher aspect ratio than ARC

MANTA has lower confinement consistent with L-mode

Elongation (κ) chosen to be consistent with vertical stability at negative triangularity, reducing VDE disruption risk

| Parameter | ARC | MANTA |
|---|------|---------|
| P_{fus} [MW] | 525 | 250-500 |
| P_{aux} [MW] | 38.6 | 10 |
| P_{SOL} [MW] | 93 | 25 |
| $f_{\text{rad}} = P_{\text{rad}}/P_{\text{heat}}$ | 0.35 | 0.6-0.8 |
| I_p [MA] | 7.8 | 10 |
| B_{T0} [T] | 9.2 | 11.08 |
| R [m] | 3.3 | 4.55 |
| a [m] | 1.13 | 1.2 |
| aspect ratio | 2.9 | 3.8 |
| V [m ³] | 141 | 181 |
| κ | 1.84 | 1.4 |
| H_{89} | 2.8 | 1.75 |
| β_N | 2.59 | 1.48 |



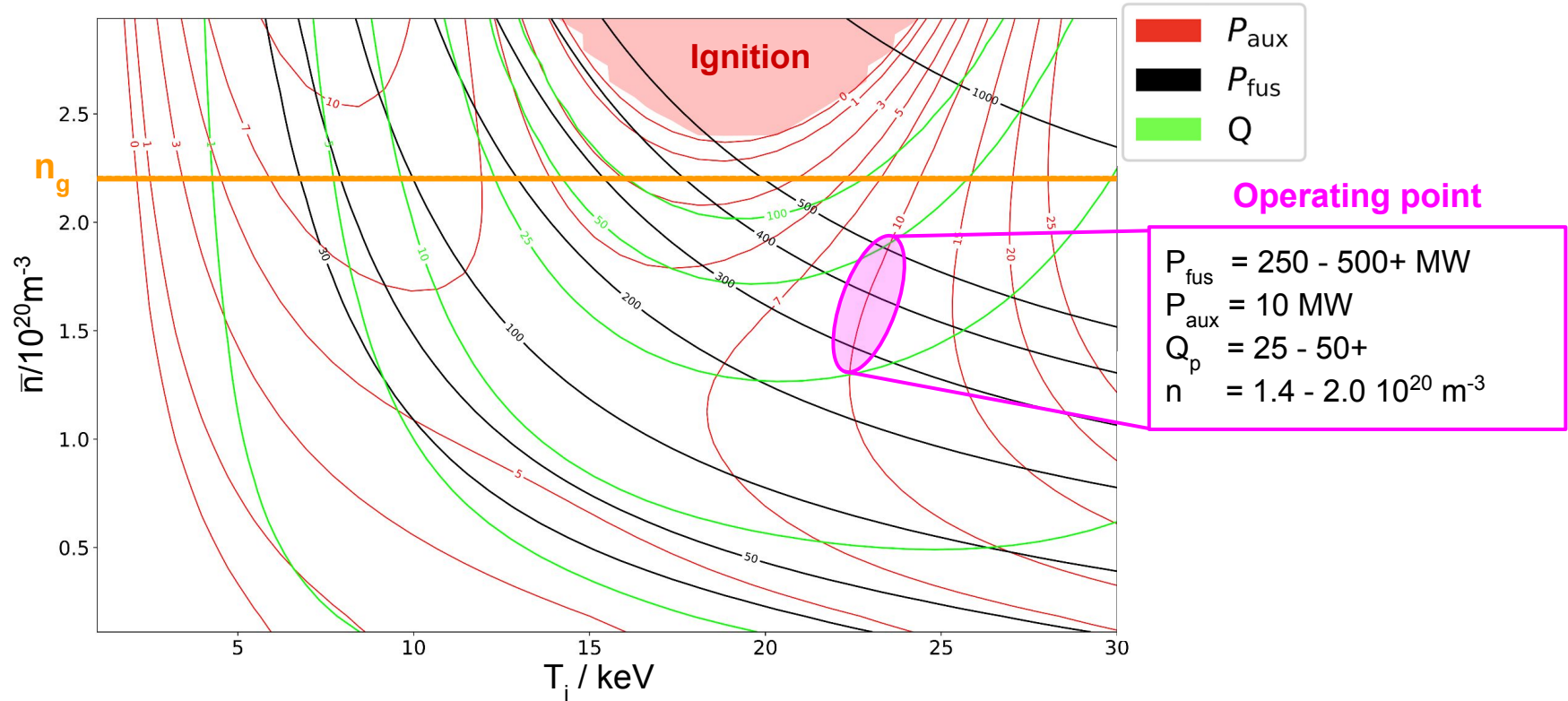
J. Song et al. 2021 Nucl. Fusion 61 096033

- Larger elongation preferable for core performance
- Vertical stability decreases with negative triangularity, limiting maximum allowable elongation
- Active control limited in pilot plant: $\gamma\tau_w \sim 1.5$

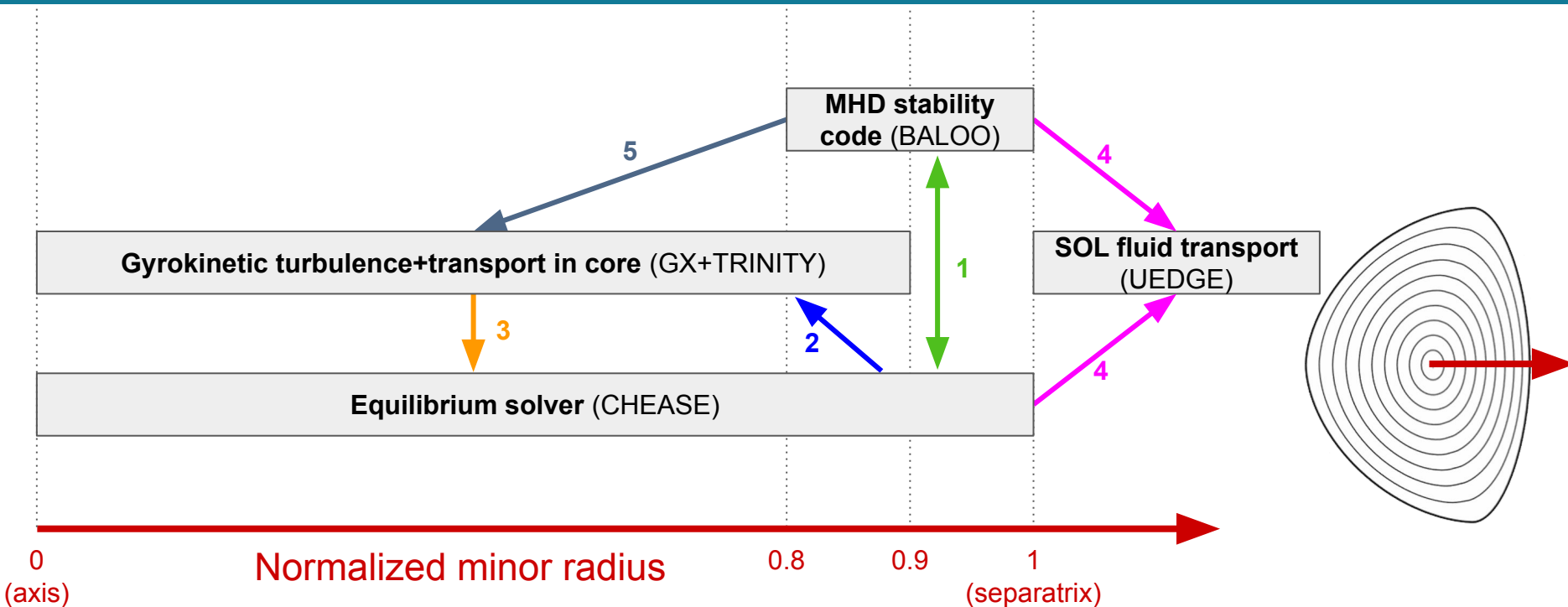
Solution:

- $\kappa = 1.4$ chosen after MANTA geometry modelled by Song

POPCON reveals wide operating regime meeting NASEM report, with assumption of enhanced confinement, keeping constant $P_{\text{SOL}}=25\text{MW}$



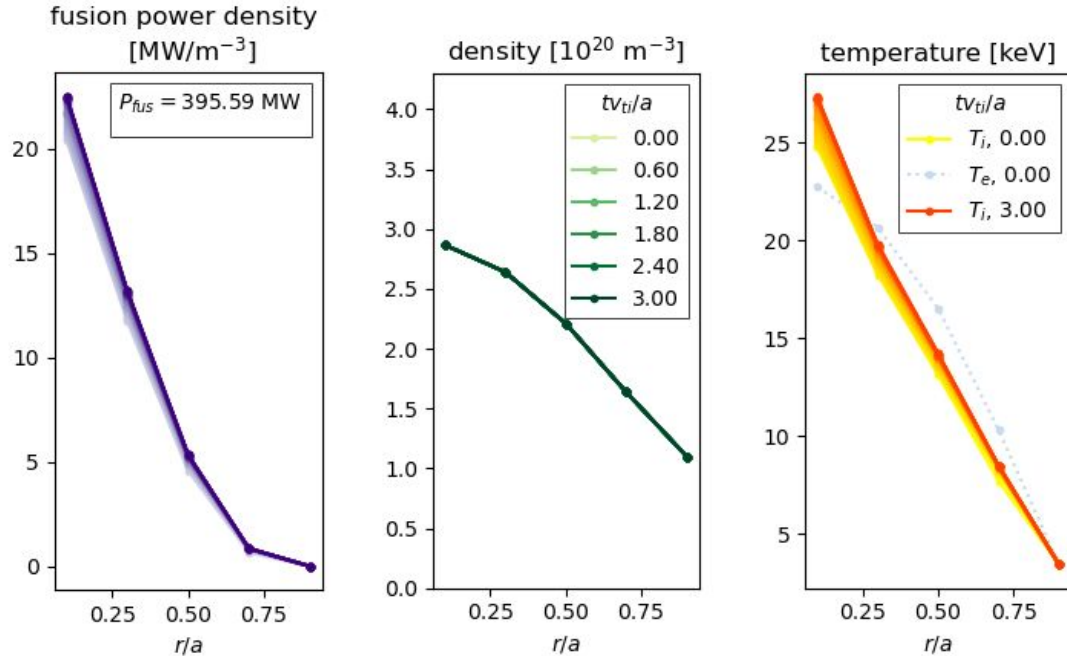
Self-consistent core and divertor design generated by iterating profiles (T,n,P) between simulation codes



GX: N. Mandell et al, 2022, arXiv:2209.06731; N. Mandell et al, 2018, JPP 84, 905840108
Trinity: M. Barnes et al, 2010, PoP 17, 056109

BALOO: R. L. Miller et al, 2015, Phys. Plasmas, 4 1062
UEDGE: T. D. Rognlien et al, 1992, J. Nucl. Mater., 196–198 347–351
CHEASE: H. Lütjens et al, 1996, Comput. Phys. Commun. 97 219–60

Initial gyrokinetic ion turbulence simulations show 400+ MW fusion power is attainable in negative triangularity



Gyrokinetic ion turbulence results:

$$\begin{aligned} P_{fus} &= 395 \text{ MW} \\ T_{avg,0} &= 25 \text{ keV} \\ n_{line} &= 2.1 \times 10^{20} \text{ m}^{-3} \text{ (} 0.95 n_g \text{)} \\ H_{89} &= 1.96 \end{aligned}$$

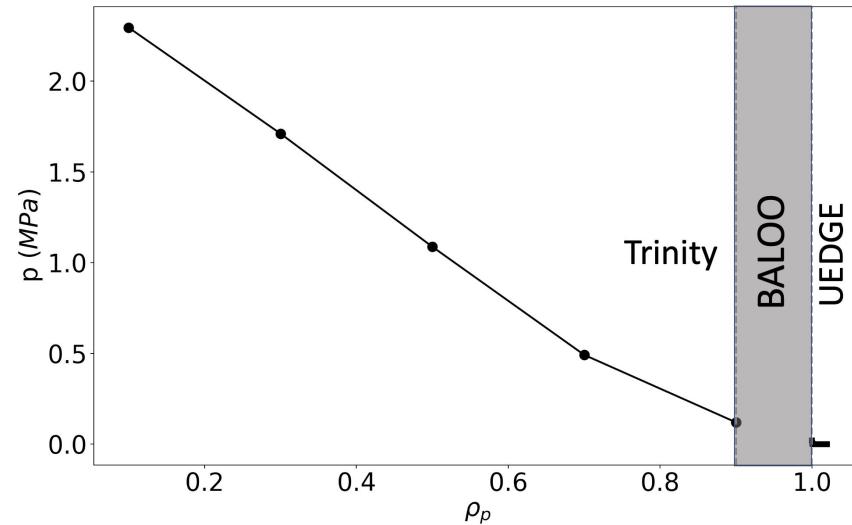
Assumptions:

- Static density profiles*
- Static electron temperature profile, adiabatic electrons

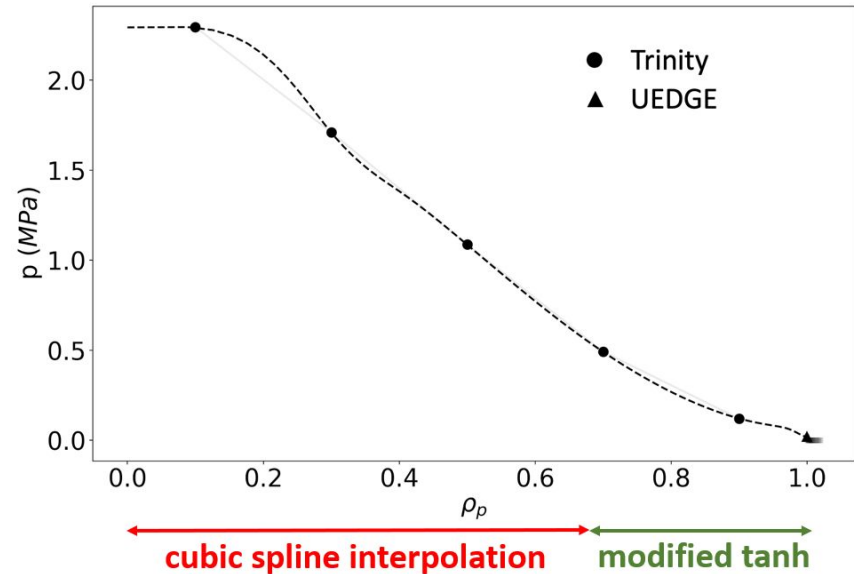
Fully kinetic, multi-species simulations in progress!

Smooth pressure profile is interpolated from Trinity and UEDGE pressure outputs

Discrete pressure profile from
TRINITY + BALOO + UEDGE

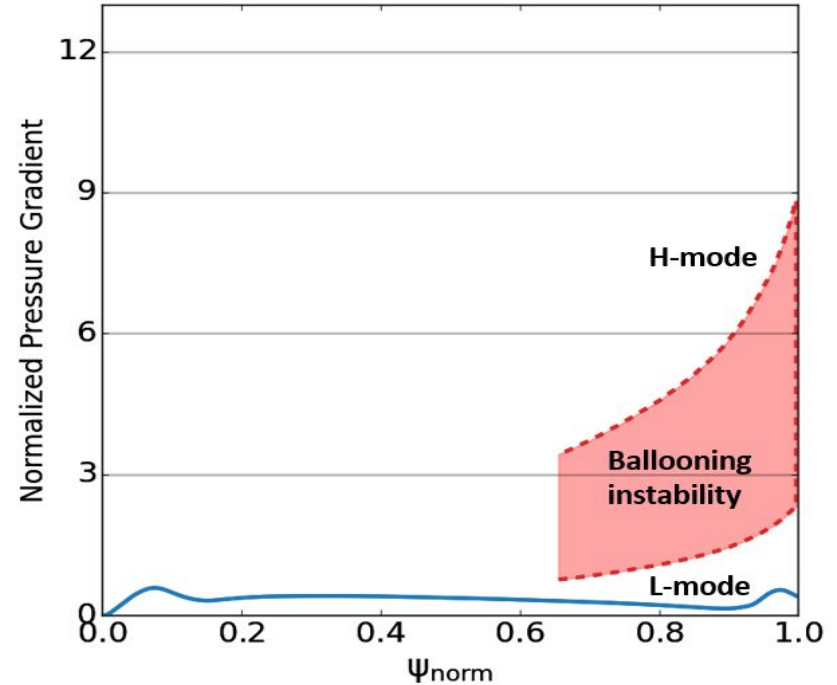


Interpolated pressure profile



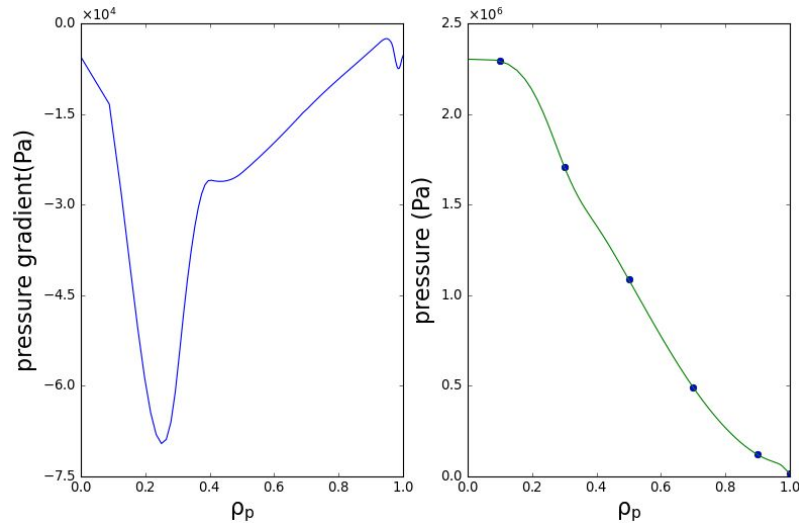
Ballooning stability code confirms H-mode is inaccessible in this negative triangularity plasma

- Edge pressure gradients are below the lower boundary of the ballooning unstable region.
- H-mode is completely inhibited with no access paths open.

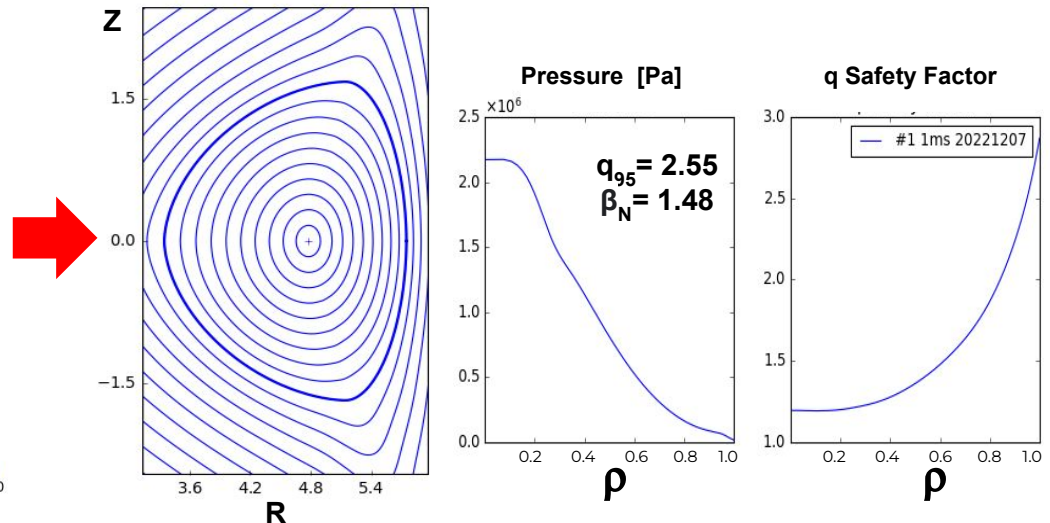


Equilibrium is generated by iterating the pressure profile

Smooth pressure profile is interpolated from Trinity and UEDGE pressure outputs



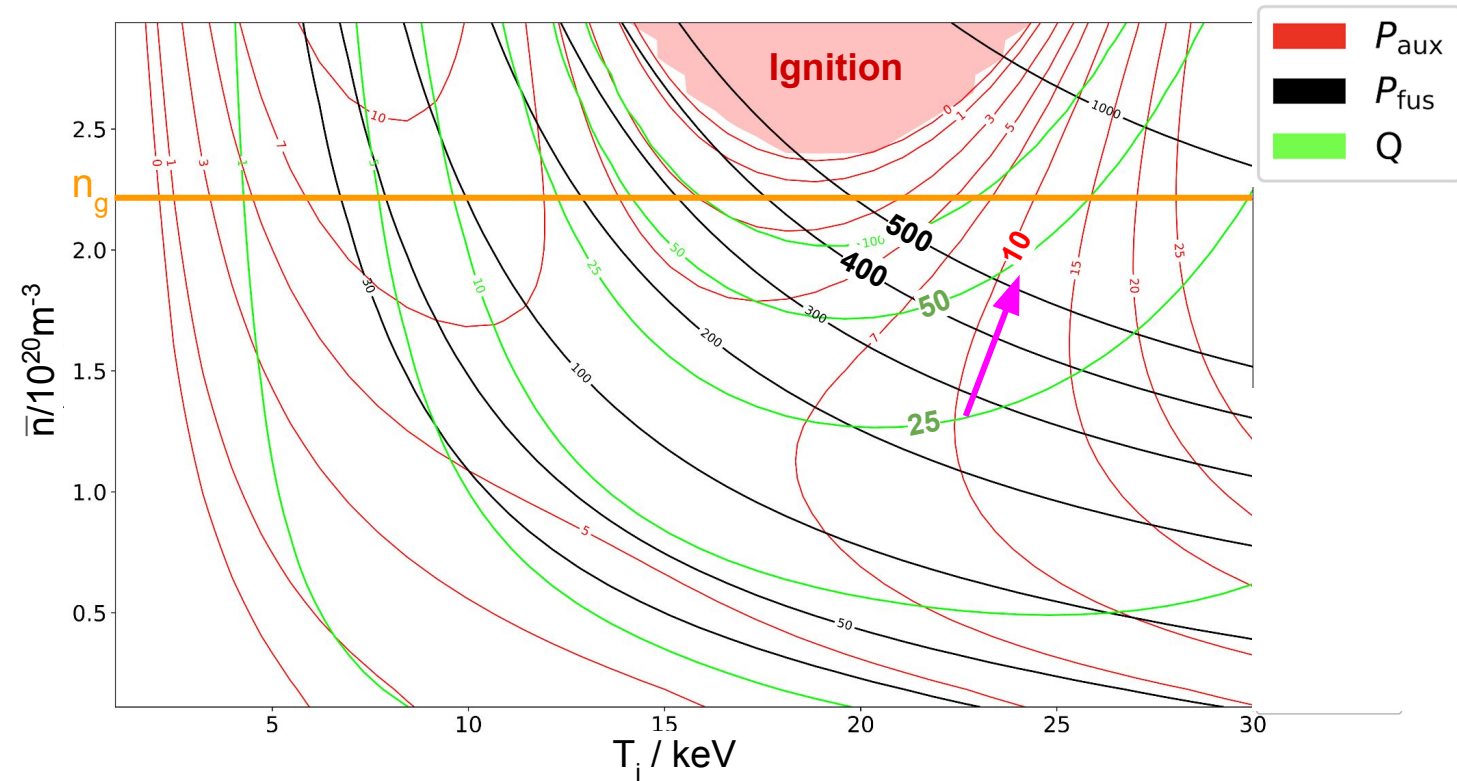
Transport and BALOO-informed equilibrium generated with CHEASE



New equilibrium is passed to UEDGE, TRINITY, iteration continues

Simulation operating range trends are consistent with POPCON

⇒ density-adjustable P_{fus} and Q , constant P_{sol} and P_{aux}



Transport results
from a density scan*

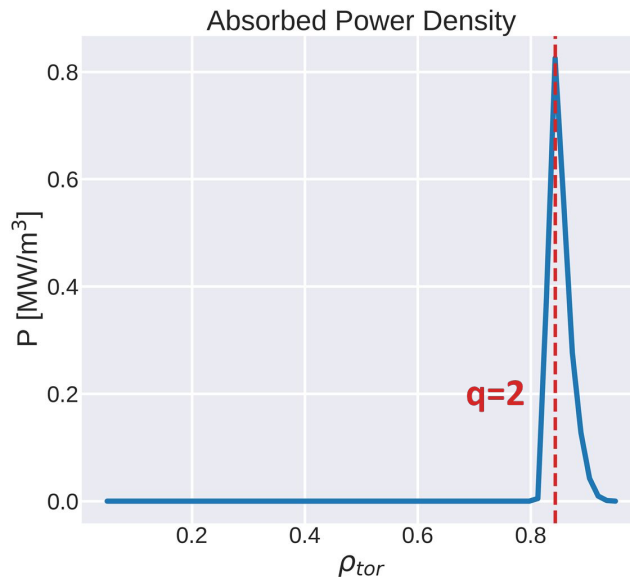
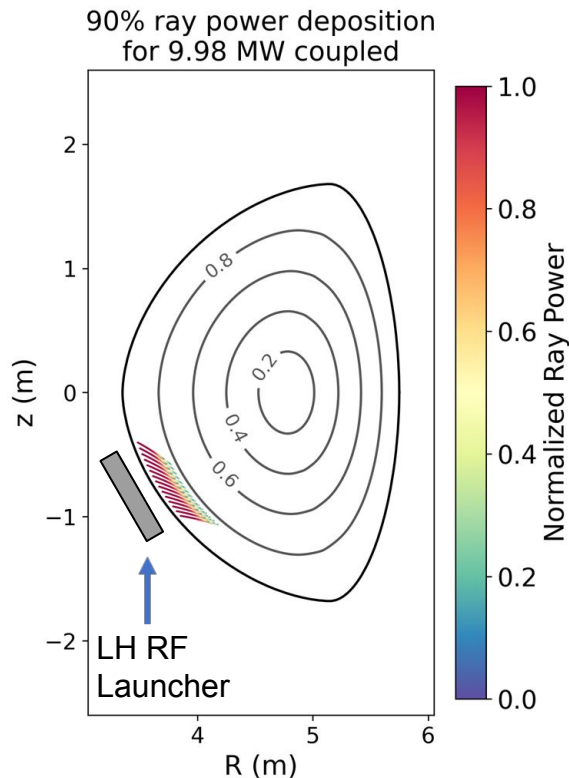
$$P_{\text{fus}} = 505.56 \text{ MW}$$
$$\bar{n} = 2.25 \times 10^{20} \text{ m}^{-3}$$

$$P_{\text{fus}} = 383.75 \text{ MW}$$
$$\bar{n} = 2.15 \times 10^{20} \text{ m}^{-3}$$

$$P_{\text{fus}} = 286.96 \text{ MW}$$
$$\bar{n} = 2.0 \times 10^{20} \text{ m}^{-3}$$

*profile shapes differ from nominal
POPCON's (not fully iterated)

Raytracing simulations show lower hybrid provides highly localised current drive optimised for neoclassical tearing mode suppression



- Peak power density on q=2 verified for test launcher angle 30° below the HFS midplane
- Launcher position avoids the highest intensity fast neutrons at the midplane while still achieving a peak of 0.83 MW/m³ at $\rho_{tor}=0.84$

Raytracing Simulation Tools

GENRAY:

A. Smirnov et al., *Bull. Amer. Phys. Soc.*, 39(7), 1994.

CQL3D:

R. Harvey & M. McCoy, *Proc. IAEA TCM on Advances in Simulation and Modeling of Thermonuclear Plasmas*, Montreal, 1992.

Tearing mode suppression

A. Reiman & N. Fisch, *Phys. Rev. Lett.*, 121(22), 2018.

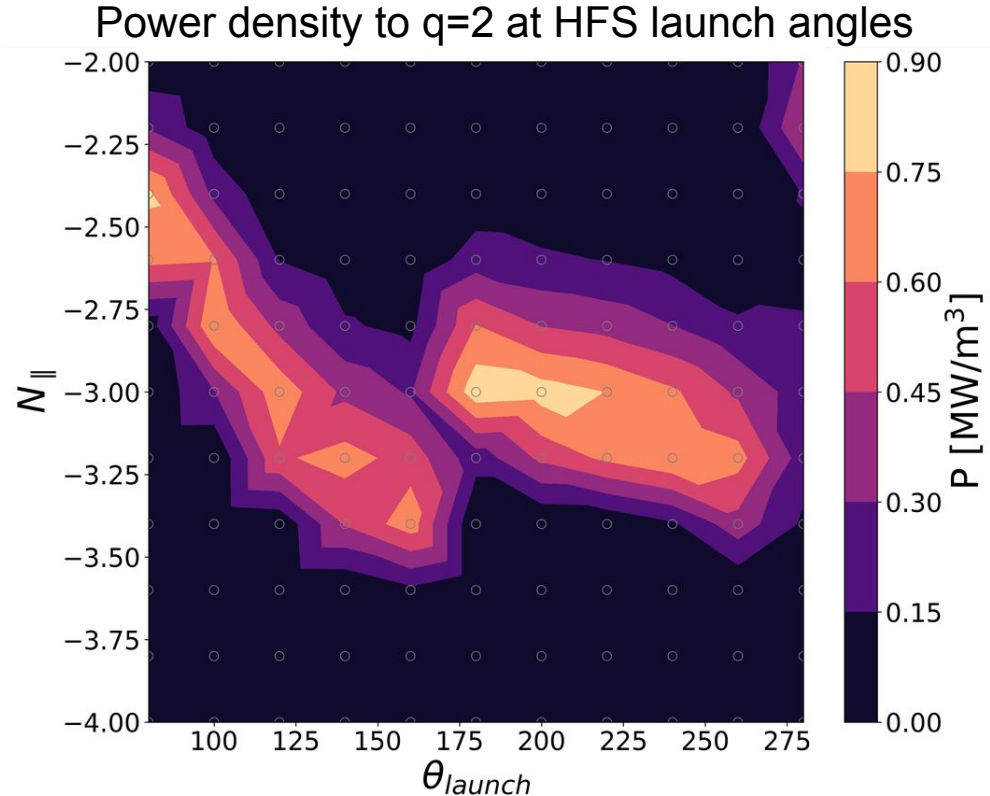
S. Frank et al., *Nuclear Fusion*, 60(9), 2020.

S. Jin et al., *Physics of Plasmas* 28(5), 2021.

S. Frank et al., *Nuclear Fusion*, 62(12), 2022.

Lower hybrid launcher located for optimizing NTM suppression at $q=2$ surface

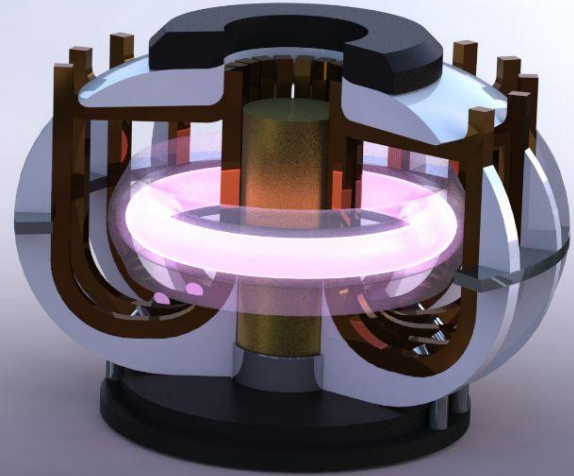
- Launcher tuned for power delivered to $q=2$ at $\rho_{\text{tor}}=0.84$ (equal to $r/a=0.88$ for present equilibria)
- Poloidal LH launch angles 175° to 224° with $N_{\parallel}=-3$ identified for high power deposition



Magnet Systems Pt. 1: TFs, PFs, and CS

Alexis Devitre
Allen Wang
Andrew Maris
Haley Wilson
Michael Liu

Mentor: Theodore Mouratidis



22.63 Fusion Engineering

APPH 9143

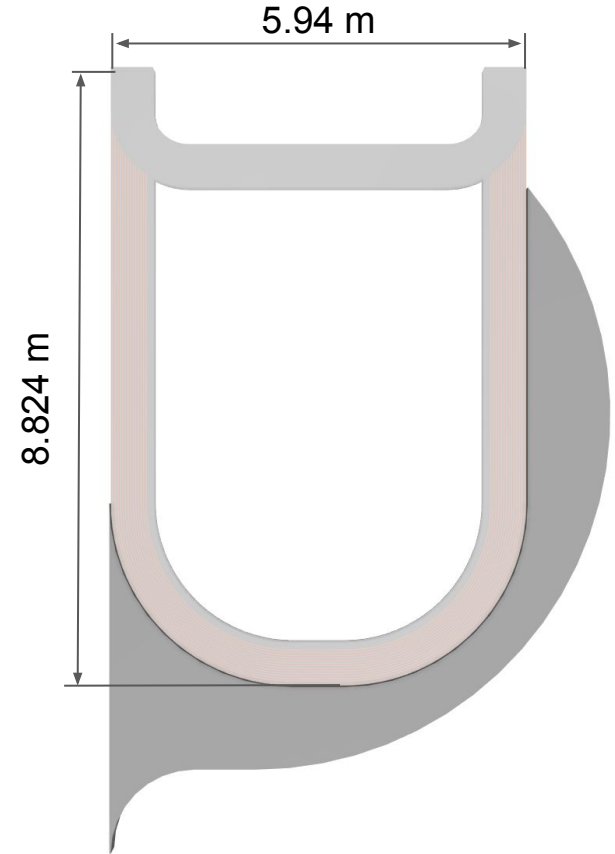


COLUMBIA ENGINEERING
The Fu Foundation School of Engineering and Applied Science

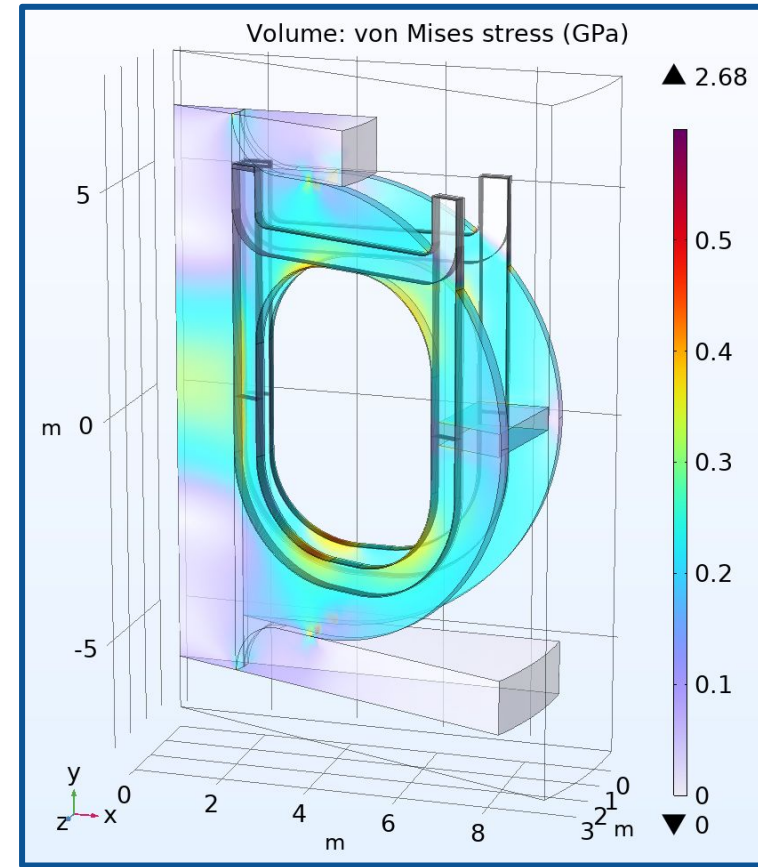
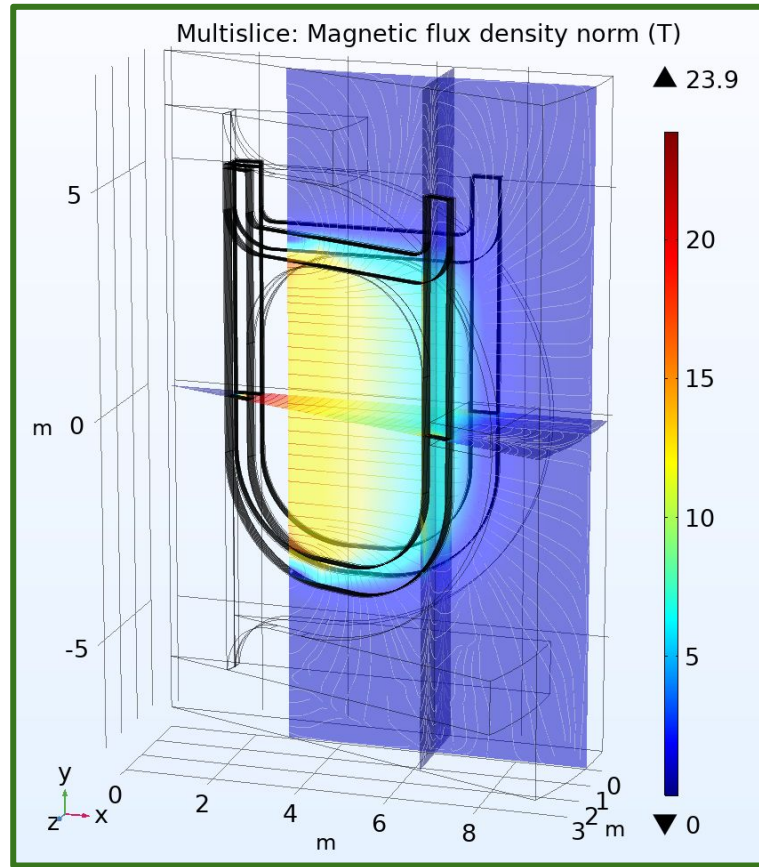
Toroidal field coils achieve design goals

Design Goals

- Top-down maintenance with demountable joints
- 11 T field on axis with REBCO superconductors
- Non-insulated coil for improved quench resilience
- 0.6 GPa structural stress limit
- Operating current $\leq 60\%$ critical current

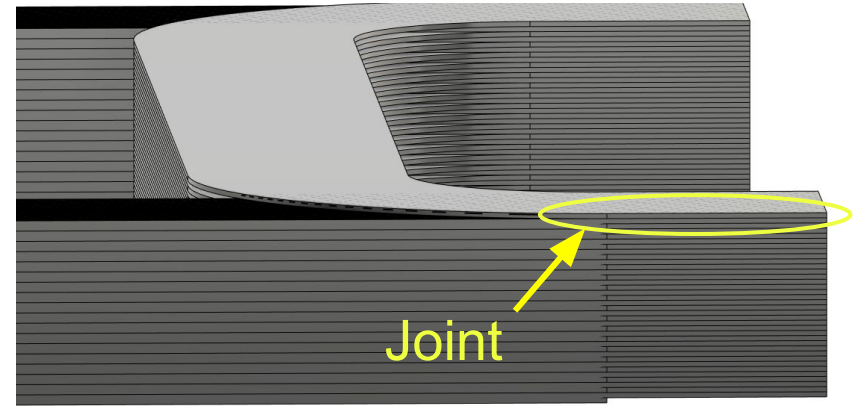
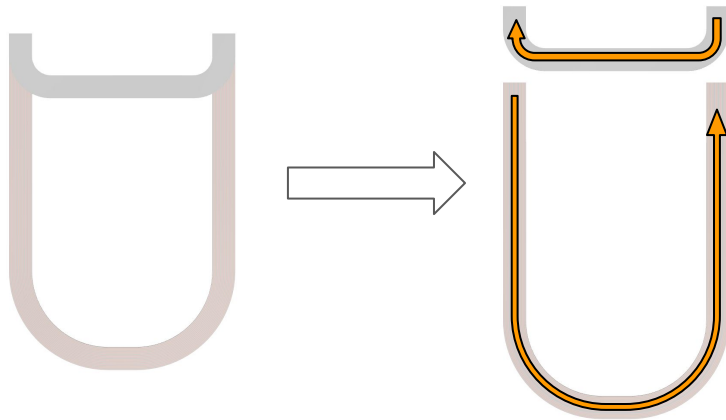


11 T field achieved on axis with tolerable stress



Pancake structure integrated with soldered joints

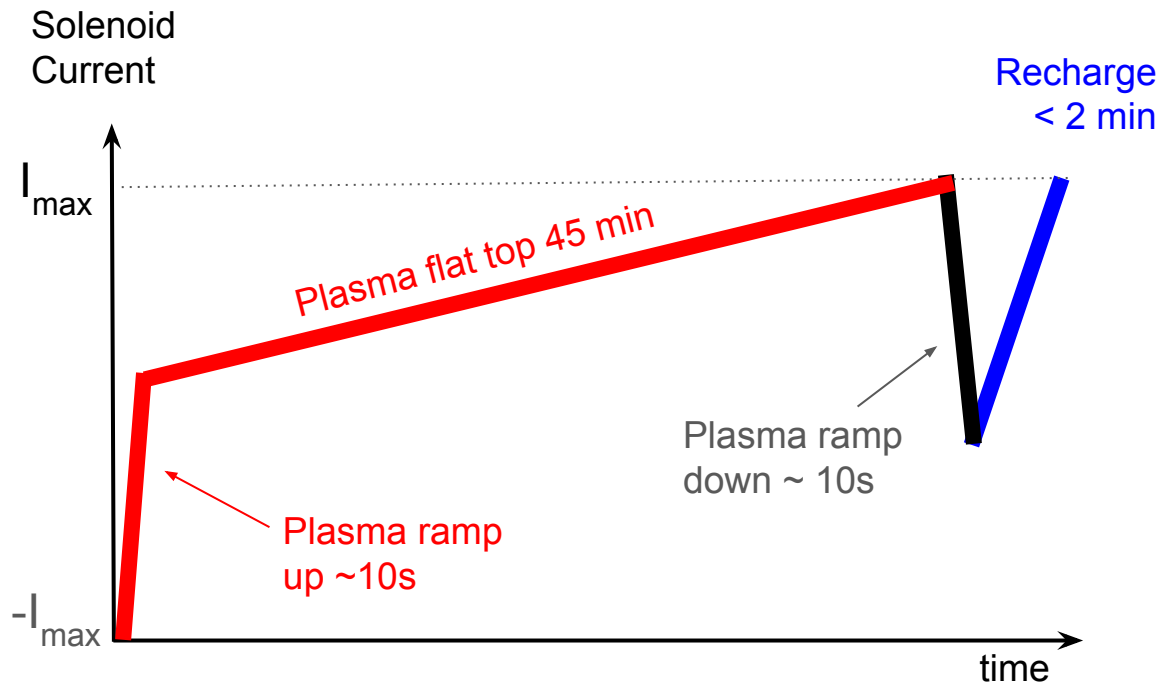
- Magnet consists of 18 “pancakes”
- Sections interleaved with low temperature solder (0.5 nΩ)
 - Demountable joints: Coils sections assembled with a recently developed low temperature solder vacuum pressure impregnation process [Mouratidis]



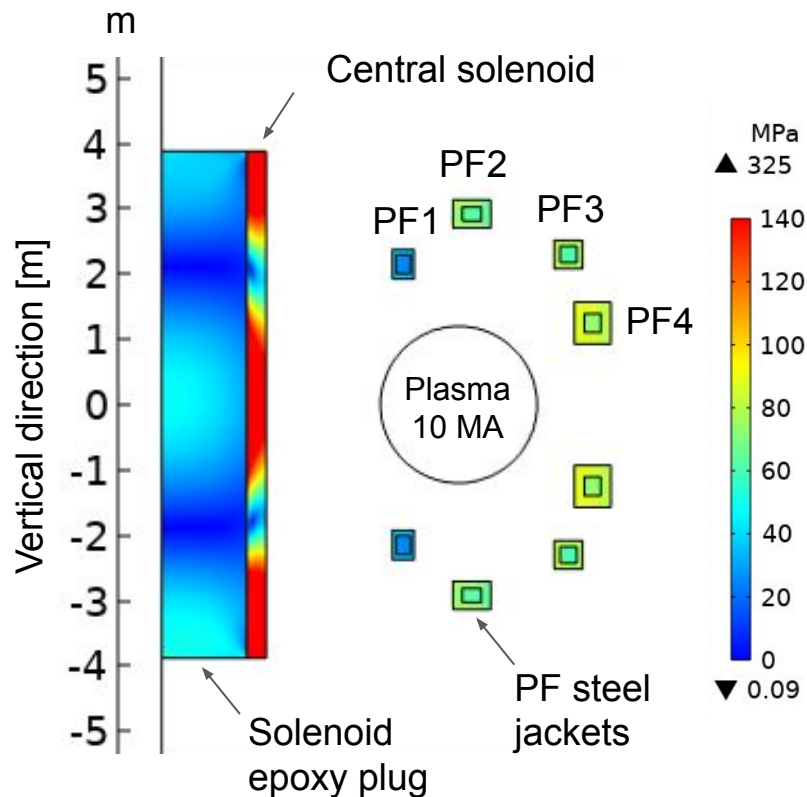
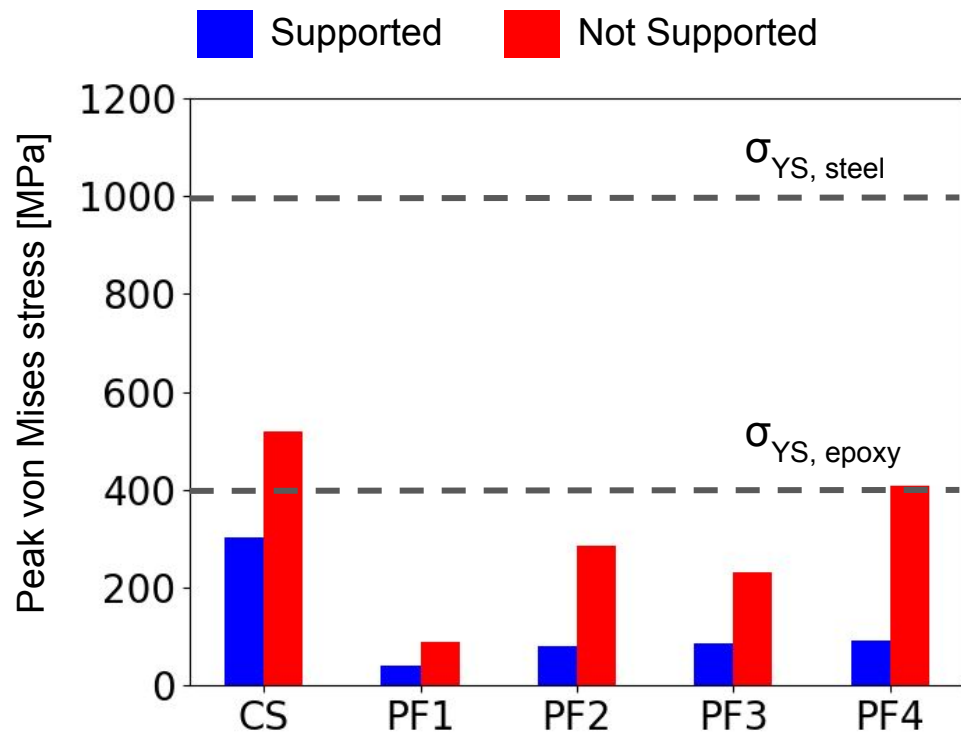
Solenoid achieves long pulses and short interpulses within the operational limits of HTS magnets

Solenoid specs

- 3.2 m bore
- 23 T peak field on HTS
- $J_e = 85 \text{ A/mm}^2$
- 305 V.s = Plasma ramp-up and 45 min flat-top
- 1 T/s charge rate = 2 min between pulses



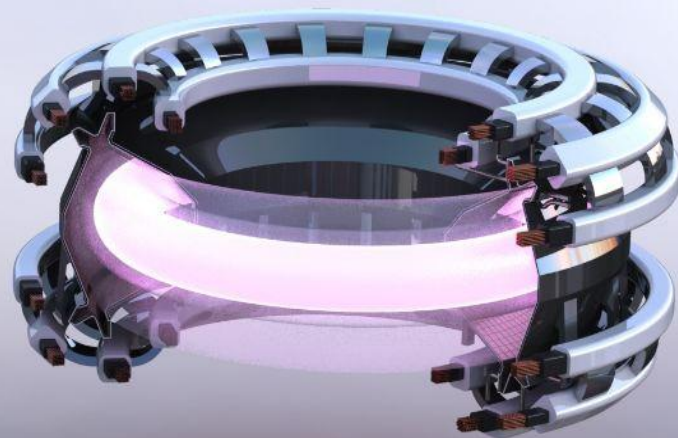
Stresses on the central solenoid and poloidal field coils are below the yield strength of structural materials



Power Handling

David Arnold
Hari Choudhury
Calvin Cummings
Andrés Miller
Grant Rutherford
Julia Witham

Mentors: Oak Nelson and Mike Wigram



22.63 Fusion Engineering

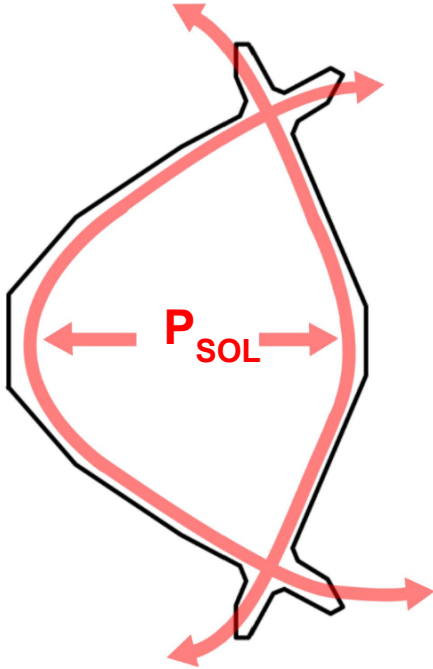
APPH 9143



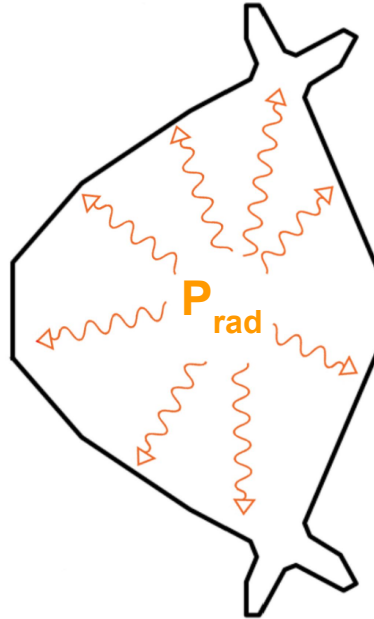
COLUMBIA | ENGINEERING
The Fu Foundation School of Engineering and Applied Science

Core plasma exhausts substantial power onto structural components

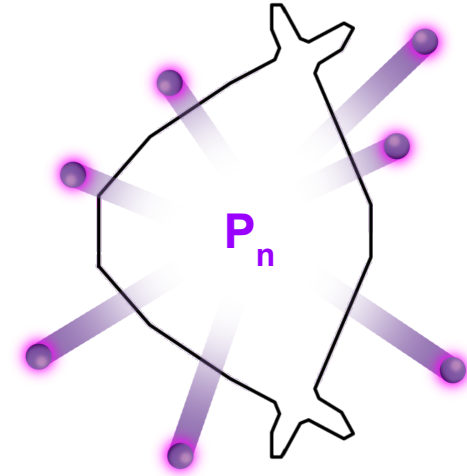
P_{SOL} : power conducted along field lines to the divertor target



P_{rad} : power radiated from the core due to seeded impurities

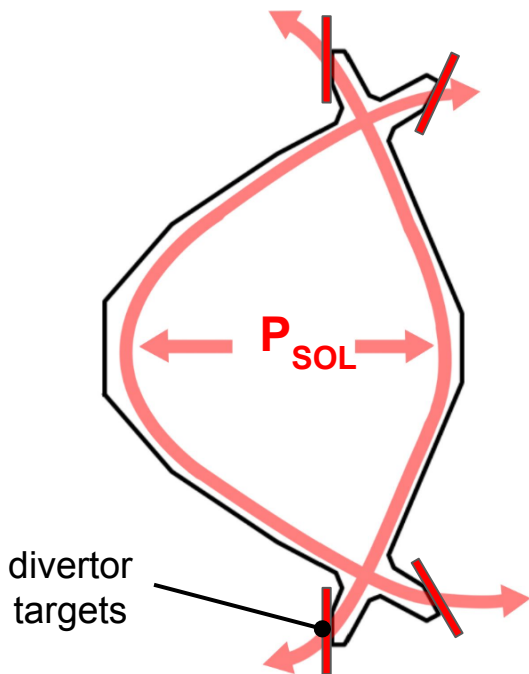


P_n : power from fusion neutrons

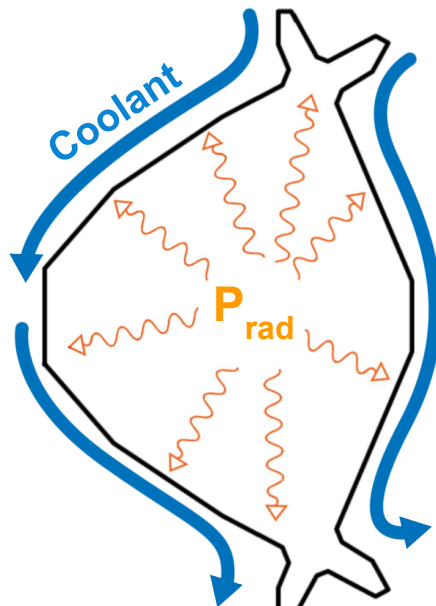


Exhausted power sets design constraints for machine wall, vessel cooling and poloidal field coils

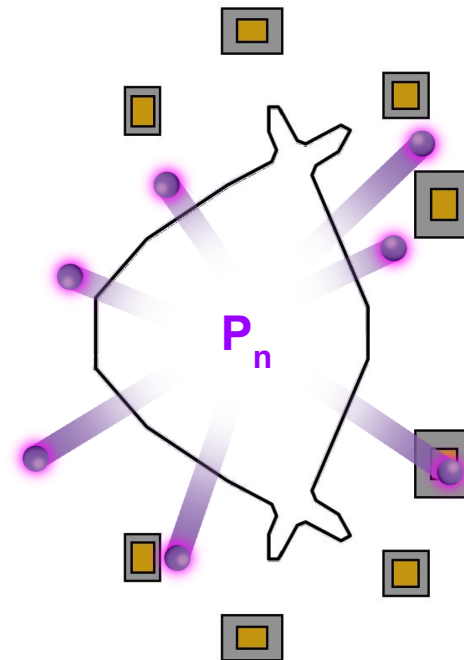
P_{SOL} sets divertor complexity and lifetime



P_{rad} forces active cooling of the vacuum vessel



P_n constrains poloidal field coil locations

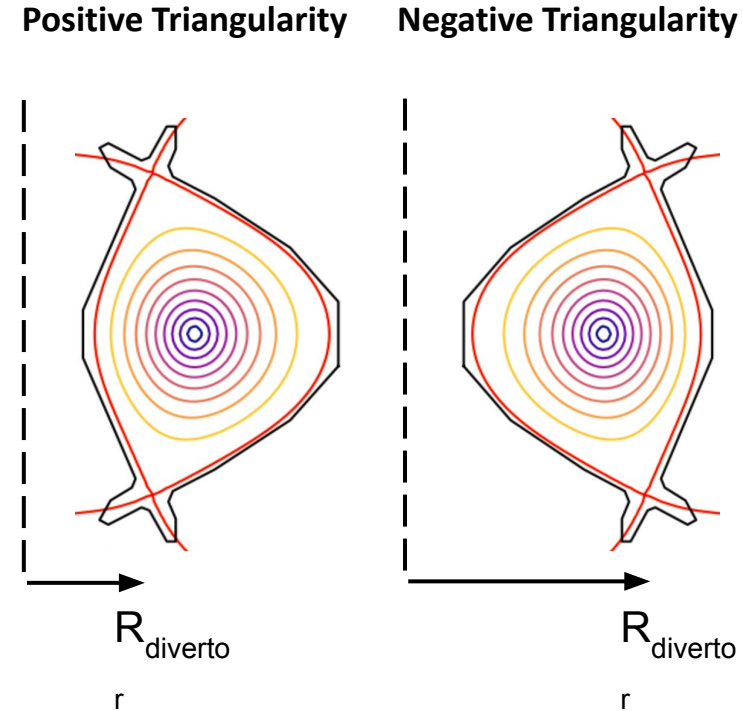


Negative triangularity and L-mode reduce divertor heat flux

- Negative triangularity increases divertor circumference and **spreads out heat flux**
- L-mode allows for increased radiated power and prevents formation of ELMs
→ **less power** to divertor plates
- Divertor challenge metrics are **significantly lower** in NT L-mode operation

| Divertor metric | ITER | MANTA |
|---|------|-------|
| $P_{\text{SOL}} B_T / R$ | 85.5 | 60.9 |
| $(P_{\text{SOL}} B_T / R) / n_{\text{sep}}^2$ | 534 | 60.9 |

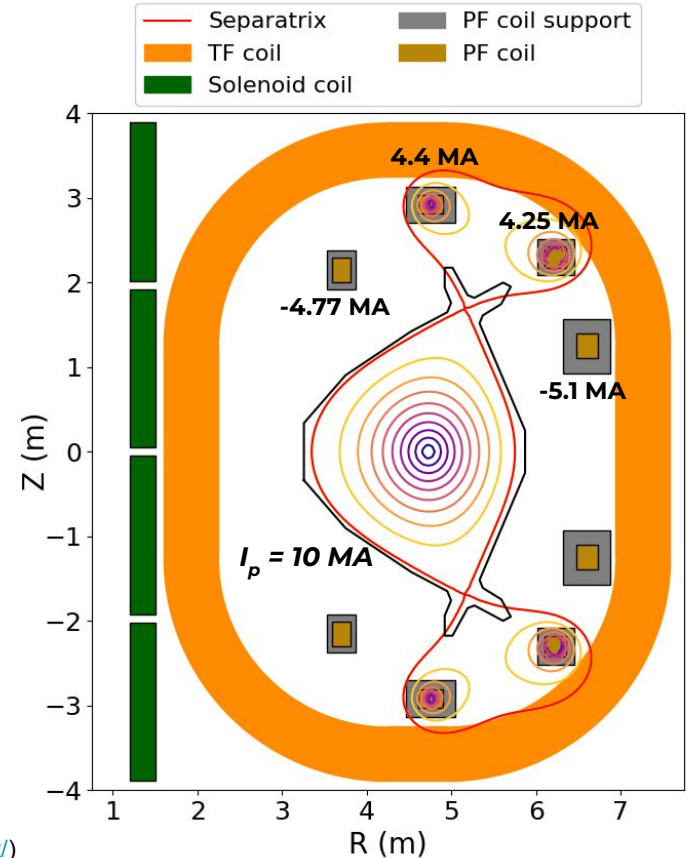
- **Goal:** Keep divertor and poloidal field (PF) coils as simple as possible



Poloidal field coils optimized for fewest coils and smallest currents

- Poloidal field coils placed inside TF
- PF coil locations and currents determined by FreeGS^[1]
- 4 sets of PF coils achieve desired plasma shape with acceptable coil currents
- Coil lifetimes validated by neutronics to be reasonable
- Resulting divertor features low technical complexity

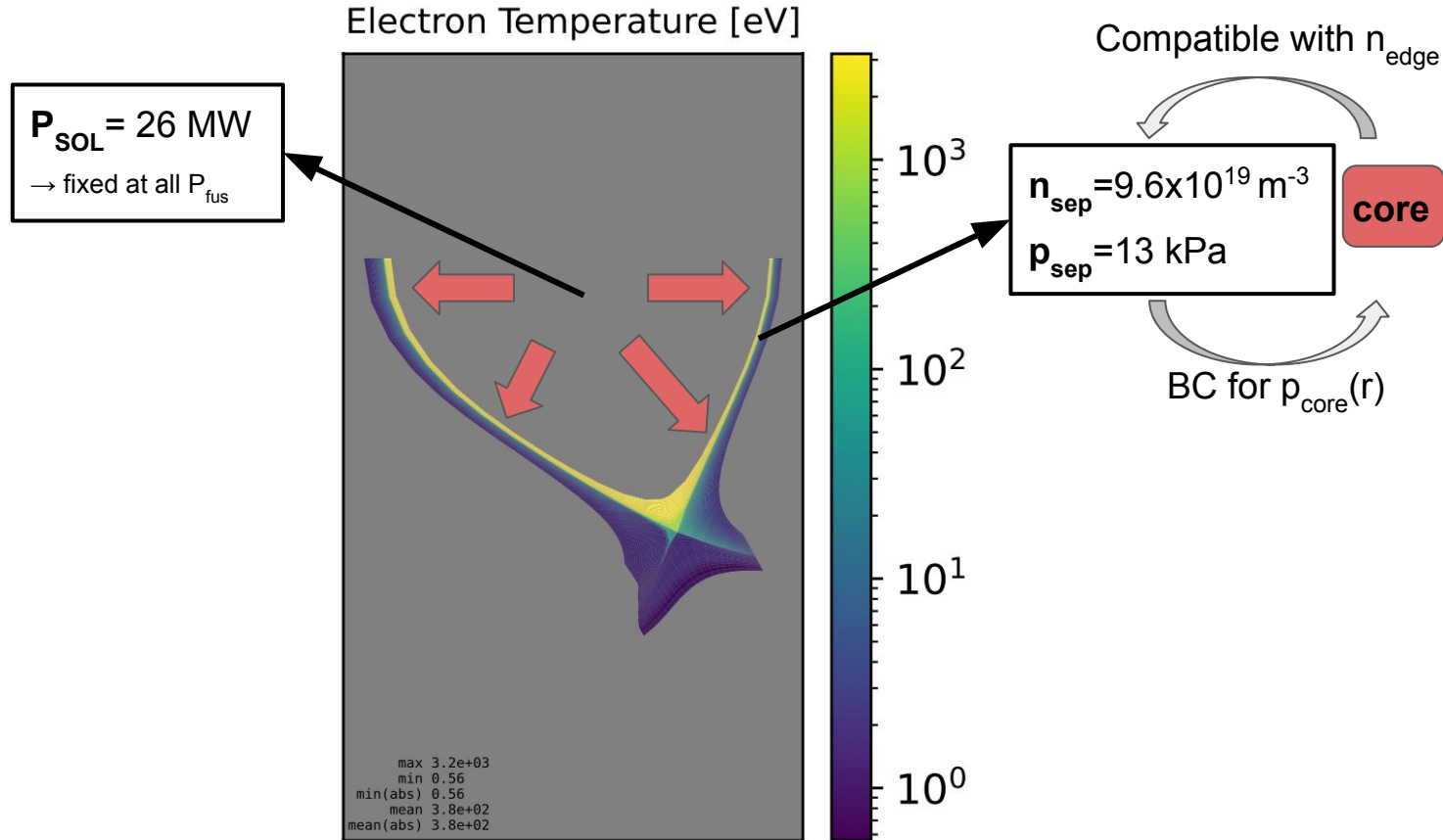
[1] Dudson B et al 2021
(<https://freegs.readthedocs.io/en/latest/>)



Self-consistent transport model determines optimal partially detached divertor geometry

UEDGE:
2D fluid
transport
code

⇒ plasma
+ neutral
SOL
modeling



Self-consistent transport model determines optimal partially detached divertor geometry

UEDGE:
2D fluid
transport
code

⇒ plasma
+ neutral
SOL
modeling

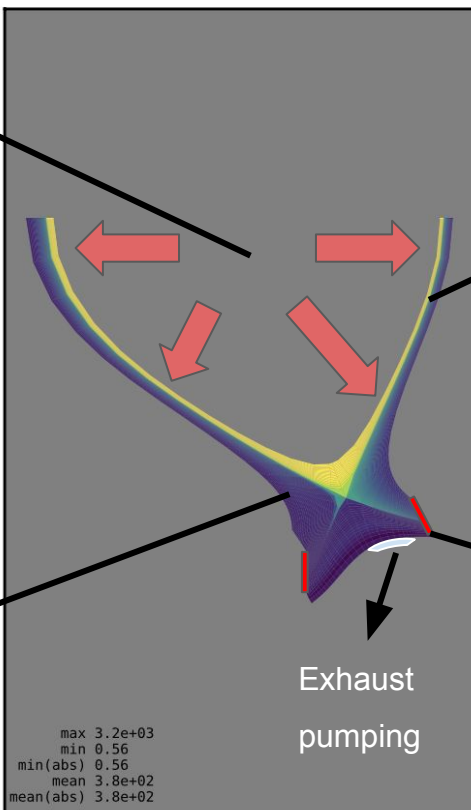
$$P_{\text{sol}} = 26 \text{ MW}$$

→ fixed at all P_{fus}

$$n_{\text{Ne}} = 1.1 \times 10^{-3} \cdot n_e$$

→ impurities exhaust heat
through radiation

Electron Temperature [eV]



10^3

10^2

10^1

10^0

Compatible with n_{edge}

$$n_{\text{sep}} = 9.6 \times 10^{19} \text{ m}^{-3}$$

$$p_{\text{sep}} = 13 \text{ kPa}$$

core

BC for $p_{\text{core}}(r)$

Need $q_{\text{surf}} < 10$

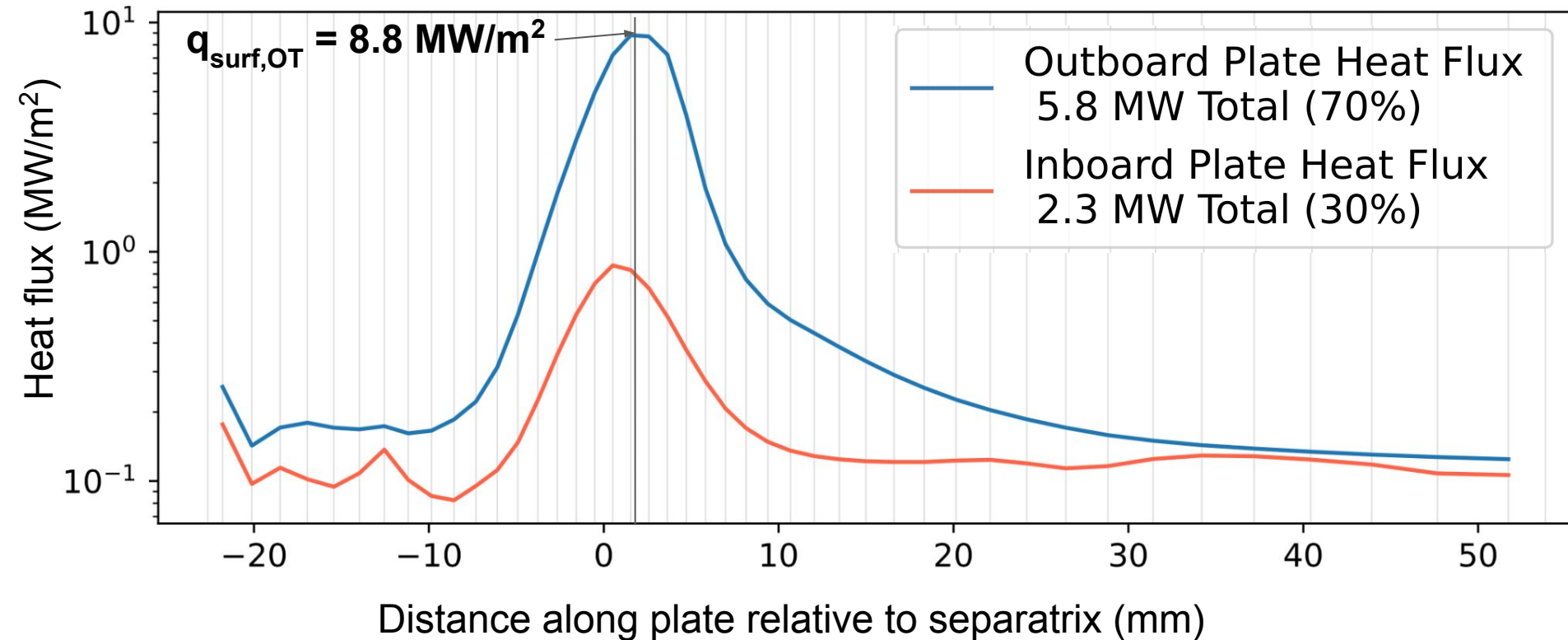
MW/m²

($T_{\text{surf}} < 5 \text{ eV}$)

→ limit on W plates

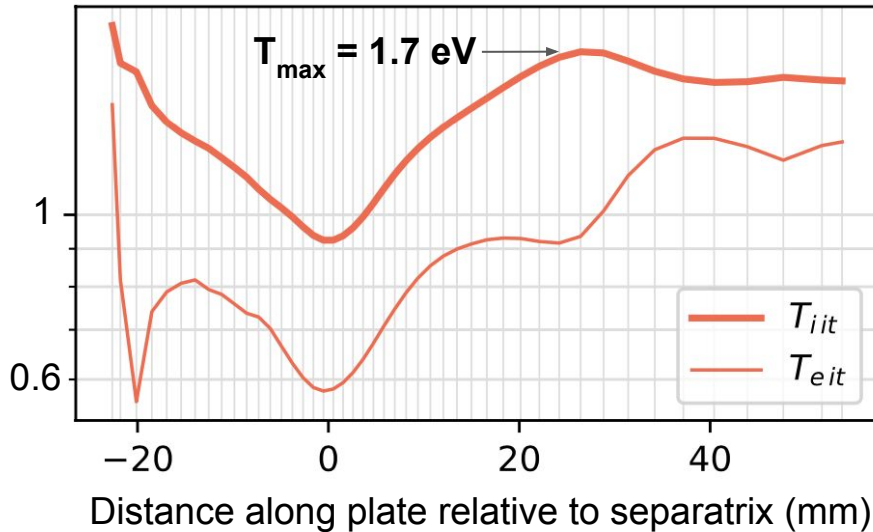
Exhaust
pumping

Partially detached plasma ensures divertor survival in full fusion-power operation

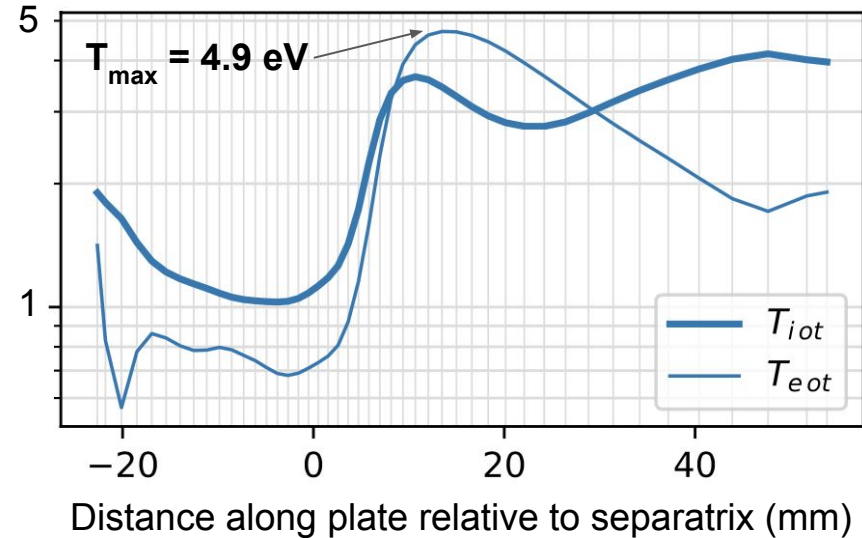


Divertor plates will survive full fusion-power operation under 5 eV without tungsten sputtering

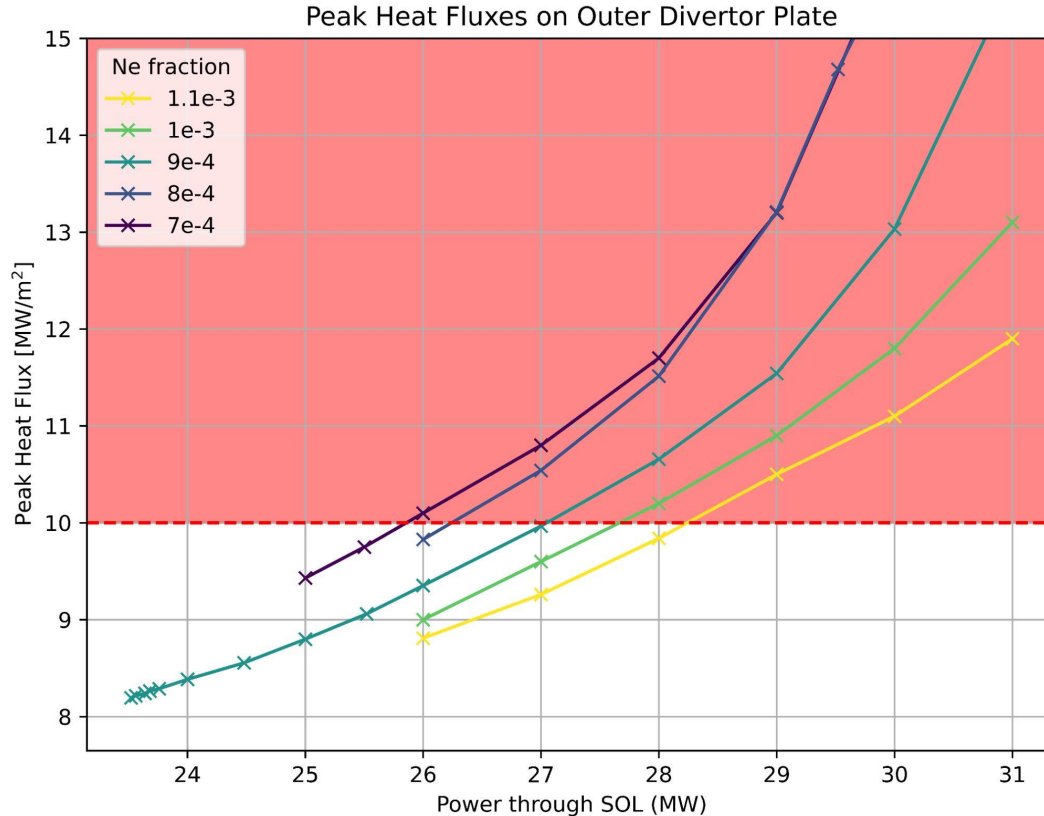
Temperature Across Inner Plate (eV)



Temperature Across Outer Plate (eV)

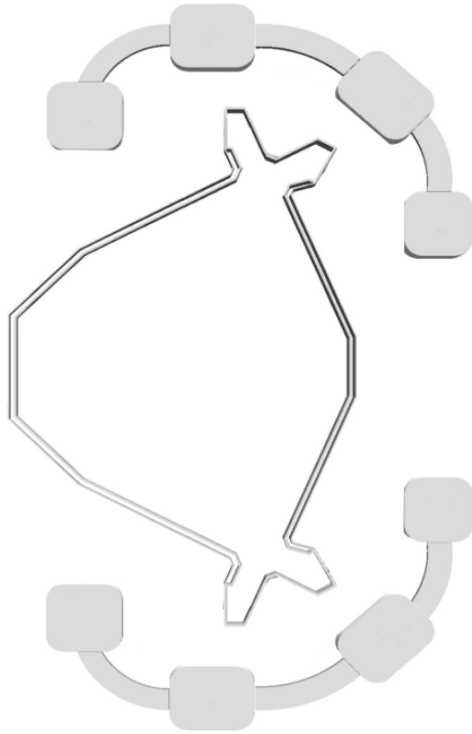


Peak heat fluxes are sensitive to SOL power and impurity fraction



- Outer plate gets ~2.3x the peak heat flux the inner plate does
- Impurities (Neon) reduce peak heat fluxes
- **Reduced SOL power and increased impurity concentration** allow for operation below material limits
- **Increasing SOL density** is also found to be **beneficial** for divertor operation

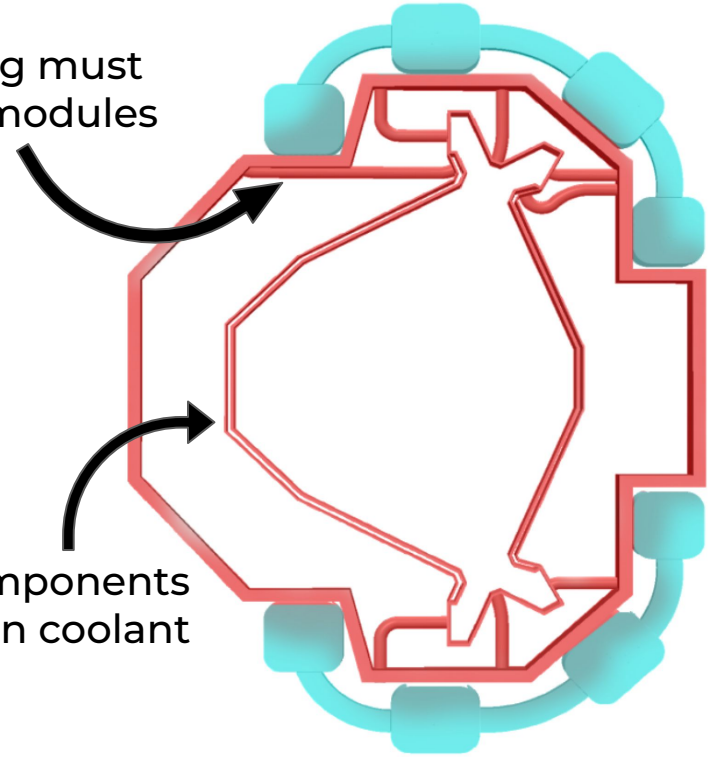
Cooling requirements drive blanket geometry



PFs require separate Cryostats

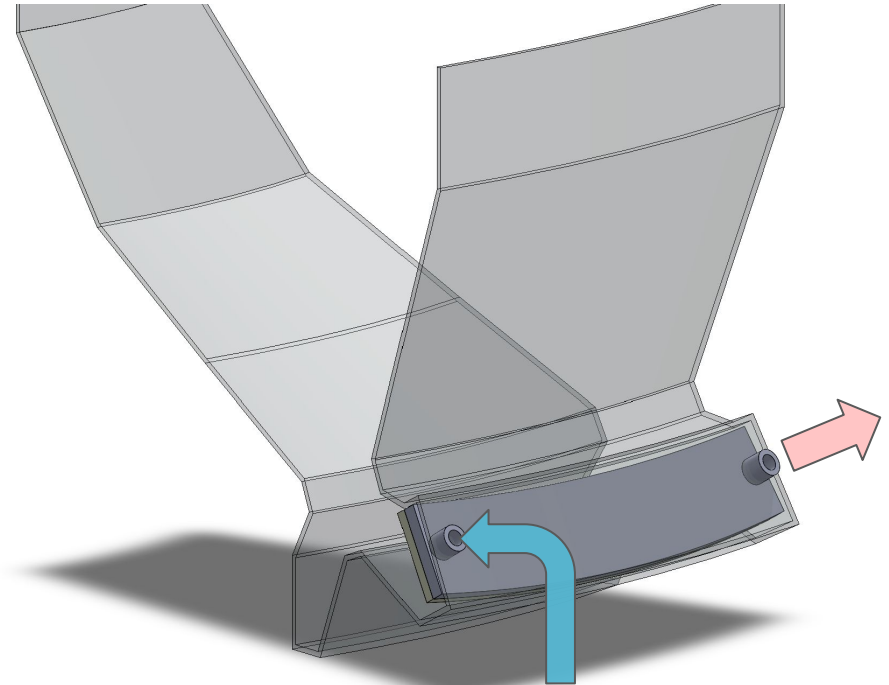
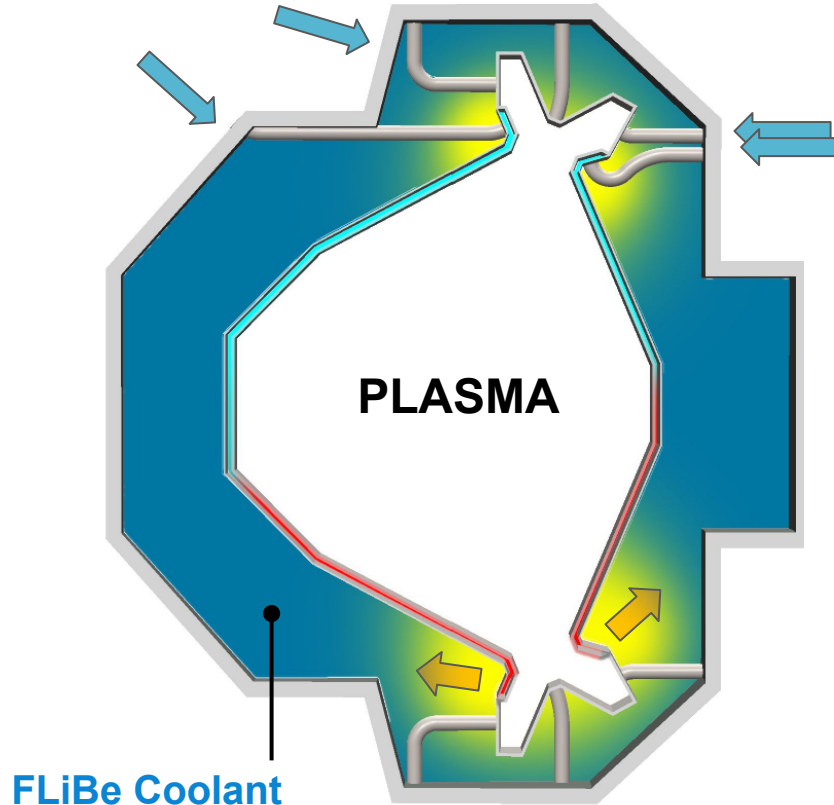
Liquid cooling must fit between modules

Hottest components immersed in coolant reservoir



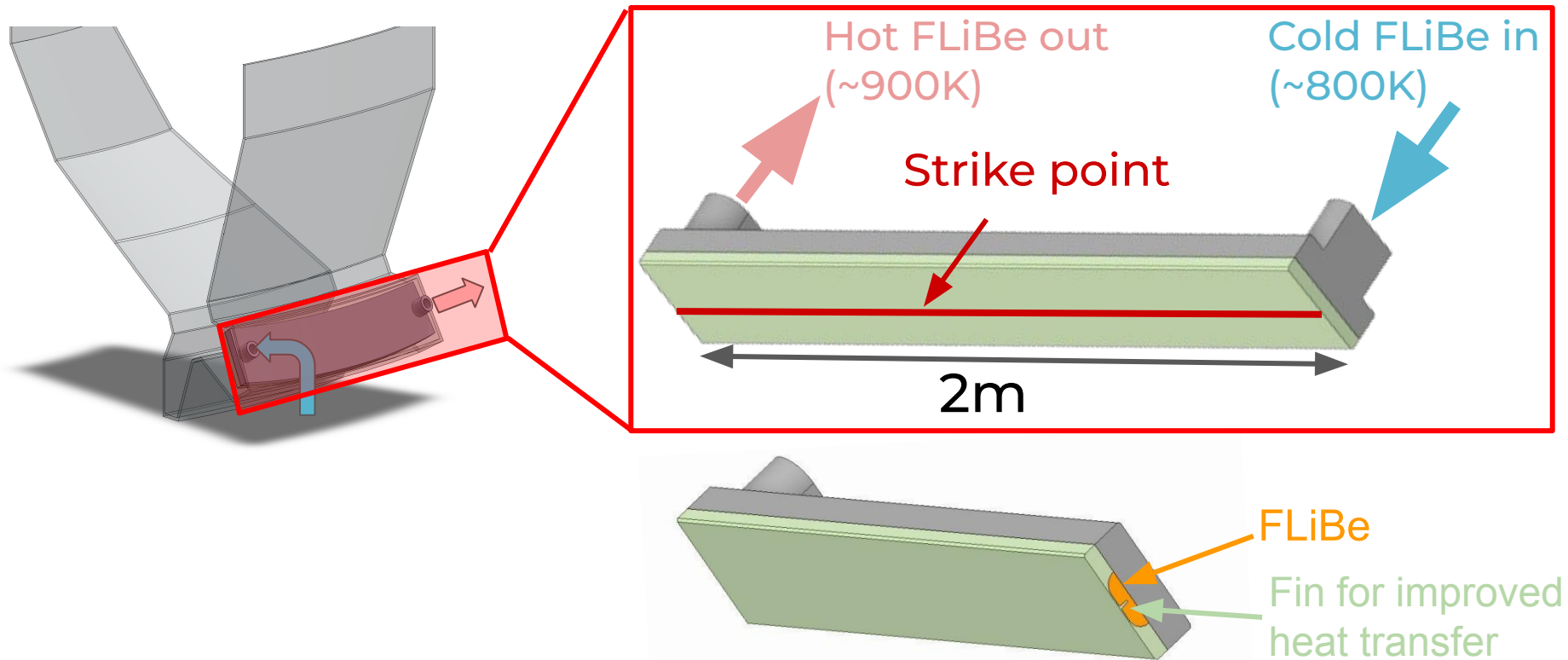
Separate modules allow thermal isolation

FLiBe Enters VV cold and exits into the Tank



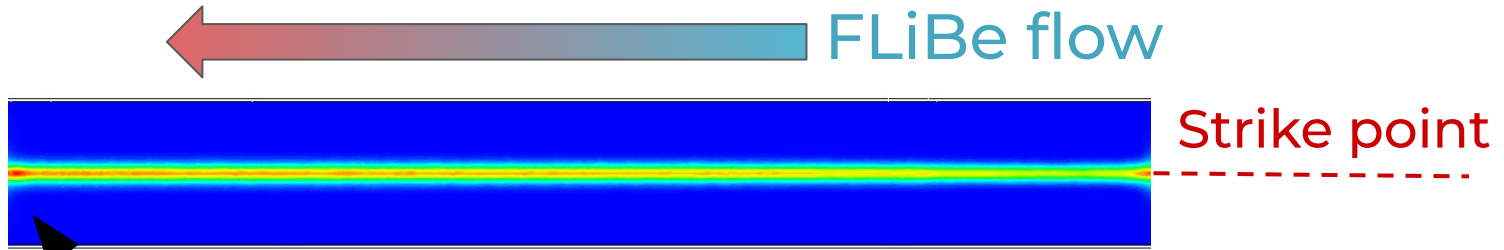
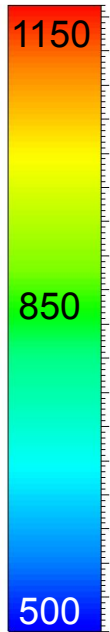
FLiBe exits divertor in-line toroidally

Divertor plates are aligned toroidally and cooled by FLiBe



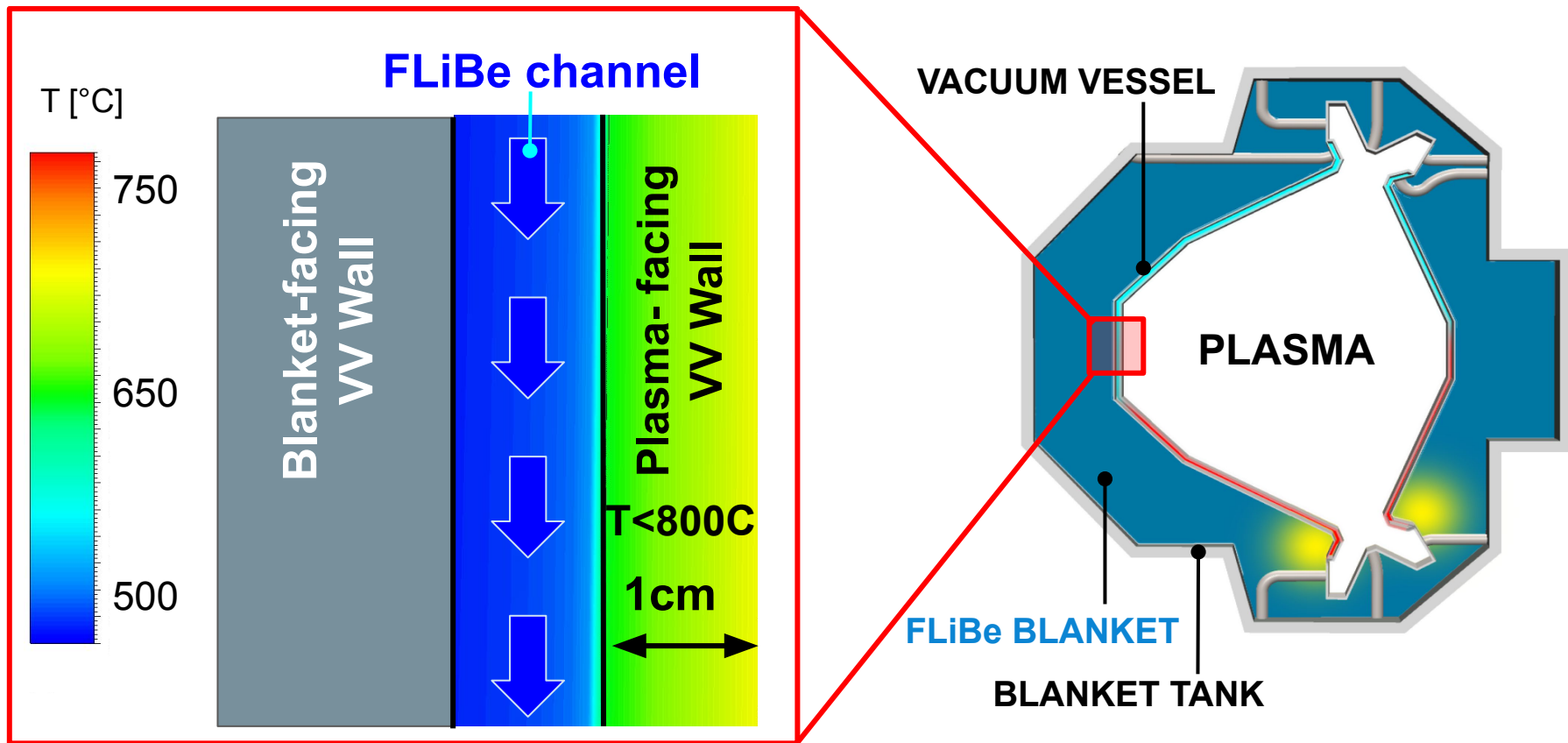
Heat flux on divertor plates successfully managed by FLiBe cooling

T [°C]



Maximum temperature < Recrystallization temperature (1200C)

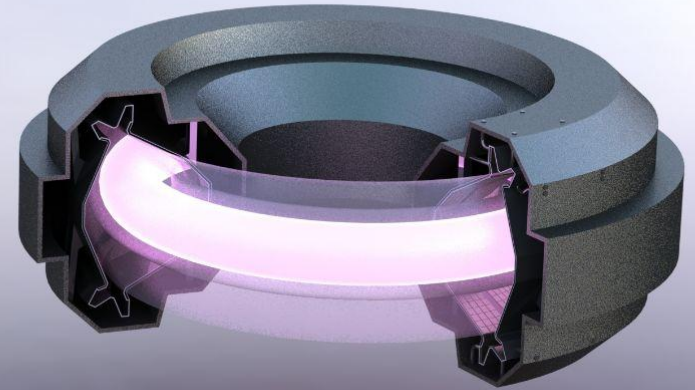
Radiative heat flux managed well by double wall vacuum vessel



Neutronics, Blanket, and Fuel Cycle

John Ball
Cody Chang
Nigel DaSilva
Joseph Jerkins
Matt Tobin

Mentors: Ethan Peterson, Sara Ferry, Stefano Segantin



22.63 Fusion Engineering

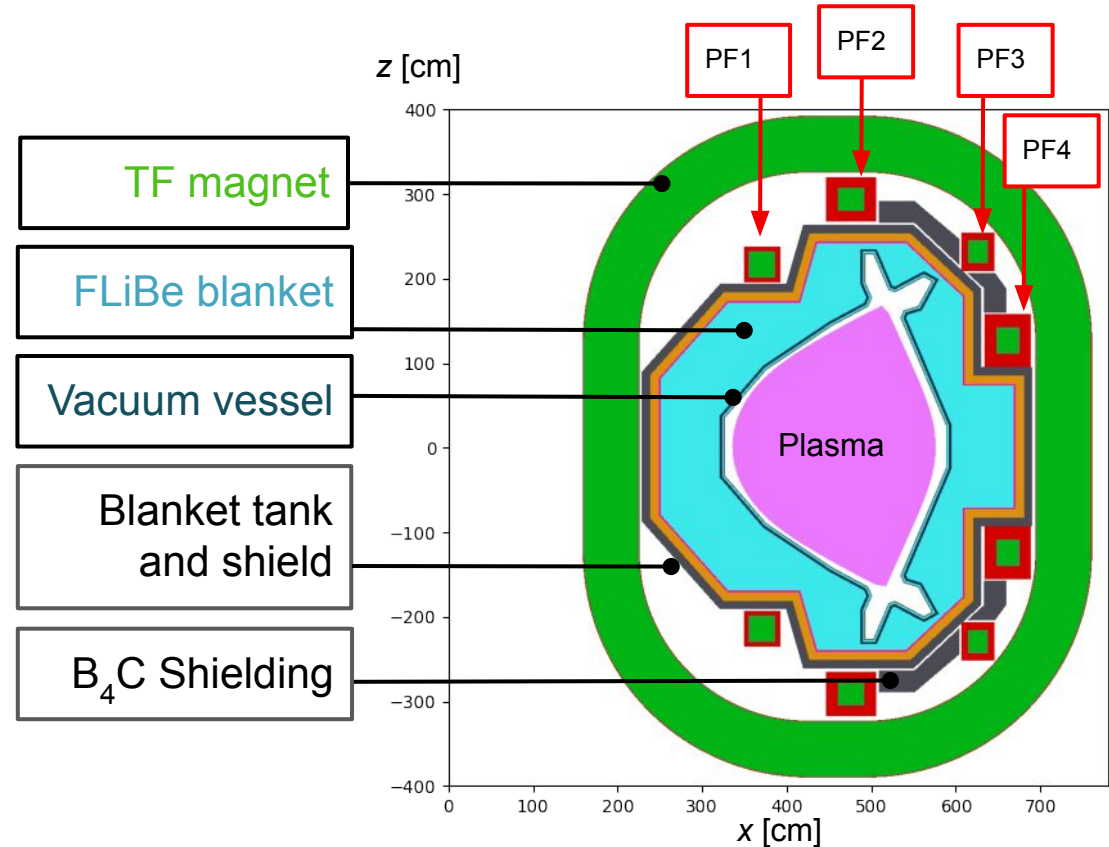
APPH 9143



COLUMBIA | ENGINEERING
The Fu Foundation School of Engineering and Applied Science

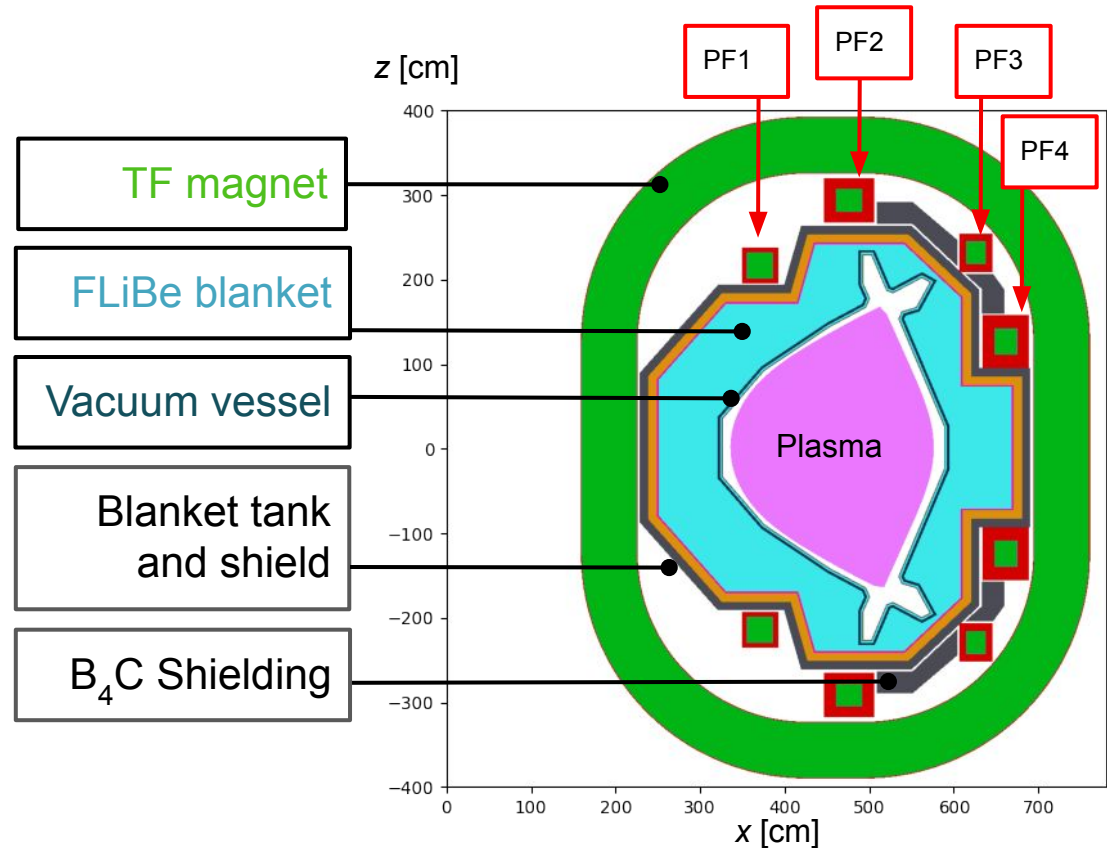
Blanket captures heat, breeds tritium, shields components

- Blanket design provides crucial constraints on the design of other systems
- Blanket analysis provides:
 - Heat deposition in components
 - Radiation damage
 - Activation
 - Tritium Breeding Ratio (TBR)
- All nuclear analysis was performed with OpenMC



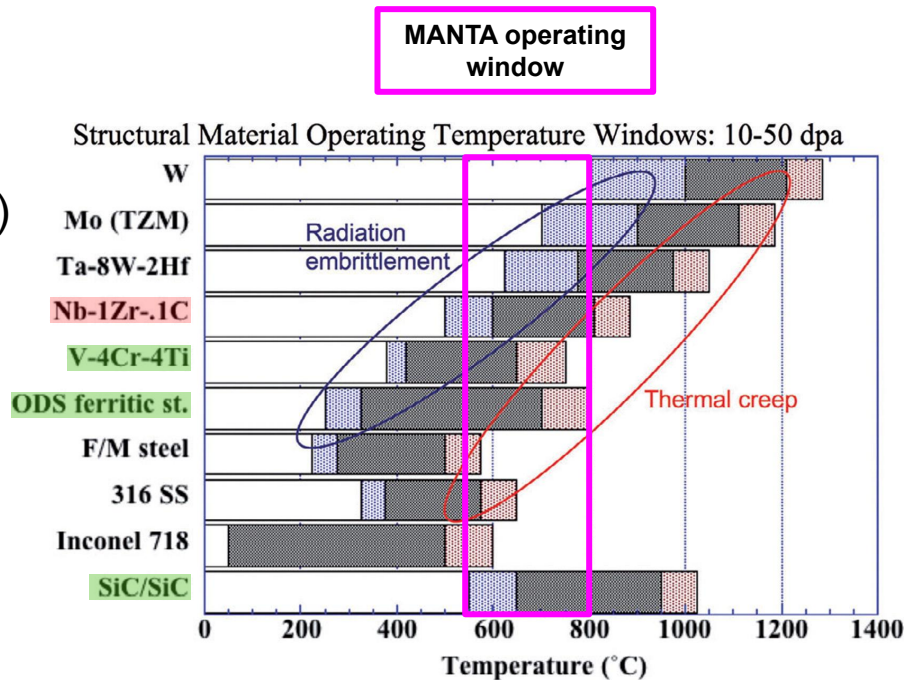
Advanced (but realistic) materials allow compact, low-activation vessel

| Component | Material |
|------------------------------|---|
| Vacuum vessel + Blanket tank | V-4Cr-4Ti |
| Magnet structure | Nitronic 50 |
| Blanket material | FLiBe |
| Neutron shielding | Boron carbide (B_4C), Tungsten carbide (WC) |
| Plasma-facing components | Tungsten |



FLiBe Temperature Drives VV Material Selection

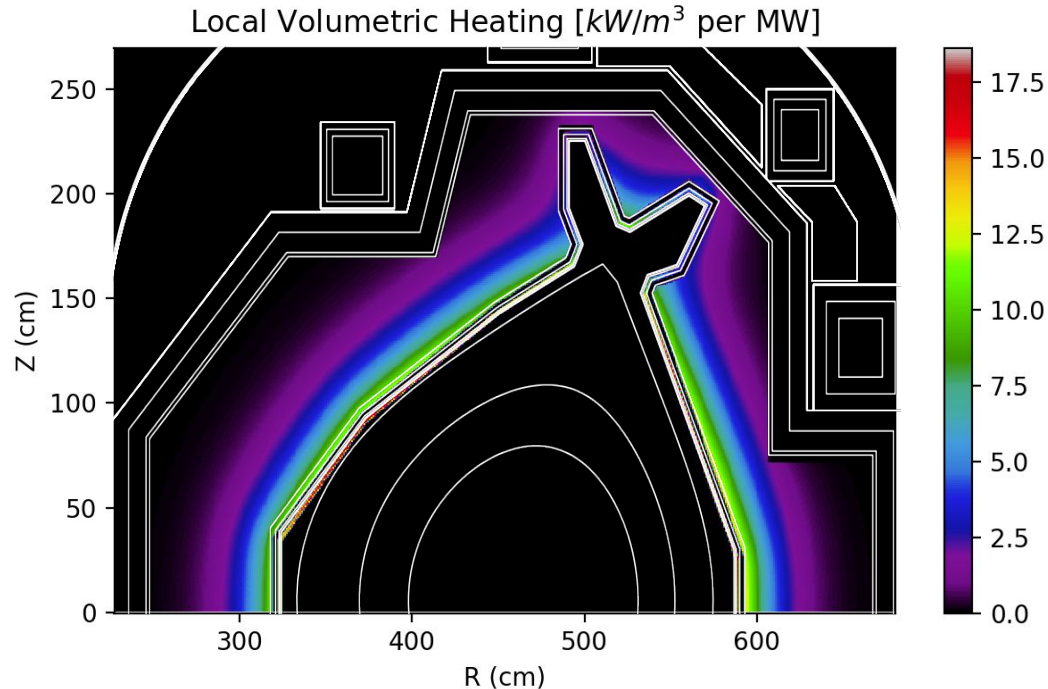
- Vacuum vessel structural material is a key element for the feasibility of the reactor
- Choice criteria:
 - High operating temperature (550-800°C)
 - Good ductility
 - High radiation resistance
 - Low activation
 - Corrosion resistance
 - TRL as high as possible
- Design modularity enables a 3-step plan for assessing materials of decreasing TRL in succession



Zinkle, S. J. and Busby, J. T. *Materials Today* 12(11) 12-19. (2009).

Blanket shaped to optimize heat deposition

- Contours in global heat deposition in FLiBe inform blanket geometry
- Power multiplication factor in the blanket is **1.11**



| Quantity | Power [MW] |
|-------------------------|------------|
| Fusion power | 395 |
| α power | 79 |
| Neutron power | 316 |
| Nuclear heating | 360 |
| Auxiliary heating power | 10 |
| Total thermal power | 449 |

Magnet Lifetimes Allow for Years of Operation

- Target lifetime: **1000 MW-years**
 - At 400 MW P_{fus} this corresponds to 2.5 full power years (FPY)
- This requirement is met or exceeded at all points in the TF magnet
- PF magnets do not meet lifetime goal

| PF# | Avg. Lifetime [MWy] |
|-----|---------------------|
|-----|---------------------|

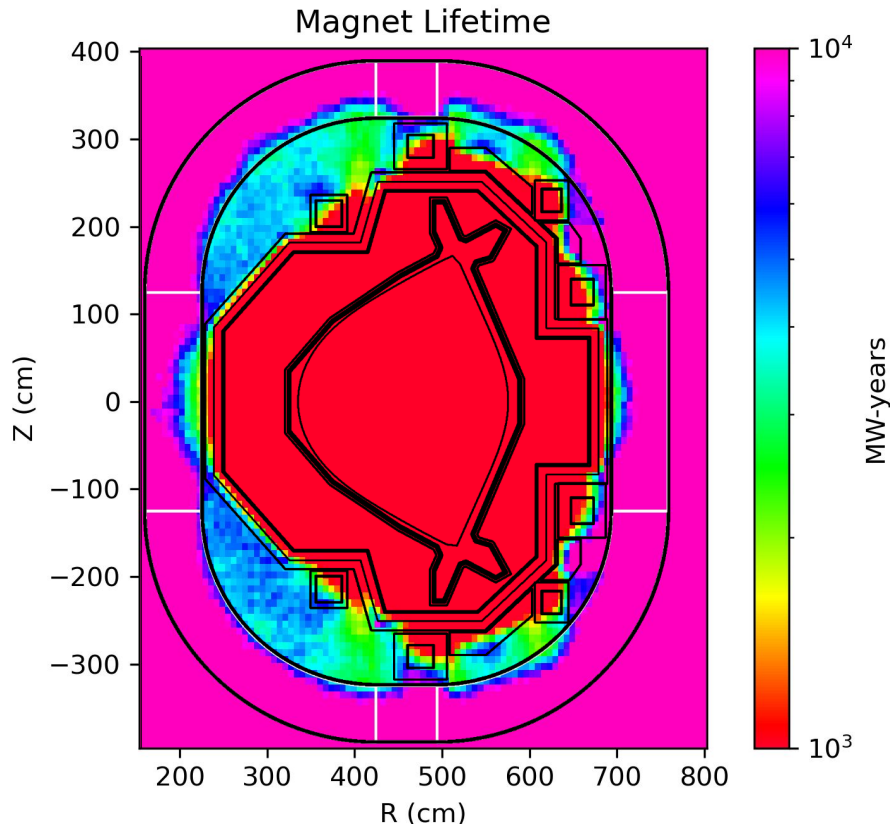
PF1 1271 \pm 25

PF2 1117 \pm 18

PF3 726 \pm 10

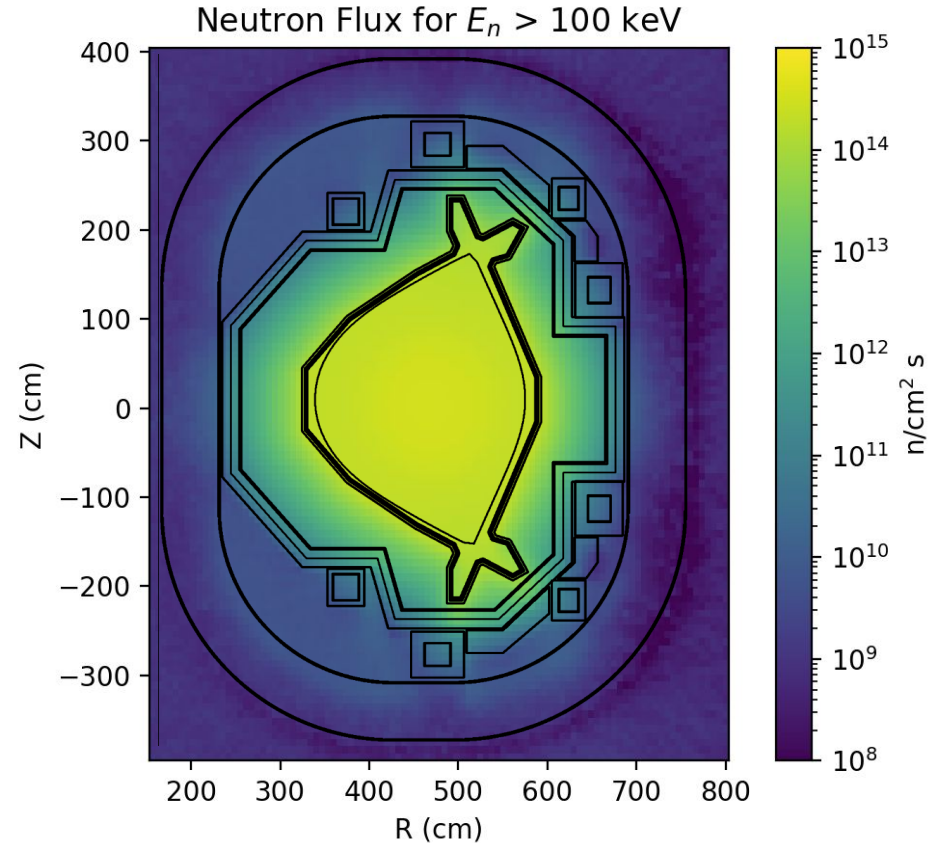
PF4 1580 \pm 60

PFs likely will
require
replacement



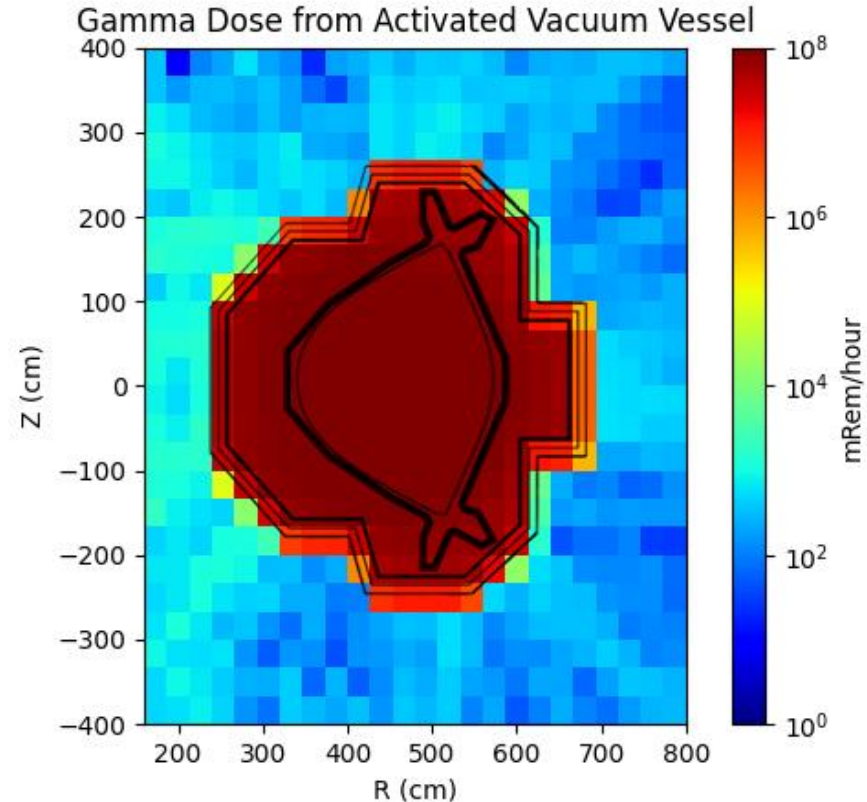
Vessel radiation damage likely acceptable for years of operation

- Material integrity is related to displacements per atom (DPA) from incident neutrons
- Vacuum vessel DPA of **2.06** per 100MWy, predicted to be within acceptable range for material operation
- True lifetime limits based on DPA are to be determined during operation



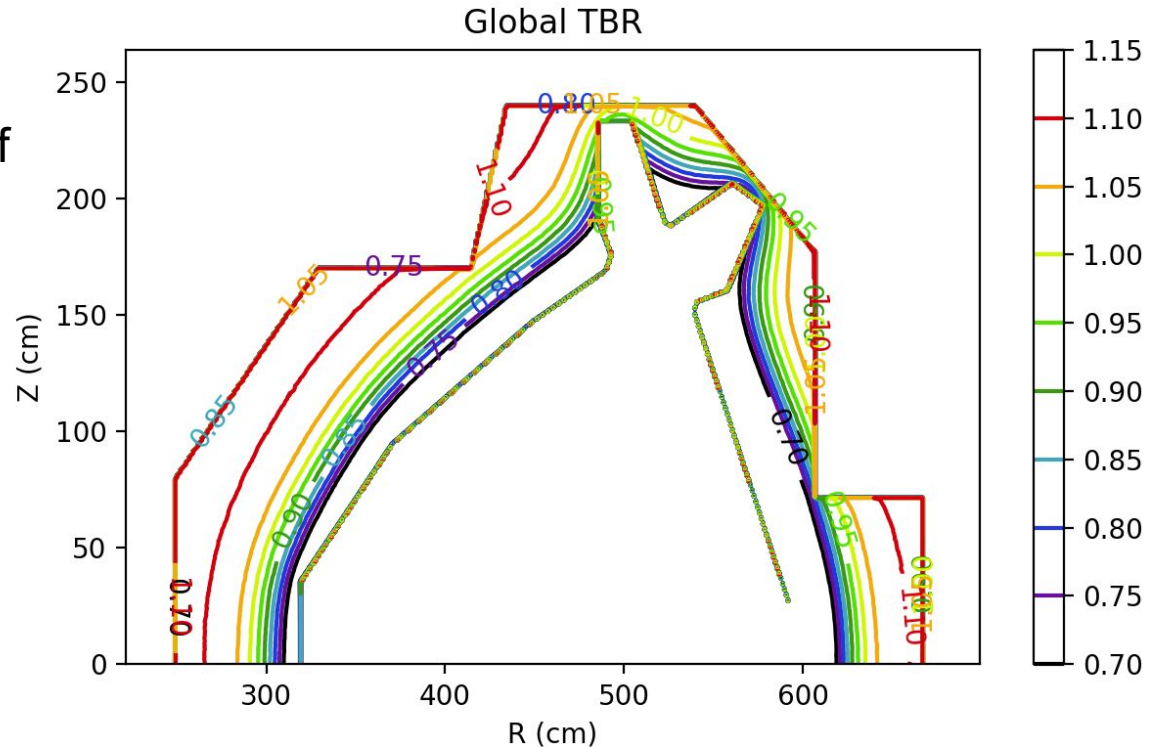
Blanket Tank Shields VV During Maintenance

- Rigorous 2-Step method used to compute gamma dose
- Depletion simulation carried out for $P_{\text{fus}} = 400$ MW for 4 years with 100% duty factor
- Simultaneous removal of blanket tank and VV with FLiBe drained → tank shields highly activated VV
- **Current blanket tank shielding reduces gamma dose from activated VV by a factor of $\sim 10^5$**



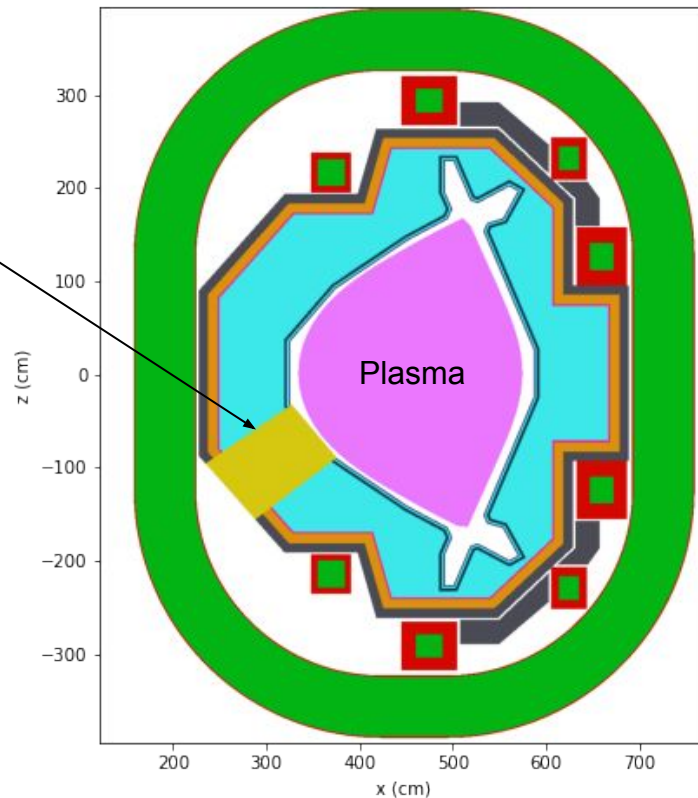
Blanket design achieves tritium self-sufficiency

- TBR determines mass of tritium required to start-up reactor, and self-sufficiency of plant over time
- Model predicts a TBR of **1.11**
- TBR contours used to optimize breeding while minimizing volume



Acceptable TBR Maintained with RF system

- RF launcher location optimized in collaboration with core team
- Modeled at right: worst-case scenario for geometry of the RF heating system feedthrough
 - Blanket material replaced with GRCop-84 at half density around one third of the torus
 - Reduces TBR
 - Final blanket geometry must avoid neutron streaming paths to the TF coil
- TBR of **1.10** (reduction of 0.01) maintained even in this worst-case scenario

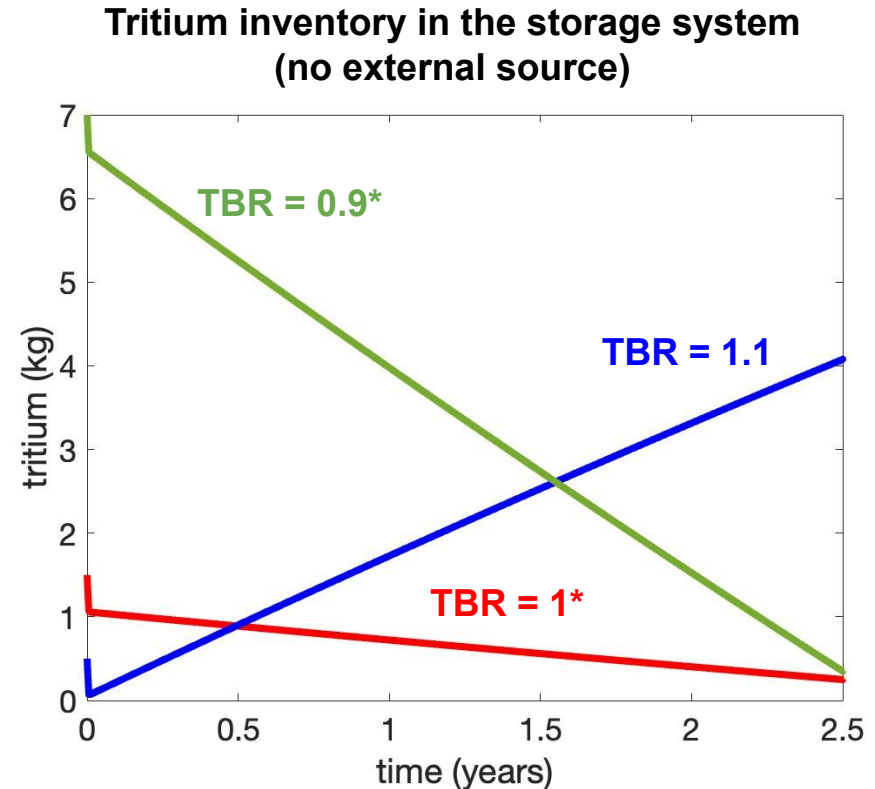


TBR of 1.10 enables startup of additional fusion power plants

- TBR > 1.02 required for self-sufficiency, where enough tritium is produced to fuel MANTA
- At TBR of 1.1, it takes **6 months** to generate startup inventory for another reactor

$P_{\text{fus}} = 400 \text{ MW}$

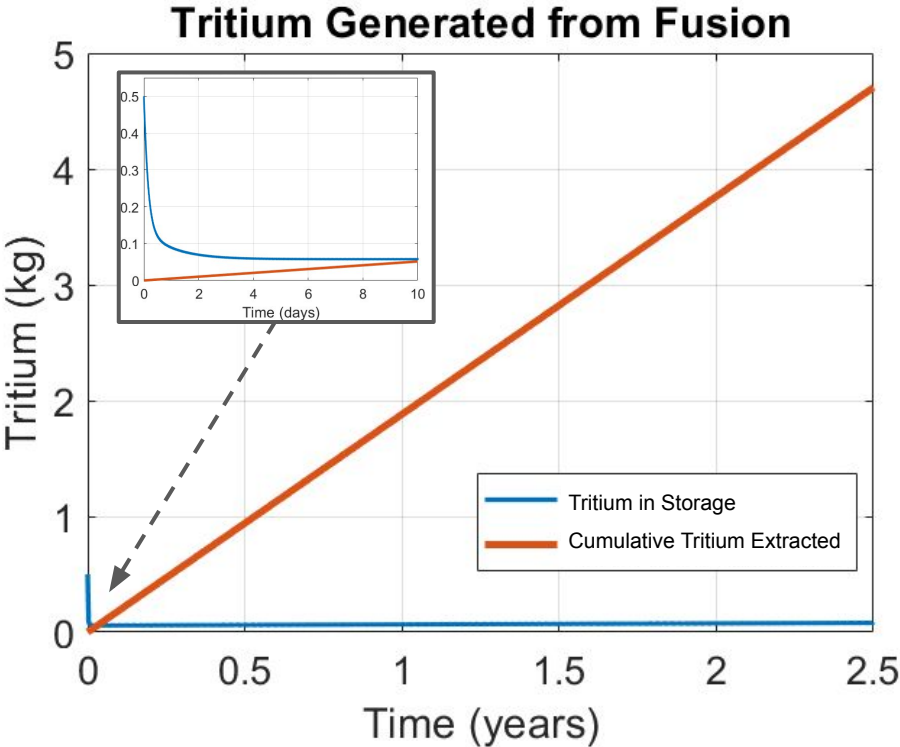
*not a measure of start-up inventory



Current fuel cycle parameters enable the production of enough tritium to fuel 7-9 more MANTA-class devices over 2.5 years

| MANTA fuel cycle parameters | |
|---------------------------------------|---------|
| Tritium breeding ratio (TBR) | 1.10 |
| Fusion power (P_{fus}) | 395 MW |
| Availability Factor (AF) | 0.9 |
| Startup T inventory ($I_{startup}$) | 500 g |
| Reserve T inventory ($I_{reserve}$) | 75 g |
| Time to system equilibrium | 1 week |
| Lifetime T production | 4.70 kg |

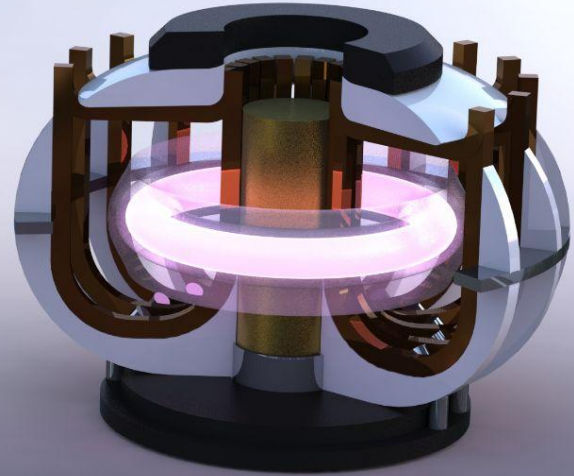
$I_{startup}$ is optimized for initial cost and net T production



Magnet Systems Pt. 2: Maintenance

Alexis Devitre
Allen Wang
Andrew Maris
Haley Wilson
Michael Liu

Mentor: Theodore Mouratidis



22.63 Fusion Engineering

APPH 9143



COLUMBIA ENGINEERING
The Fu Foundation School of Engineering and Applied Science

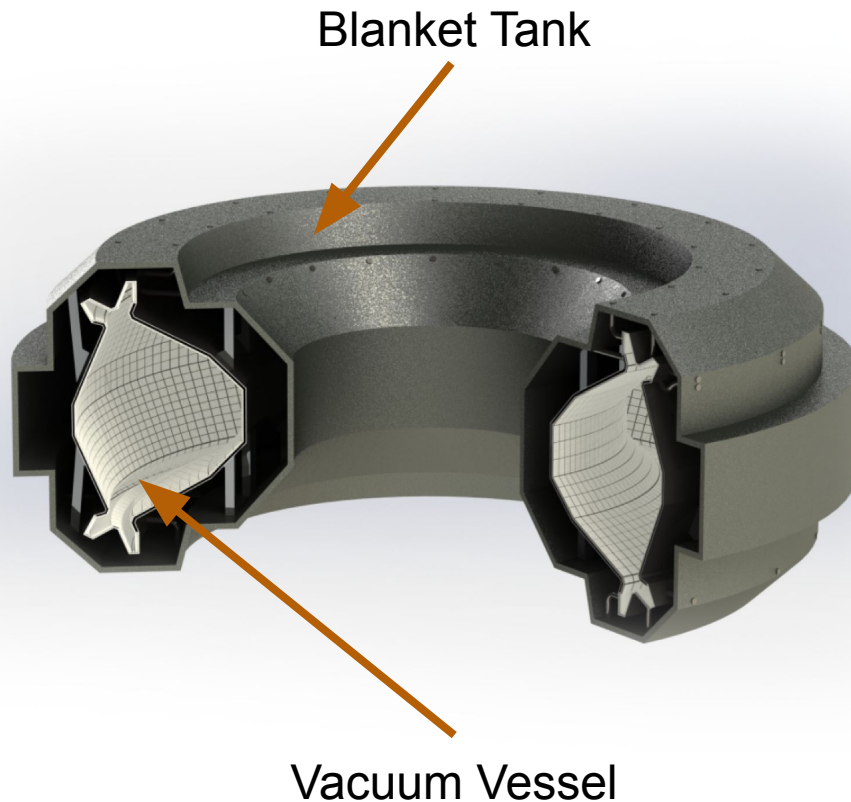
Maintenance goals met by regularly replacing internal assembly

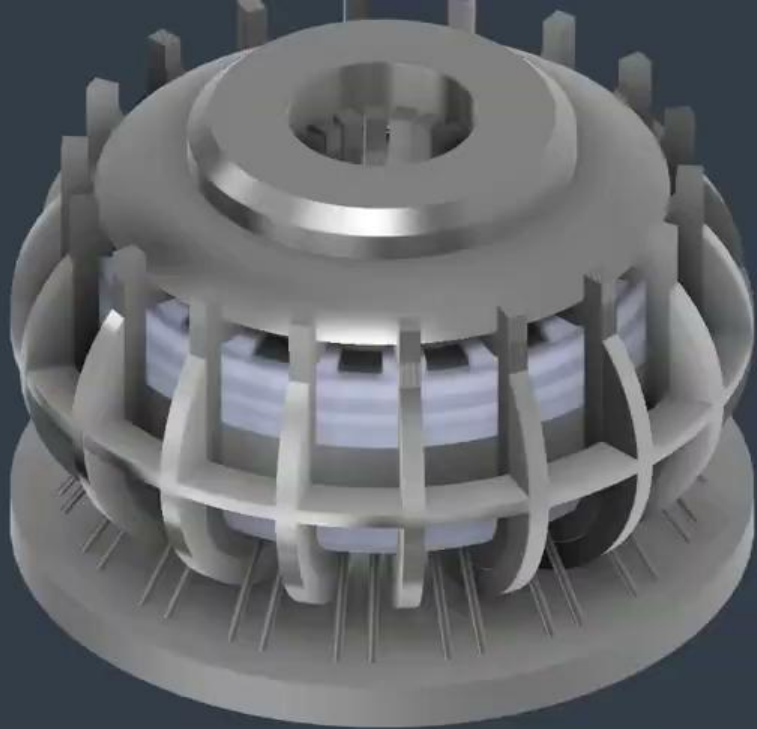
Design Goals:

- Replace the wearable Vacuum Vessel (VV)
- Ensure operational certainty by minimizing downtime

Strategy:

- Replace VV + Blanket Tank assembly together
- Spec a large cryoplant (13kW nominal, 1.5 MW peak)



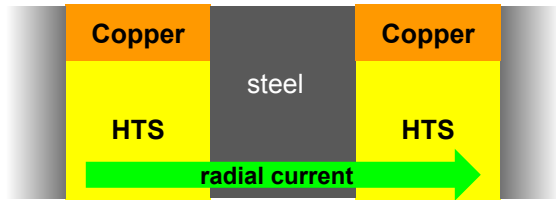


Oversized cryoplant leads to ~1 month replacement cycle

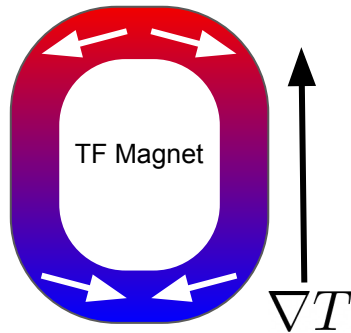
| Required steps | Baseline | MANTA |
|------------------------------|--------------------------|-----------------|
| Charge & discharge TF | ~ 3 months (scaled TFMC) | 11 days |
| Warm up & cool down cryostat | ~ 2 months (ITER, KSTAR) | 11 days |
| Detach & re-attach joints | ~1 day | ~1 day |
| Replace internal assembly | ~1 week | ~1 week |
| Wall conditioning | 2 days | 2 days |
| Total | ~ 5 months | ~1 month |

Fast replacement requires a large cryoplant

Rate-limiting effects



1. Radial current heating during TF charge and discharge



2. Thermal stress on TF when cryostat warms up and cools down

Solution

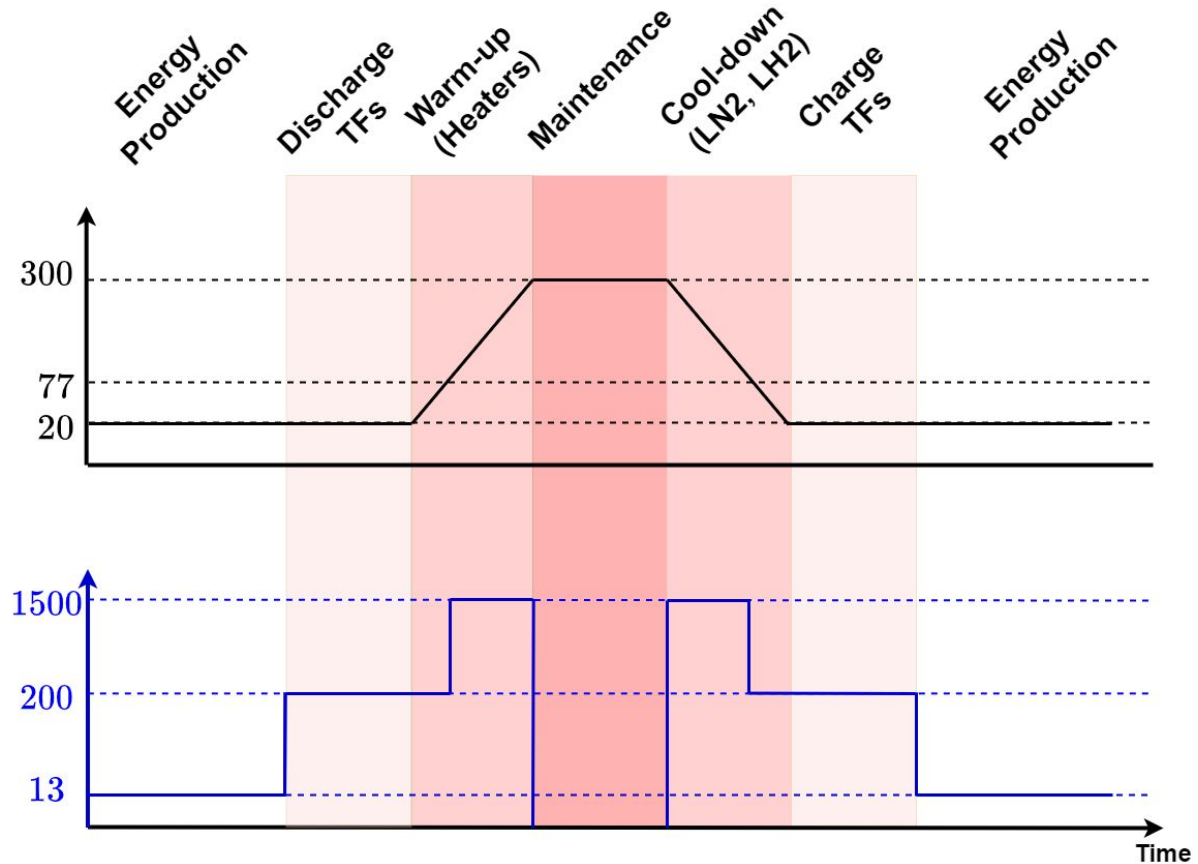
Large cryoplant

- LN_2 precoolant (cool down)
- LH_2 coolant
 - Temperature: 20 K
 - Mass flow rate: 15 kg/s

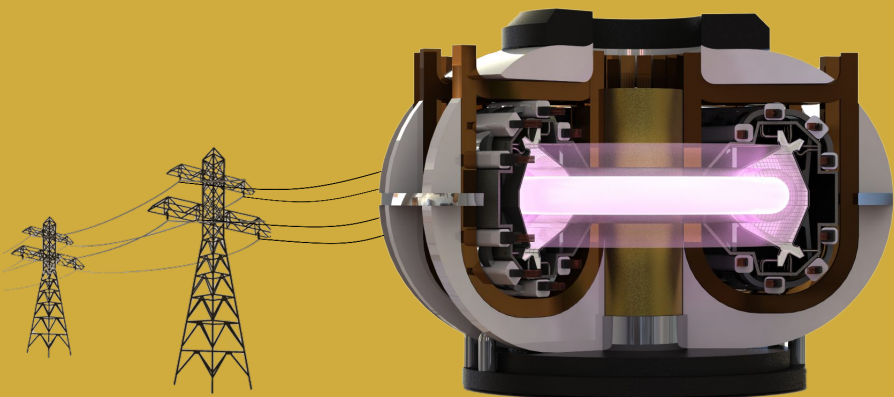
Peak heating/cooling power far beyond needs of fusion operations

TF coil temperature
[K, linear]

Warming & cooling
power [kW, log]



Economics and Balance of Plant



Shon Mackie
Dan Murphy
Audrey Saltzman
Alex Velberg
Miguel Calvo Carrera
Rian Chandra
William Boyes

Mentor: Rachel Bielajew



22.63 Fusion Engineering

APPH 9143



COLUMBIA ENGINEERING
The Fu Foundation School of Engineering and Applied Science

Thermal Cycle layout: FLiBe - Solar salt - Rankine

$P_{\text{fusion}} = 395 \text{ MW}$

FLiBe

($2\text{LiF} \cdot \text{BeF}_2$)

$T_{\text{melting}} = 459 \text{ }^\circ\text{C}$

$T_{\text{boiling}} = 1430 \text{ }^\circ\text{C}$

Solar salt

($60 \text{ NaNO}_3 - 40 \text{ KNO}_3$)

$T_{\text{melting}} = 220 \text{ }^\circ\text{C}$

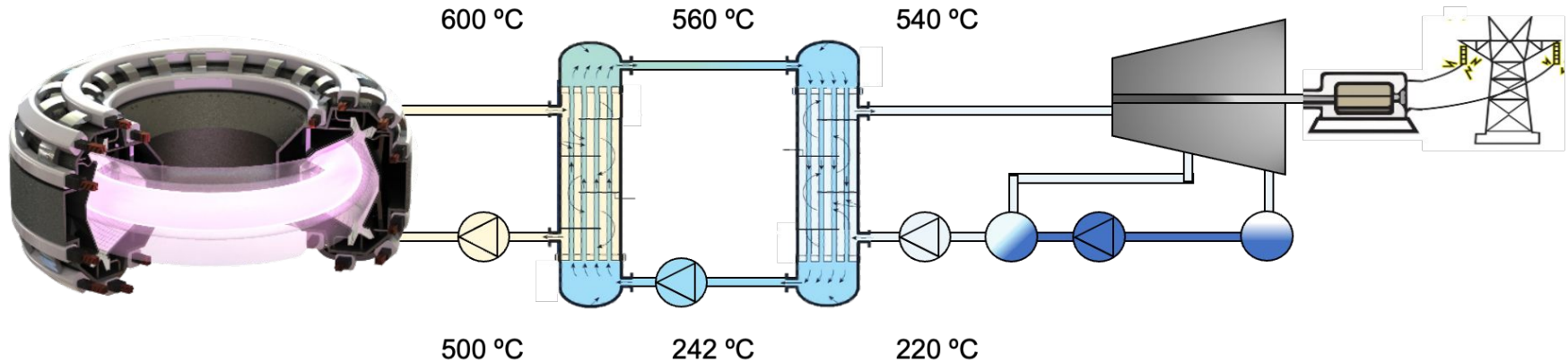
$T_{\text{boiling}} = 600 \text{ }^\circ\text{C}$

H₂O Rankine

Subcritical: 150 bar: $\eta = 36.0\%$

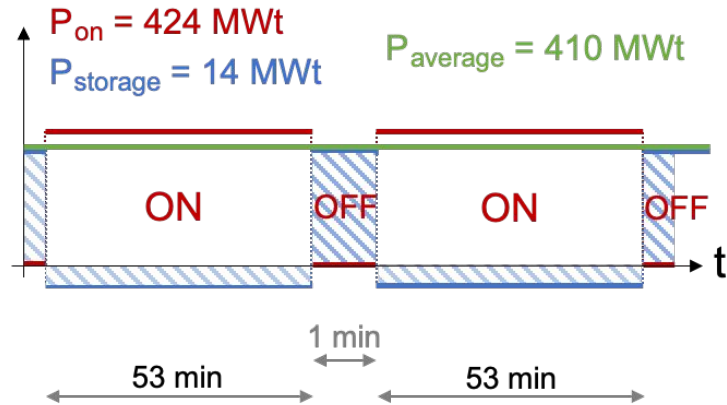
Supercritical: 300 bar: $\eta = 38.5\%$

$P_{\text{e, grid}} \sim 110 \text{ MW}$

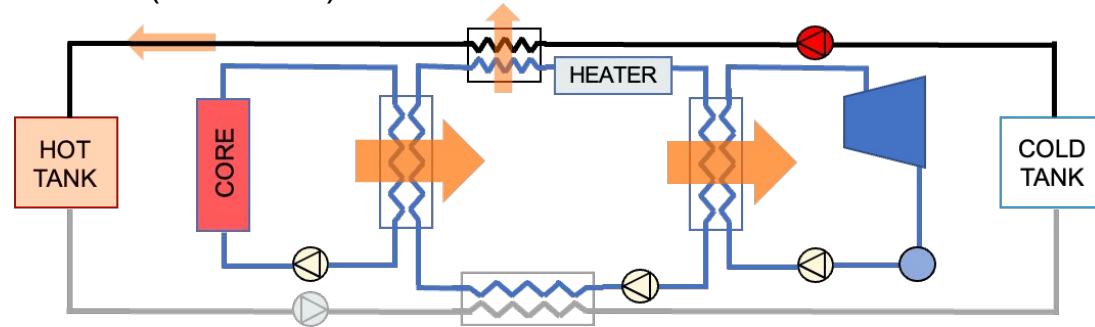


Sohal M., Ebner M., Sabharwall P. and Sharpe P., 2013 Engineering Database of Liquid Salt Thermophysical and Thermochemical Properties

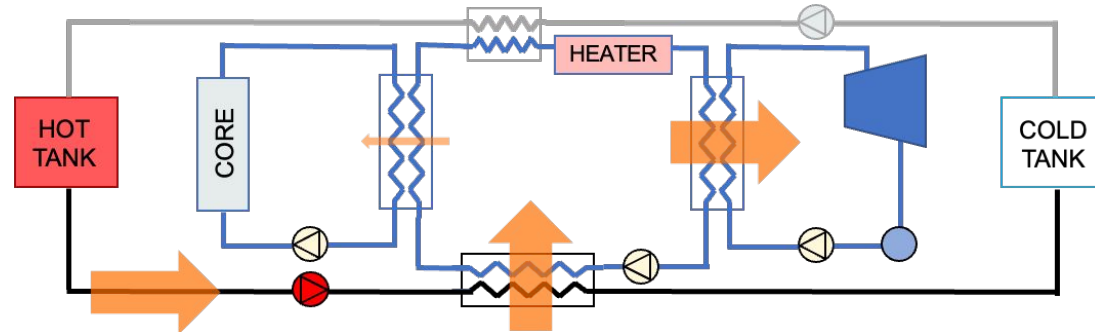
Thermal Storage: from pulsed core to steady-state



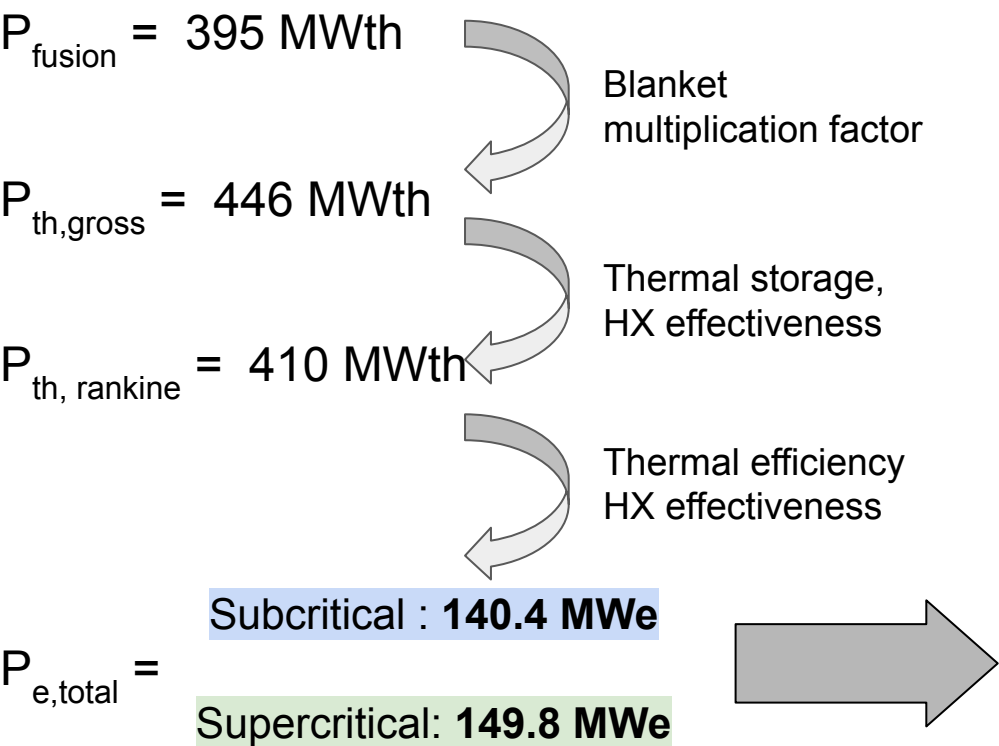
ON (t ~ 53 min)



OFF (t ~ 1 min)

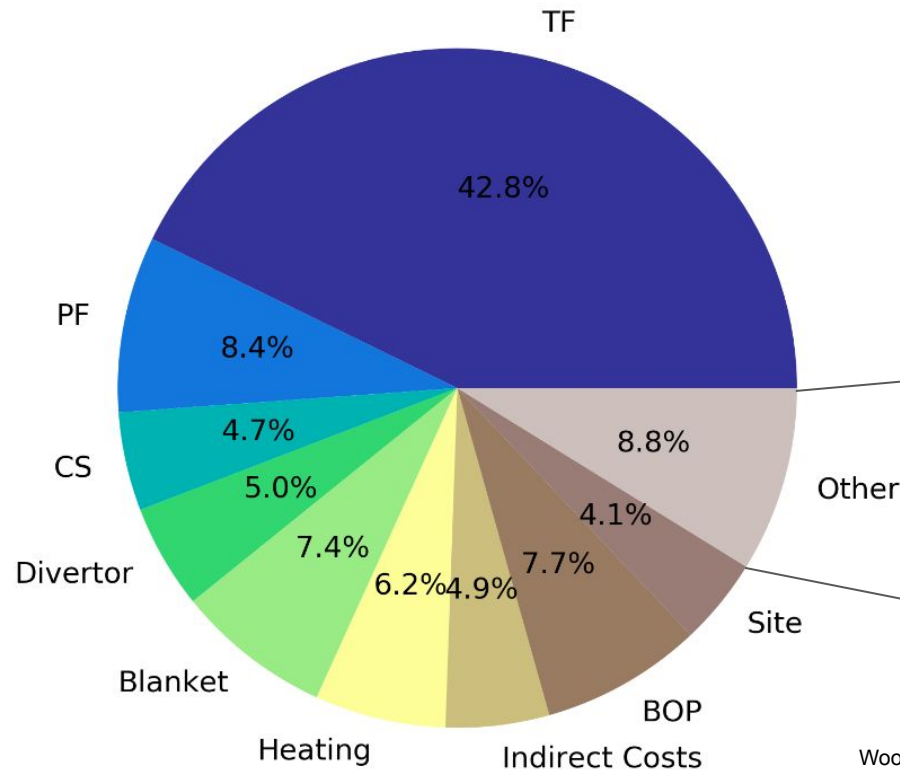


Balance of Plant: $P_e > 50\text{MW}$, $Q_e > 1$ Satisfied

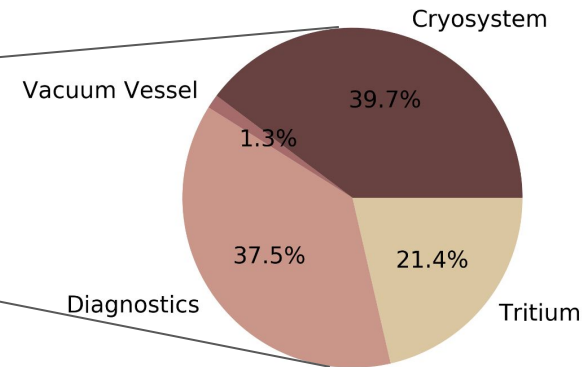


| Power Budget | | |
|--------------------------------|-------------|---------------|
| | Subcritical | Supercritical |
| $P_{\text{auxiliary heating}}$ | 20 MWe | 20 MWe |
| $P_{\text{cryogenics}}$ | 0.9 MWe | 0.9 MWe |
| P_{pumps} | 5.2 MWe | 12.3 MWe |
| P_{systems} | 26.1 MWe | 33.2 MWe |
| $P_{\text{electric, grid}}$ | 114.3 MWe | 116.6 MWe |
| $Q_{\text{electrical}}$ | 5.3 | 4.5 |

Overnight cost is \$3.0B, below \$5B requirement



- ▶ ~\$25 million / MWe, comparable to offshore wind pilot plant built in 2020
- ▶ Consistent with Sheffield Model prediction of \$3.3B



Woodruff S, Miller R, Chan D, Routh S, Sakti Basu and Rao S 2017 Conceptual Cost Study for a Fusion Power Plant Based on Four Technologies from the DOE ARPA-E ALPHA Program

Brownfield siting offers cost savings

Cost Savings

Brownfield site construction could save **\$232M**
(~8% of total cost)

\$3.02B - Greenfield Estimate

- \$107M turbine (subcritical Rankine)
- \$ 35M electrical plant
- \$136M construction costs
- + \$ 45M legacy plant decommissioning

\$2.79B - Brownfield Estimate

Energy Justice

Repurposing of a legacy fossil fuel plant builds **relationships with the community** under **informed consent - based siting**

The Fusion Pilot Plant will:

- Retain jobs in the community
- Eliminate a major polluter in the community
- Put the community on the forefront of a cutting edge scientific development

Raimi, Daniel. "Decommissioning US power plants." *Decisions, costs, and key issues. Resources for the Future (RFF) Report* (2017).

Beyond NASEM: MANTA provides operational certainty

- What if MANTA were run as a power plant?
- Revenue streams: Electricity + Tritium
- Variable costs: Financing + Operations + Electricity usage
- Capacity factor set by magnet replacement + central solenoid pulse time

Net Cost Remains \$3.0B (2.5 Year Project)

- Scale up: 25 yr project, 600 MW fusion \Rightarrow 227 MW electric
 - Levelized Cost of Electricity: \$145.0/MWh

Historic wholesale price of electricity: ~\$47.59/MWh (NYC)
LCOE of natural gas: \$39/MWh (US)

Pilot Model Begins to Approach Competitiveness

Source: Bureau of Labor Statistics,
Energy Information Agency

Class outcome exceeds NASEM requirements

Primary Goals

$$P_{\text{out}} > 50 \text{ MWe}$$

$$\text{Cost} < \$5\text{B}$$

$$Q_e > 1$$

Achieved Results

$$P_{\text{out}} \sim 110 \text{ MWe}$$

$$\text{Cost} \sim \$3.0\text{B}$$

$$Q_e \sim 5$$

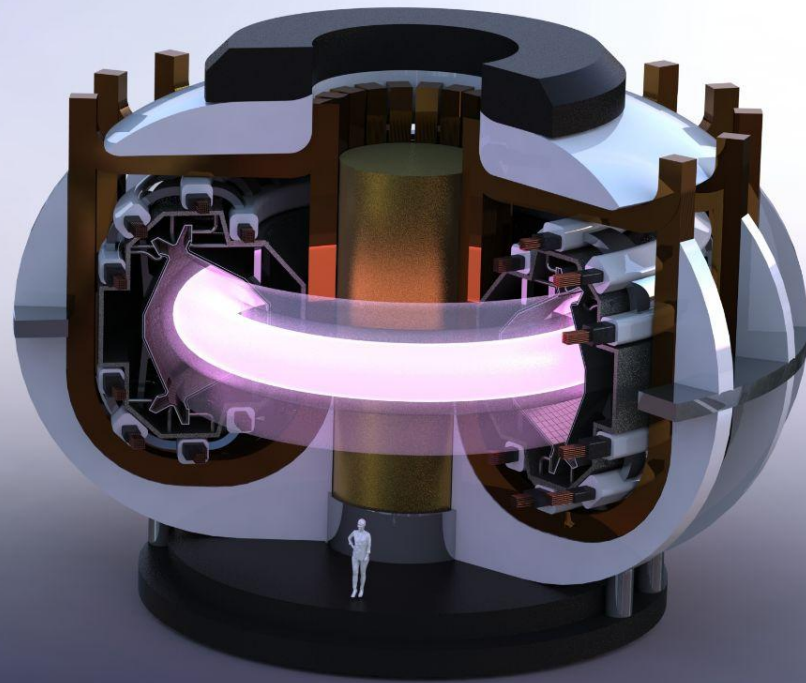
| Parameter | Initial Target | Attained Value |
|-------------------------|------------------|----------------|
| Lifetime | 1000 MWy | 1000 MWy ✓ |
| P_{fusion} | 200 MW | 395 MW ✓ |
| $T_{\text{production}}$ | 10^3 s | ✓ |
| $f_{\text{available}}$ | 0.9 | 0.92 ✓ |
| Q_{P} | 15 | 39.5 ✓ |
| P_{SOL} | 25 MW | 25 MW ✓ |
| $B_{\text{T on-coil}}$ | 21 T | 24 T ✓ |
| TBR | 1 | 1.1 ✓ |

What's new? A list of MANTA's first-time achievements

- Negative triangularity ARC modelling
- Radiative L-mode in negative triangularity
- GX+Trinity turbulent transport simulations
- Fully integrated core and edge design workflow (across separatrix)
- Modular structure for VV and PF replacement
- Designed for short downtime
- Adjustable operating point with constant P_{sol}
- Variable pulsed power with constant Q_e
- Tritium economic viability studies
- Intentional quenching to speed cool-down
- ?? add :)

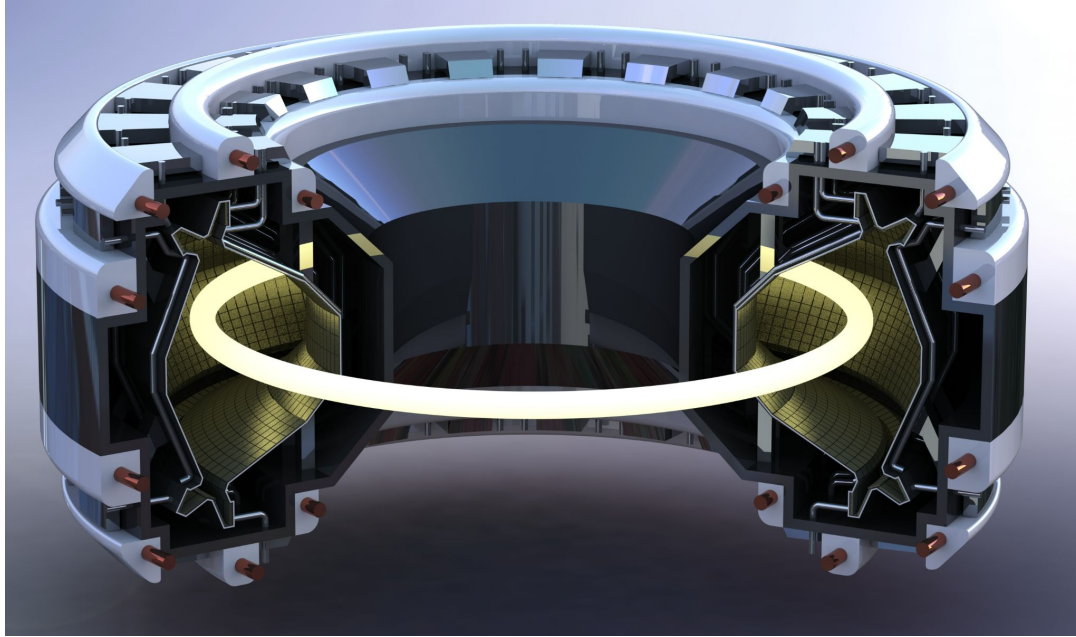
Key innovations and insights exceed NASEM requirements

1. Large aspect ratio, low elongation, and negative triangularity **reduce physics and technology risk**
2. **Variable fusion power** at constant, manageable divertor power exhaust
3. **Pulsed plasma** but **constant electricity** production > 50 MWe
4. Flexible fusion core **replacement strategy** enables rapid test of multiple designs through many environmental cycles
5. Tritium breeding **sufficient for operation** and inventory



Negative triangularity fusion pilot plant design

Fusion design course Fall 2022 | MIT 22.63 / Columbia APPH9142



Backup

BACKUP: Scaled TFMC

“Scaled TFMC” is a scaling up of TFMC parameters assuming cooling power scales with perimeter of the magnet and inductance + current scale to the quantity needed for MANTA

Magnet Operating Current

Magnet Inductance

$$t_{charge} \approx \frac{I_{op} L_{coil}}{\sqrt{R_c P_{cool}}}$$

Characteristic Resistance

Magnet Thermal Cooling

| | MANTA/TFMC |
|---|------------|
| Iop [kA] | 47/40 |
| Stored Magnetic Energy [GJ] | 5.6/0.11 |
| Implied Relative Inductance (E=0.5*L*Iop^2) | 36.9 |
| Relative Perimeter | 24 |
| Assumed Relative Cooling Power | 24 |
| Relative Charge Time (Cooling + Inductance) | 7 |

TFMC data from Zach Hartwig's public presentation at 49:00 in this [youtube video](#)

Three structural material paths pursued in sequence

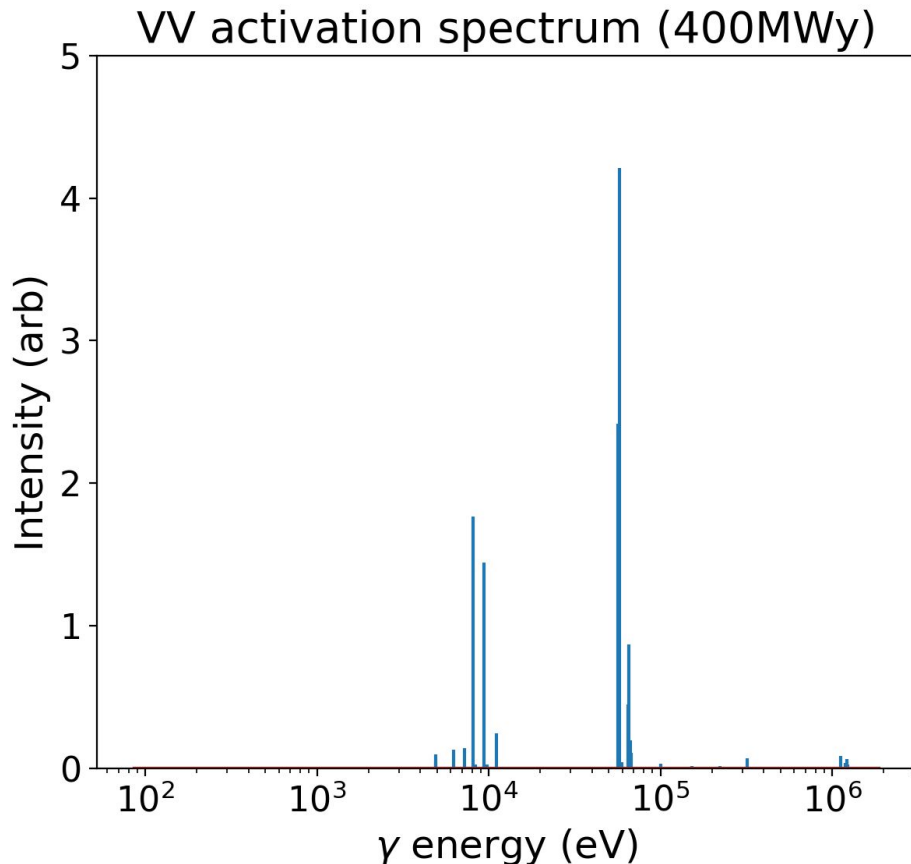
| | Plan A | Plan B | Plan C |
|--|--|--|--|
| Material | V-4Cr-4Ti | RAFM-ODS | SiC/SiC |
| Operating temperature¹ | 400-650 °C | 300-700 °C | 650-950 °C |
| Activation² | 2.2×10^4 Bq/kg | 6.7×10^8 Bq/kg | 1.4×10^4 Bq/kg |
| TRL | 4-5 | 4-5 | 3-4 |
| Advantages | <ul style="list-style-type: none"> •Technological readiness •Thermal properties •Radiation resistance | <ul style="list-style-type: none"> •F/M are widely characterized •Of main interest in other fusion industries •Mechanical strength •Radiation resistance | <ul style="list-style-type: none"> •Low thermal expansion •Corrosion resistance •Mechanical strength •Si and C natural abundance |
| Research directions | <ul style="list-style-type: none"> •Corrosion barriers •H anti-permeation barriers •Joining & welding •Industry-scale production | <ul style="list-style-type: none"> •Corrosion barriers •H anti-permeation barriers •Industry-scale additive manufacturing | <ul style="list-style-type: none"> •Reduced brittleness configurations to be found •Characterization in FLiBe corrosion •Characterization under irradiation •Industry scale production |

¹Zinkle, S. J. and Busby, J. T. *Materials Today* **12**(11) 12-19. (2009).

²In terms of highest activity of component elements after 2 full power years irradiation in a DEMO-like environment, followed by 10 years of cooling.
Gilbert, M. R., et al. *Nucl. Eng. and Tech.* **49** 1346-1353 (2017).

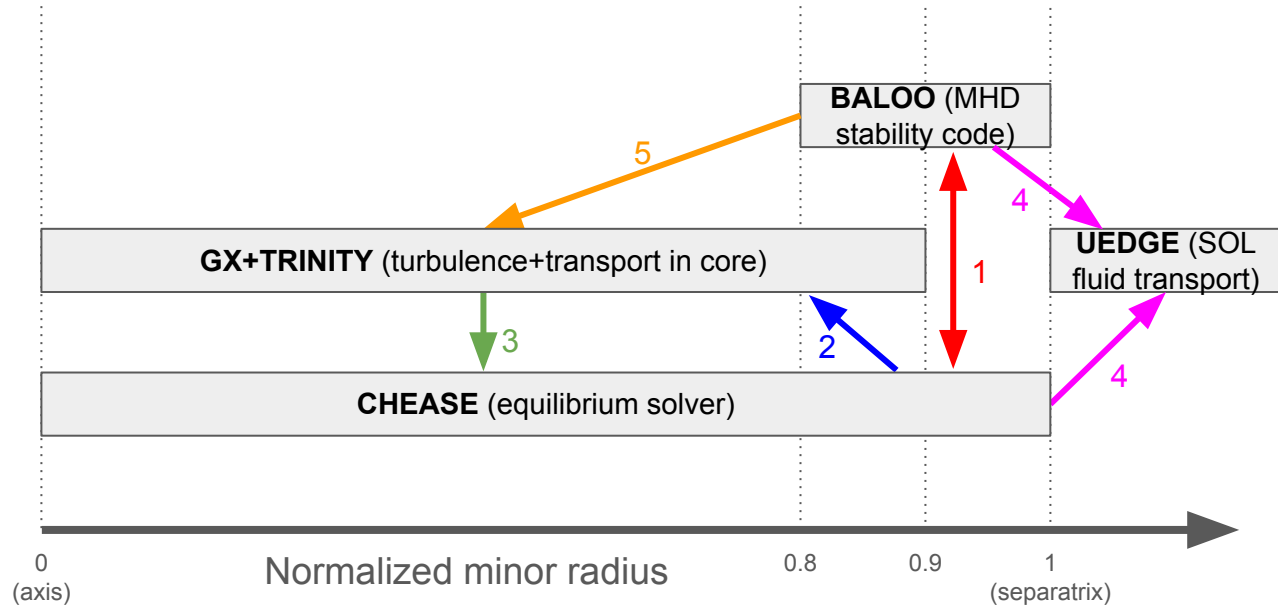
VV activation gammas are reasonably low energy

- Spectrum taken immediately after 1 year at full power
- Majority of gammas produced by VV after are below 100keV
- Dose outside blanket is low, but doing maintenance inside VV is difficult without waiting for cool down



BACKUP: Self-consistent design workflow

1. With initial EQDSK, hand to BALOO, adjust for high performance L-mode edge gradients and hand back to CHEASE
2. CHEASE create new eqdsk with baloo edge gradients → hand to TRINITY
3. TRINITY self-consistently models temp and density profiles with edge points given by BALOO and eqdsk from CHEASE → gives new profiles to CHEASE
4. CHEASE adjusts equilibrium with accurate profiles -> give this and baloo info to UEDGE
5. BALOO's profiles are interpolated and compared to TRINITY's → edge profile values are adjusted and fed to TRINITY again to start new iteration



Gyrokinetic ion turbulence simulations show 400+MW fusion power is attainable in negative triangularity

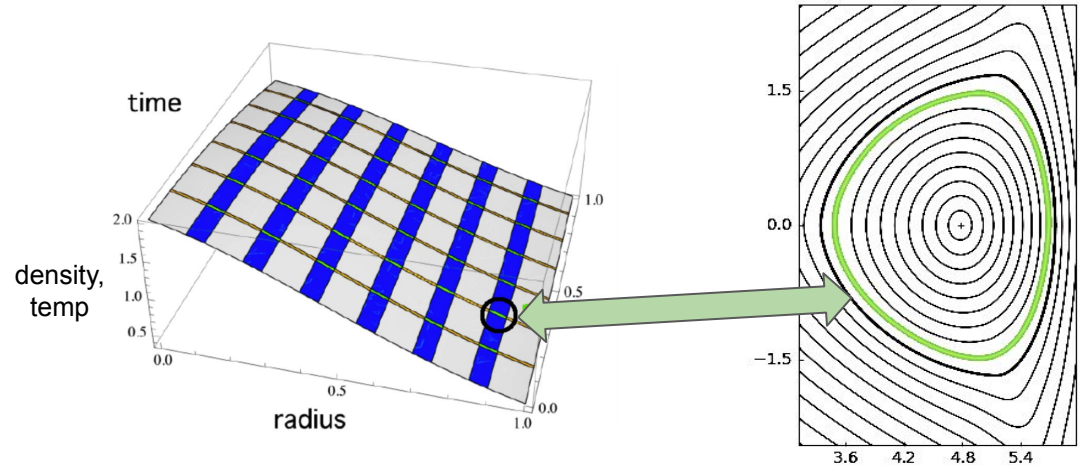
GX: GPU-native gyrokinetic code (turbulence timescales)

+

Trinity: transport solver (transport timescales)

GX-TRINITY coupling:

1. GX calculated gyrokinetic heat flux at discrete radii
2. TRINITY adjusts global profiles using GX fluxes
3. Steps 1 & 2 are repeated until solution has converged



Peaking factor of static density profiles used in gyrokinetic ion turbulence simulations has been observed in ASDEX L-mode shots

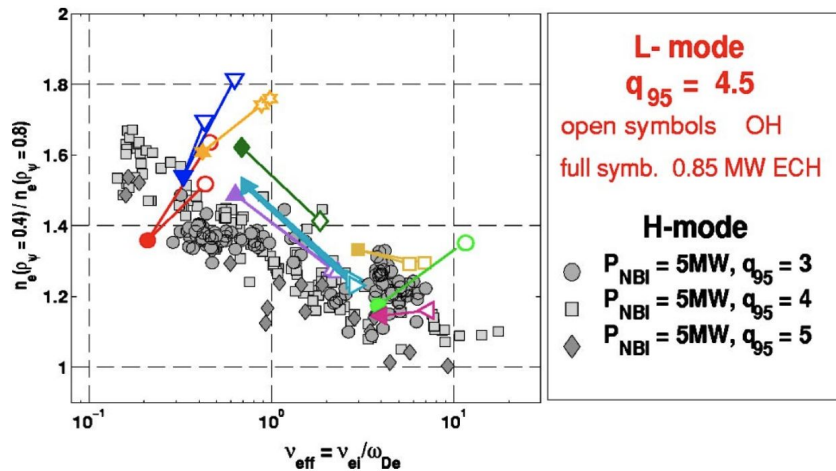
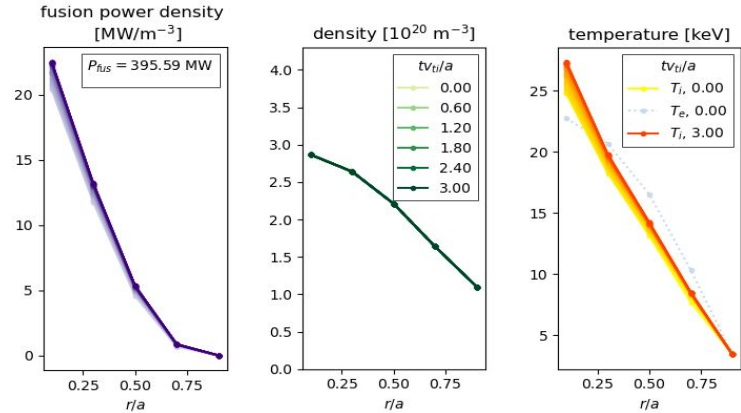


FIG. 2. (Color online). Density peaking, $n_e(\rho_\psi=0.4)/n_e(\rho_\psi=0.8)$ vs ν_{eff} for H mode with NBI heating (small symbols, in gray scale online) and for L mode (big symbols, in color online) plasmas.



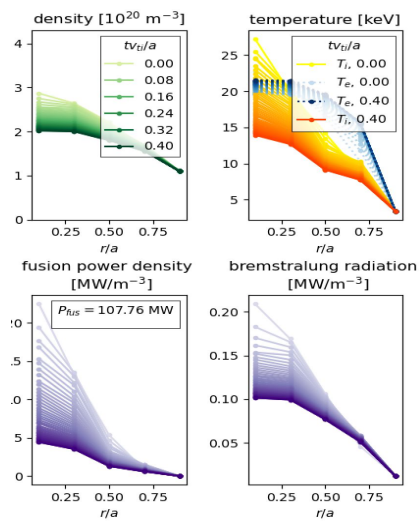
Assumptions:

- Static density profiles*, peaking = 1.6
- Static electron temperature profile, adiabatic electrons

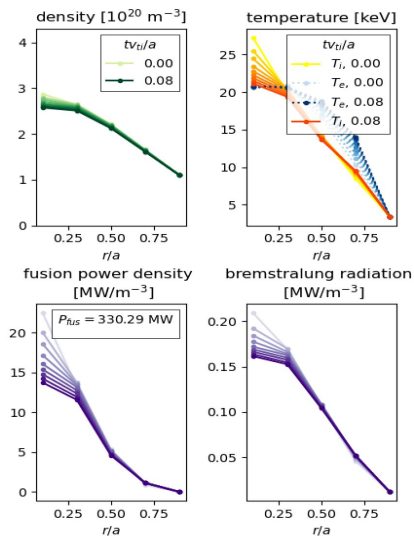
Effect of impurities is necessary to achieve acceptable confinement during kinetic electron gyrokinetic transport calculations

- Well-documented effects of impurities improving transport [1][2][3] are crucial to achieve our required confinement and fusion power goals
- Current TRINITY-GX cannot support multiple ion species
- Preliminary single-ion TRINITY runs demonstrate positive effect of impurities on transport

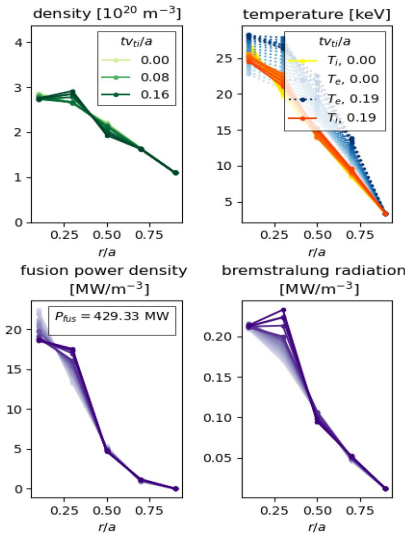
No Impurity: $Z=1$, $dil = 1$



Some Impurity: $Z_{eff}=1.15$, $dil = 0.85$



High impurity: $Z=1.8$, $dil = 0.55$



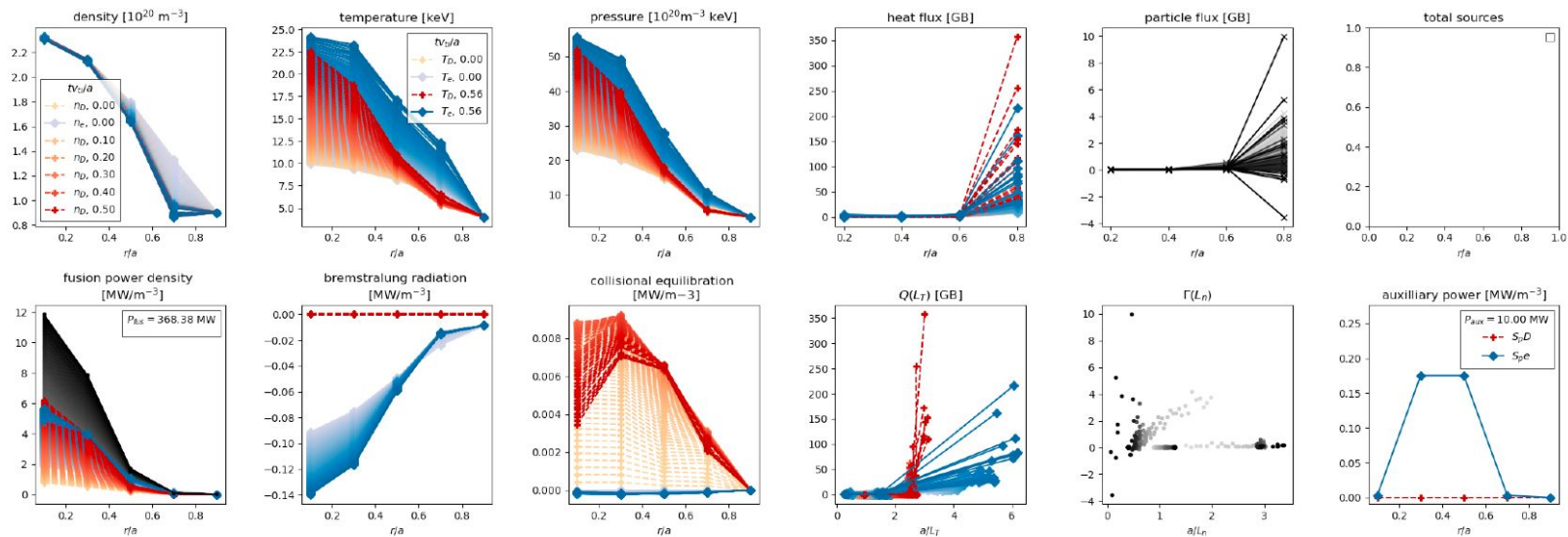
[1] Dominguez R and Staebler G 1993 Nucl. Fusion 33 51–62

[2] Tokar M Z, Jaspers R, Koslowski H R, Kr amer-Flecken A, Messiaen A M, Ongena J, Rogister A A, Unterberg B and Weynants R R 1999 Plasma Phys. Control. Fusion 41 B317–B327

[3] Tokar M Z, Jaspers R, Weynants R R, Koslowski H R, Kr amer-Flecken A, Messiaen A M, Ongena J and Unterberg B 1999 Plasma Phys. Control. Fusion 41 L9–L15 [49] Federici G, Bachmann C, Baru

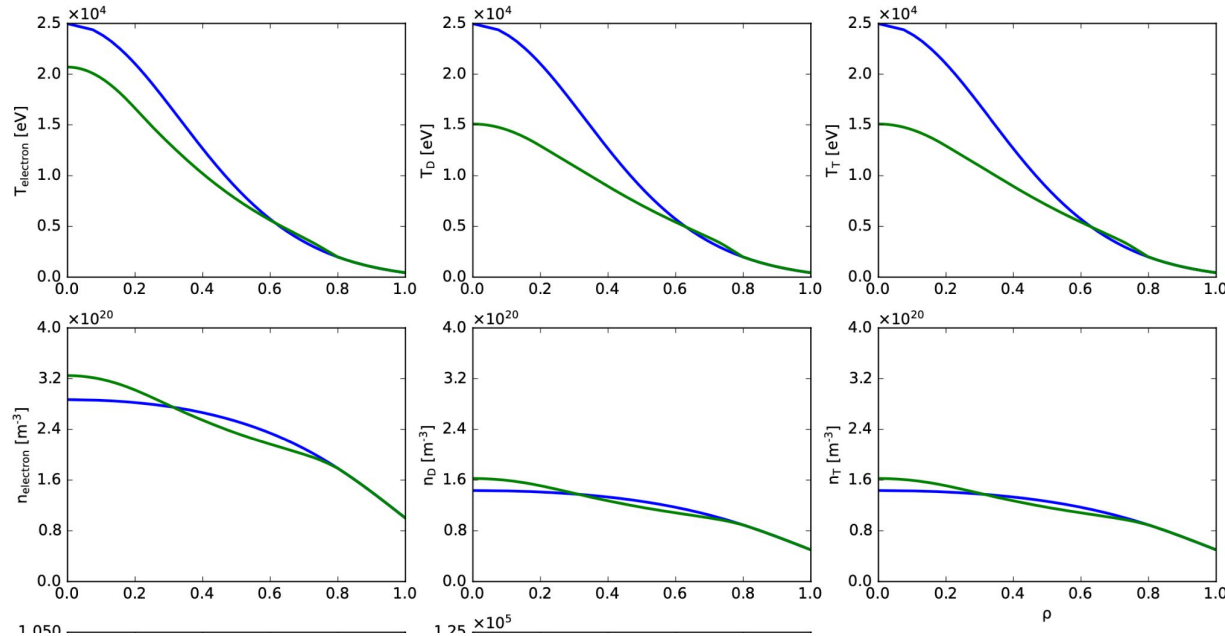
Preliminary multi-species runs produce $P_{fus} \sim 400\text{MW}$

- Next steps:
 - Density puffing
 - Heating consistent with RF
 - Impurities



Effect of impurities is necessary to achieve acceptable confinement during kinetic electron gyrokinetic transport calculations

Initial TGYRO/TGLF (SAT0 model) transport runs suggest impurities necessary to achieve Q_p consistent with POPCONS



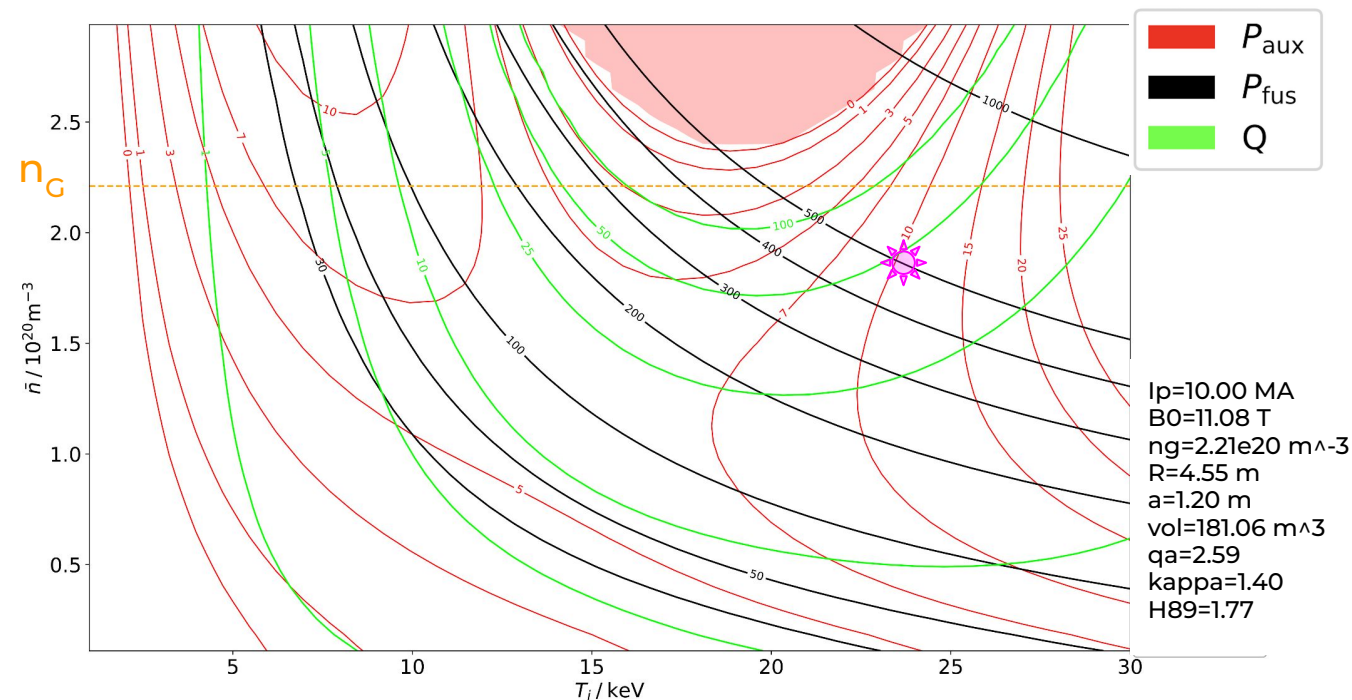
$$P_{\text{fus}} = 365 \text{ MW}$$

$$P_{\text{aux}} = 40 \text{ MW}$$

$$n_{\text{fueling}} = 1 \text{e}20 \text{ m}^{-3}/\text{sec}$$

$$H89 = 1.6$$

BACKUP: operating point on POPCON shows slight discrepancies

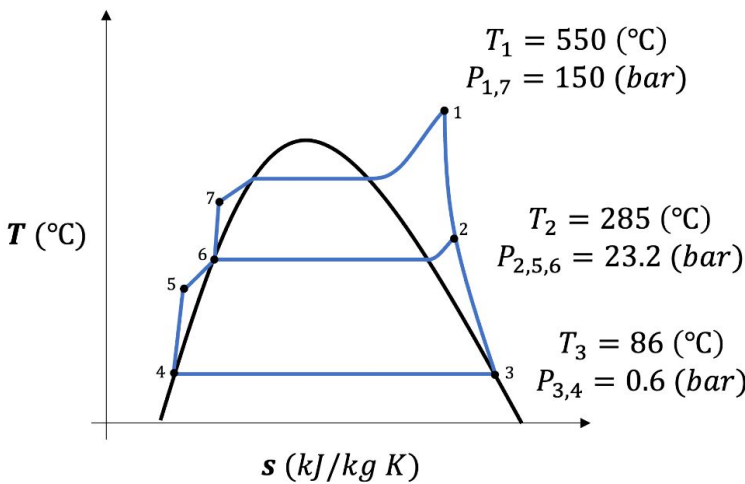


Main sources:

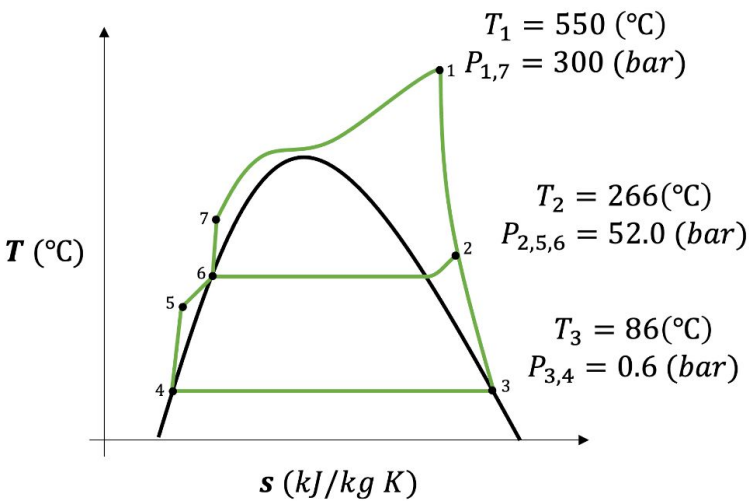
- Parabolic profiles are not entirely consistent
- H89 scaling may not exactly apply to negative triangularity
- POPCON assumes equal ion-electron temperatures
- Line averages vs volume averages

Backup: Optimized Rankine cycle diagrams

Subcritical Rankine



Supercritical Rankine



$$\eta = \frac{[\Delta h_{turb,1-2} + (1 - y)\Delta h_{turb,2-3} - (1 - y)\Delta h_{pump,4-5} - \Delta h_{pump,6-7}]}{h_1 - h_7} \quad y = \text{tapped fluid fraction}$$

$\eta_{subcritical} = 36.0\%$

$\eta_{supercritical} = 38.5\%$

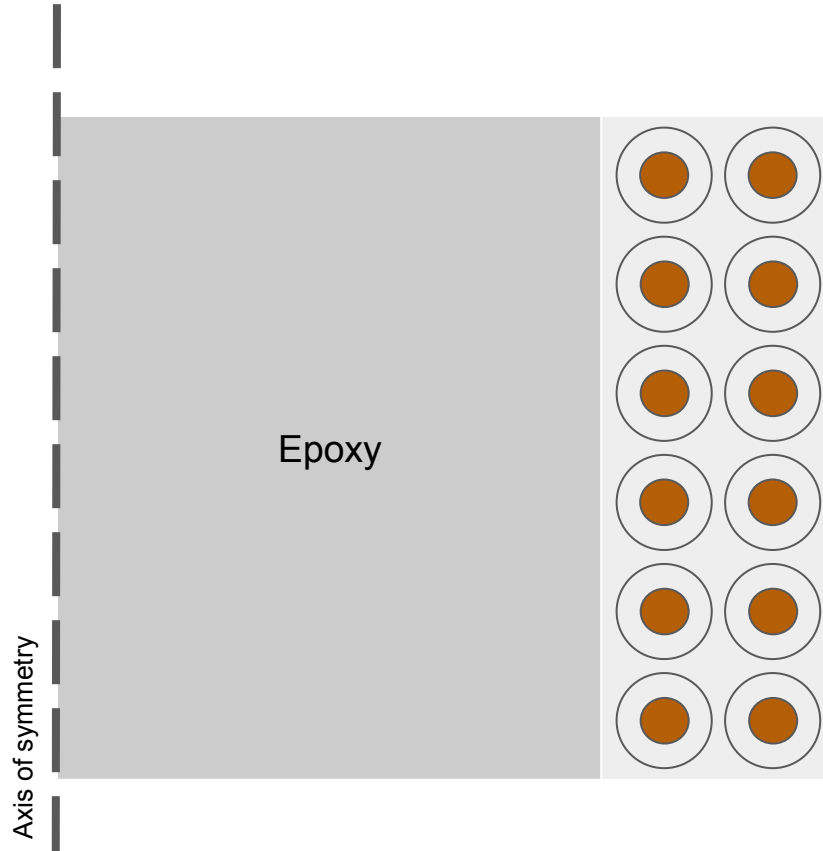
Backup: Cost Breakdown

| Cost | Millions \$ |
|----------------|-------------|
| Land | 15 |
| Structures | 110 |
| Turbine Plant | 107 |
| Electric Plant | 35 |
| Misc Plant | 17 |
| Heat Rejection | 11 |
| TF | 1293 |
| PF | 253 |

| Cost | Millions \$ |
|---------------|-------------|
| CS | 142 |
| Cryosystem | 106 |
| Divertor | 150 |
| Blanket | 224 |
| Fueling | 27 |
| VV | 4 |
| Heating | 189 |
| Heat Transfer | 60 |

| Cost | Millions \$ |
|---------------|-------------|
| Waste | 2.0 |
| Power storage | 0.2 |
| Tritium Eqpt | 30 |
| Diagnostics | 100 |
| Indirect Cost | 149 |
| | |
| | |
| | |

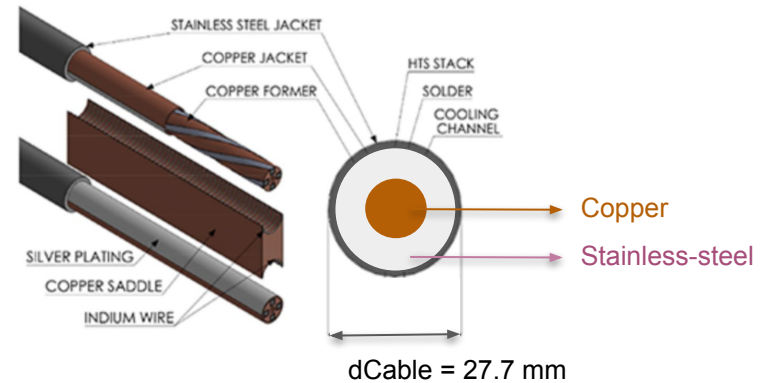
Central Solenoid constructed as an array of viper cables



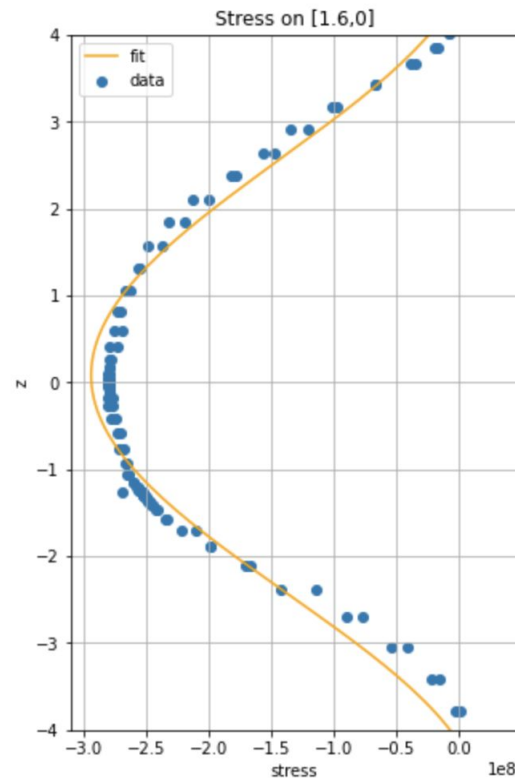
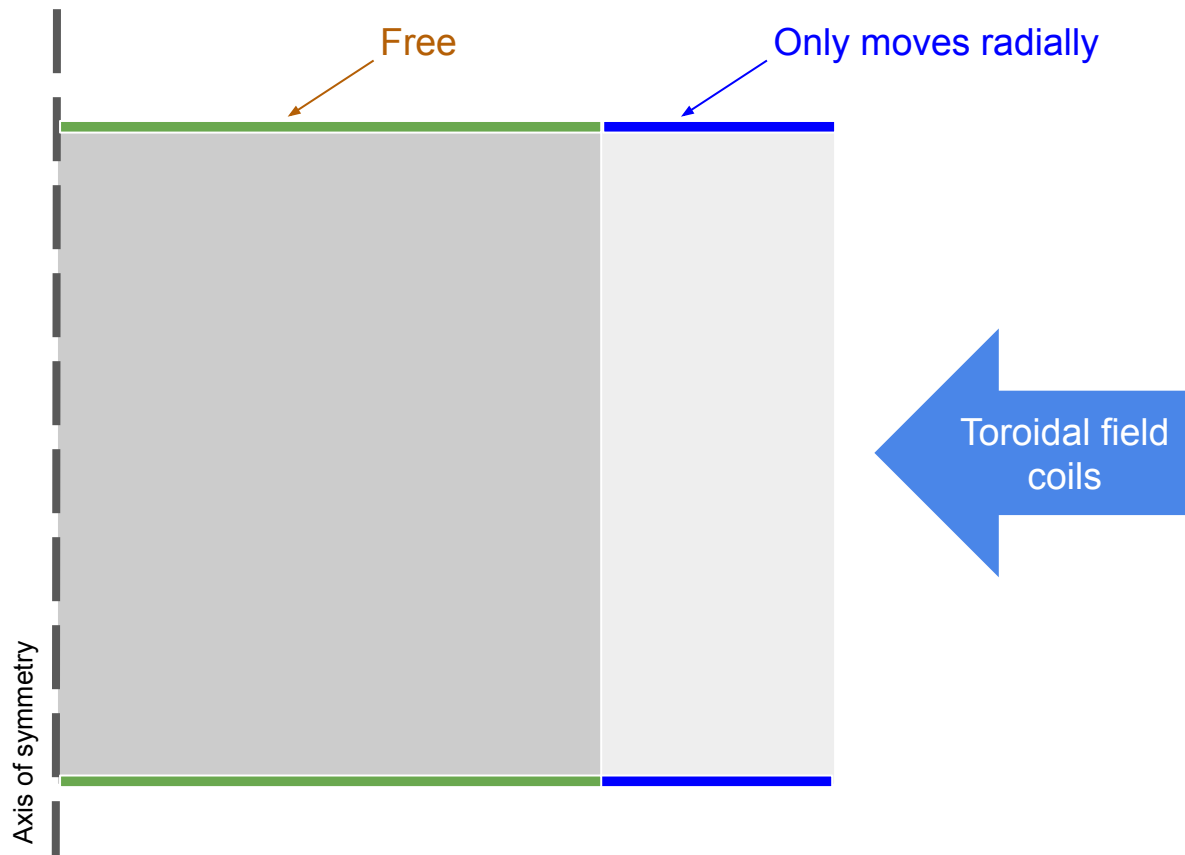
$$\text{Turns} = \text{width}/d_{\text{Cable}} \times \text{height}/d_{\text{Cable}}$$

$$J_e = 85 \text{ A/mm}^2$$

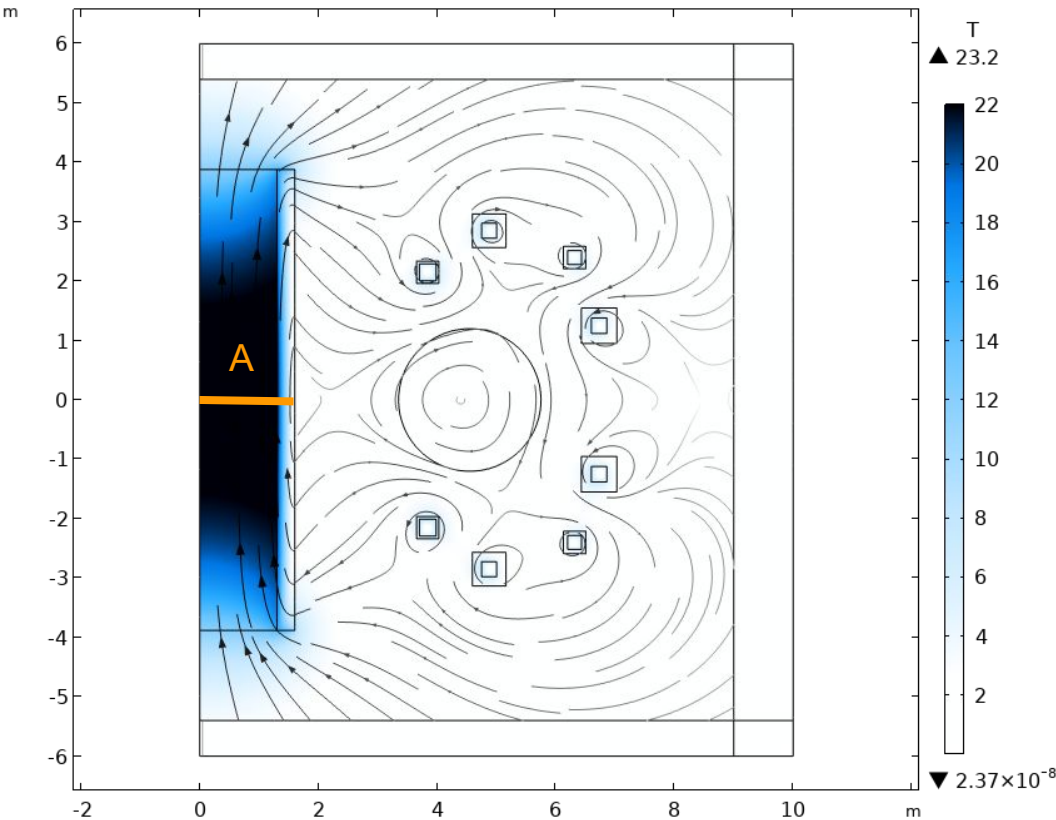
$$E = 0.55 E_{\text{steel}} + 0.45 E_{\text{Copper}}$$



Boundary conditions are carefully selected to obtain realistic stresses



Central Solenoid modeled with Poloidal Field Coil and plasma contributions



The **plasma** is a single-turn 10 MA coil, the **poloidal field coils (PF)** are modeled like the central solenoid.

Flux swing: integral of the magnetic flux through the surface area A

Slide Drafts

Order of Presentation drafting slide

- Dennis intro and summary + constraints
- Key innovations and insights
- Motivate Negative Triangularity
- Click-through from core out to integration (shows modular design of reactor & division of labor - magnet cage, VV, FLiBe tank, etc [Integration group])
 - Geometry (R,a, elongation, plasma volume)
 - Demountable magnet image
 - LIB (drainable)
 - Overnight cost for all components, Brownfield v Greenfield discussion (maybe BvG goes towards end?)
- go through each magnet system - structurally the reactor can withstand magnetic forces
- Core scenario development - physics says we can actually reach fusion power goal
- divertor/power handling - reactor won't melt
- neutronics - radiation load is tolerable
- Fuel Cycle - reactor is fuel self-sufficient
- Thermal Cycle and electricity generation (logically this follows from neutron heating of FLiBe) - we get net electricity
- maintenance, including distinction between environmental cycle and plant life time - plant maintenance is reasonable
- Economics: LCOE and tritium revenue - we'll turn a profit
- Summary and Conclusions

BACKUP: Electrical Properties

| Property | Value |
|---|--------|
| Pancakes [-] | 18 |
| Turn/Pancake [-] | 16 |
| Turns [-] | 288 |
| Operating Current [kA] | 47.2 |
| Inductance [H] | 5.6 |
| Stored Energy [GJ] | 6.27 |
| Joint Resistance [nOhms/joint] | 0.5 |
| Radial Resistance per Turn [nOhms] | 200 |
| Rib Thickness [m] | 0.021 |
| HTS Area [mm^2] | 106.2 |
| HTS Assumed Critical Current [A/mm^2] | 740 |
| HTS Operating Current Over Critical Current [-] | 0.6 |
| Characteristic Resistance for Charging [nOhms] | 27,288 |

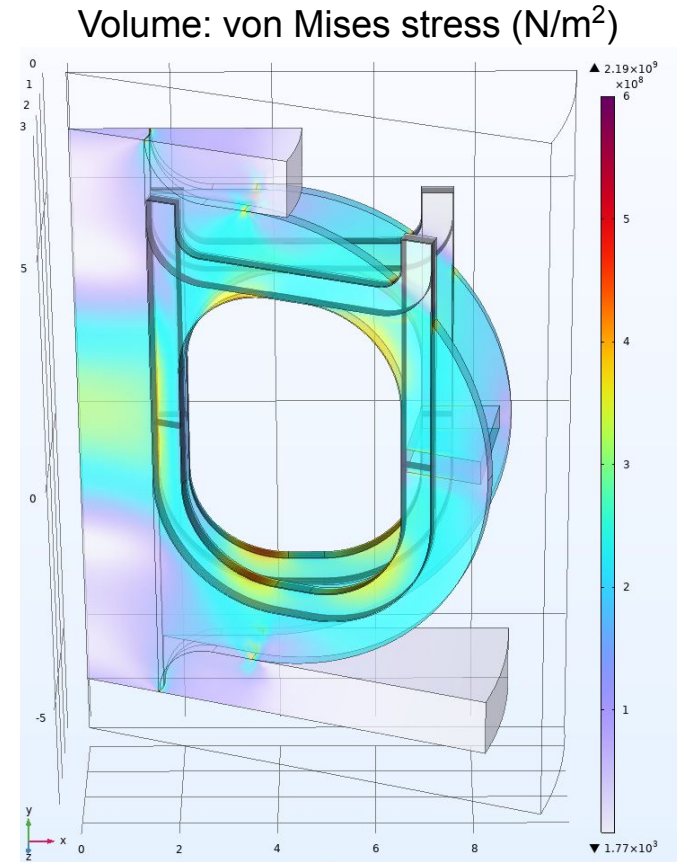
For More Data: [\[link\]](#)



Diagram Showing HTS Circuit Pathway

Joints provide top-down maintenance

- “Devil’s Horn” joint shape provide top-down access
- Demountable magnet allows PF coil within the TF cage
- First order cross current on joint lead to low joint stress
- Same internal geometry
 - Case top corners filled with steel



Toroidal Field (TF) Coils - Rounded Window

Design Goal:

- Reasonable stress on the magnet (0.6 GPa)
- Incorporate demountable joint
- Allow top-down maintenance scheme
- Say magnetic field requirements from core physics

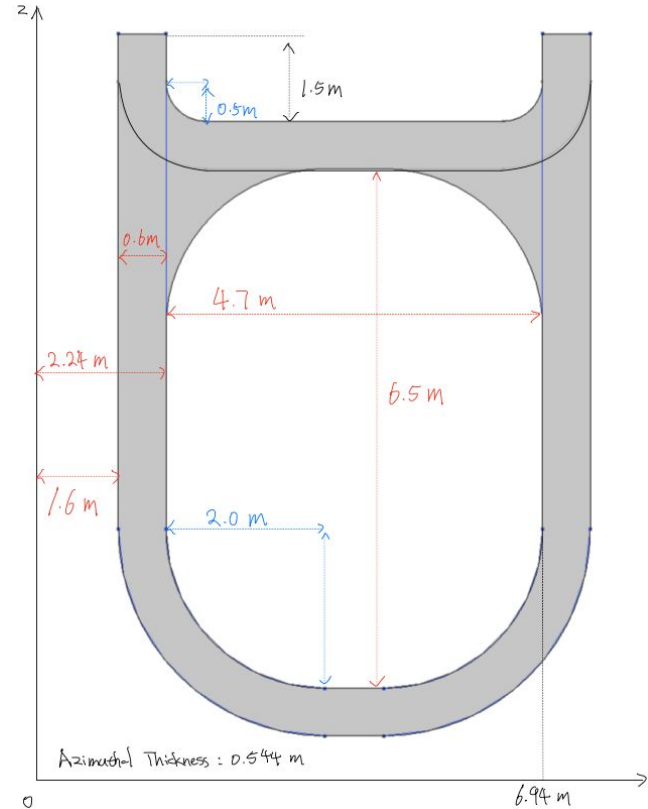
Toroidal Field (TF) Coils - Rounded Window

Design Goal:

- Reasonable stress on the magnet (0.6GPa)
- Incorporate dismantable joint
- Allow top-down maintenance scheme

Choice: Rounded Window Frame

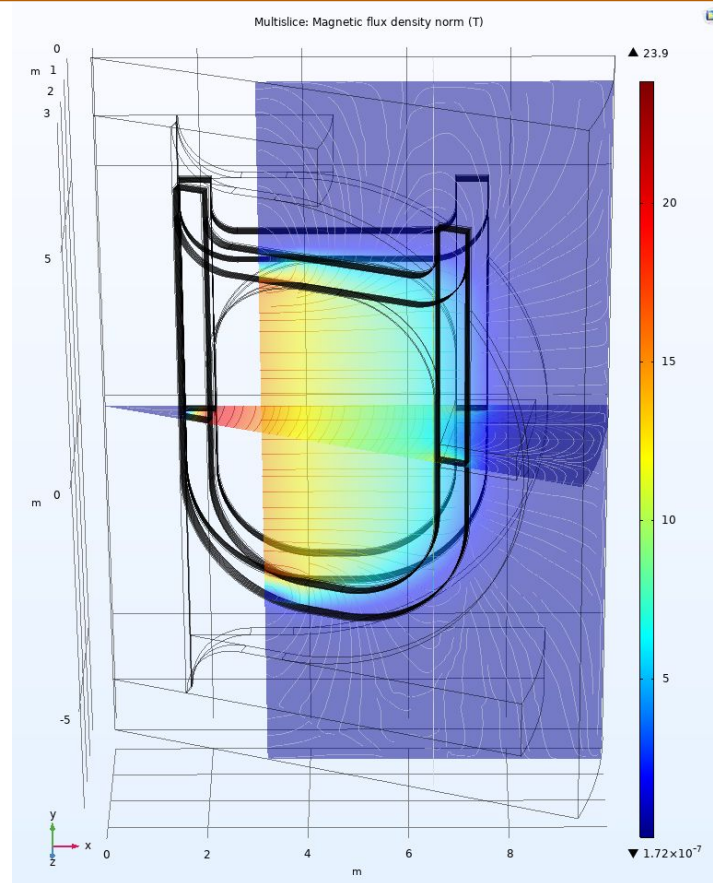
- Simple shape
- High corner curvature reduces stress
- 18 coils in total, with 13.6 MA-turns per coil
- Top joint placement
- Pancake structure of magnet pieces



Design provide 24T Max field, 11T on axis

Choice: Rounded Window Frame

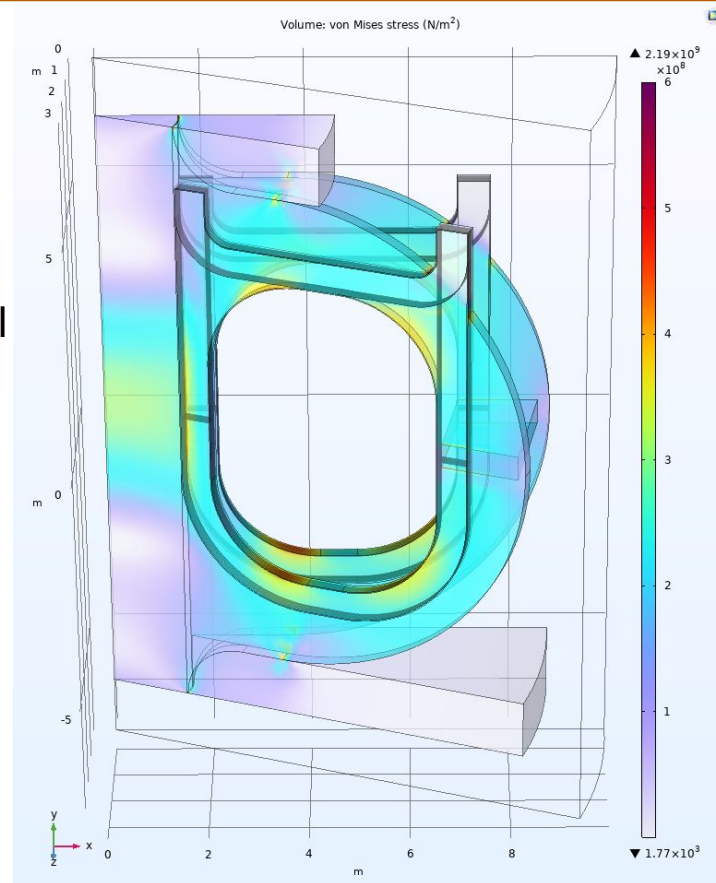
- Simplistic shape
- High corner curvature to reduce stress
- 18 coils in total, with 13.6 MA-turns per coil
- Top joint placement
- Pancake structure of magnet pieces
- 24T Max Inboard field, 11T on axis
 - Consistent with core parameter



0.6GPa desired max stress on coil

Choice: Rounded Window Frame

- Simplistic shape
- High corner curvature to reduce stress
- 18 coils in total, with 13.6 MA-turns per coil
- Top joint placement
- Pancake structure of magnet pieces
- 24T Max Inboard field, 11T on axis
 - Consistent with core parameter
- 0.6GPa Max stress on the coil
 - Support structure stress can be reduce by properly rounding out corners



Cooling system achieves 11 day cryo cycle

Cooling system design driven by thermal cycle time needs

- Liquid H₂ coolant @ 20K
- Thermal power
 - During shots: 14.5 kW (0.82 MWe)
 - Between shots: 11.5 kW (0.64 MWe)
 - Cryo cycle maximum power: 1.5 MW (25 MWe @ T = 28K)
 - Max mass flow rate?

Rate-limiting step

Limit set by

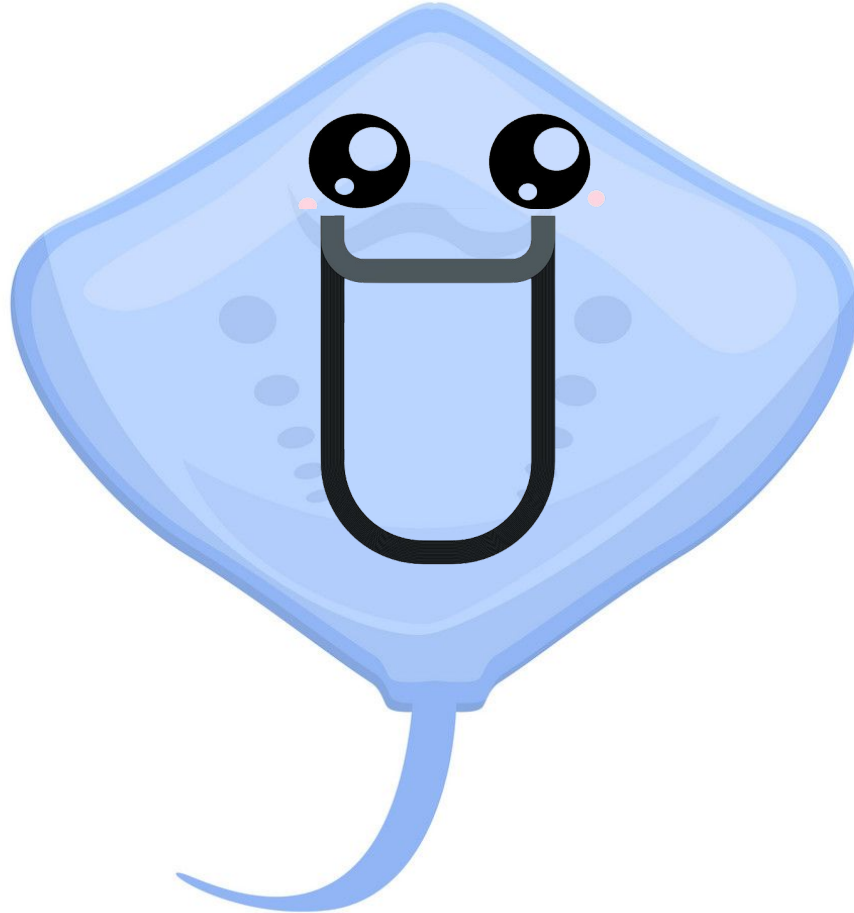
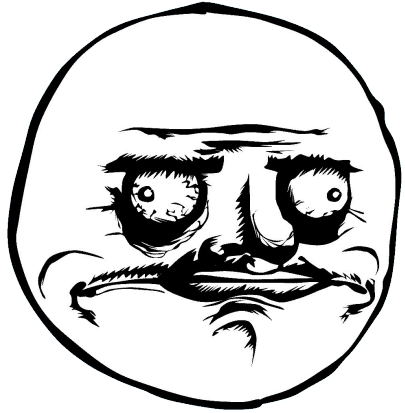
Charge/discharge TF

Radial current heating

Warm up/cool down cryostat

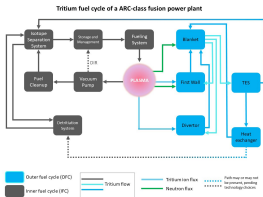
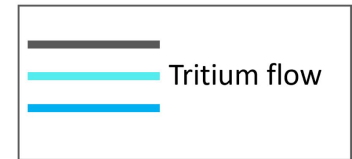
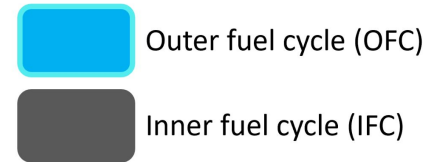
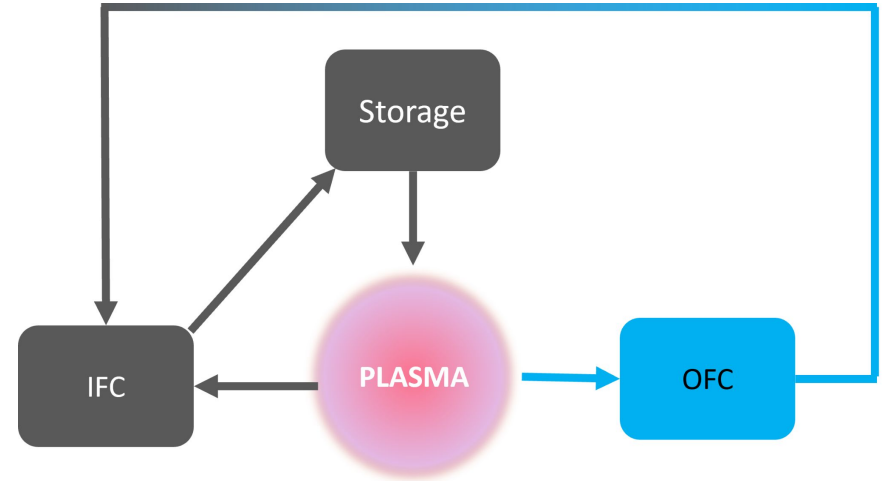
Thermal stresses

Most Important Backup Slide



Tritium transport modeling shows that MANTA is self-sufficient and able to produce excess tritium for sale

- Fuel Cycle models how tritium flows through the FPP
 - Not necessarily MANTA-specific



S. Ferry & S. Meschini, 2022

Lower separatrix densities ??benefit/degrade?? divertor operation

backupslide

**Figure to be added of peak
heat fluxes vs separatrix
density**